
**University of Almeria**

# Evaluation of electrochemical processes assisted by solar energy for water depuration

**Irene Salmerón García**

PhD Thesis

Almeria, 2020



# Universidad de Almería

**Departamento de Ingeniería Química**

**Doctorado en Biotecnología y Bioprocesos Industriales aplicados a la Agroalimentación y Medioambiente**


## Evaluation of electrochemical processes assisted by solar energy for water depuration

---

## Evaluación de procesos electroquímicos asistidos por energía solar para la depuración de aguas

Memory presented for the title of Doctor:


**Irene Salmerón García**


Almería, September 2020

**Thesis supervisor:**


**Isabel Oller Alberola, PhD.**

Research Fellow OPI

CIEMAT-PSA

# 1. Objectives and experimental plan

# 1 Objectives and experimental plan

## 1.1 Objectives

The objective of this PhD Thesis lies in the application of novel technologies based on electrochemical oxidation processes enhanced by its combination with solar energy for the treatment of industrial wastewater as well as for the elimination of organic microcontaminants (OMCs) contained in urban wastewater. In addition, the combination with other technologies such as membrane nanofiltration (NF) systems is also considered for efficiency improvement.

To achieve the general objective, the following specific objectives (defined as targets) are proposed, which have been developed in each of the papers that conforms this PhD Thesis:

- ***Target 1:*** Characterization, modelling and start-up of a solar photoelectro-Fenton (SPEF) pilot plant consisting on Electro MP-Cells from ElectroCell with Nb-BDD as anode and carbon-PTFE GDE as cathode for onsite generation of $H_2O_2$. Optimization of the main operating parameters (pH and *j*) by using response surface methodology.
- ***Target 2.*** Combination of a NF membrane system with the SPEF pilot plant as a tertiary treatment of UWWTP retentate. Evaluation of different electro-oxidative processes combined or not with solar energy for the elimination of OMCs in simulated and actual NF retentate.
- ***Target 3.*** Examination, diagnosis and preliminary autopsy of carbon-PTFE GDE cathode surface by scanning electron microscopy (SEM) and X-ray microanalysis. Assessment of $H_2O_2$ onsite production variations.
- ***Target 4.*** Development and application of new photoelectrocatalytic processes at laboratory scale for the simultaneous elimination of OMCs and pathogens in freshwater. Assessment of the enhancement achieved when a Pt counter cathode is replaced by a carbon-felt cathode able to electrogenerate $H_2O_2$.
- ***Target 5.*** Pre-treatment of complex industrial wastewaters by electrogenerated chlorine species by using commercial Dimensionally Stable Anodes (DSA), made of a titanium base coated with a conducting layer of a metal oxide or a mix of them, and combined with solar energy at pilot plant scale. Main objective lays on increasing biodegradability enough for the subsequent application of a lower-cost biological treatment.

## 1.2 Experimental plan

For the successful achievement of the proposed objectives, the tasks detailed below have been set out and performed:

***Task 1.*** Optimization of an electrochemical pilot plant equipped with four Electro-Cells of Nb-BDD anodes for the onsite generation of $H_2O_2$ and carbon-PTFE GDE cathode.

1.1 Modelling and optimization of $H_2O_2$ electro-generation by response surface methodology.

Application of a Central Composite Experimental Design for the optimization of main operation parameters of the electro-oxidation pilot plant: pH and current density. A set of 19 runs will be defined on the experimental matrix, setting variations of pH among 3, 5 and 7, and *j* among 30, 65 and 10 mA $cm^{-2}$. The statistical analysis of the results will allow obtaining a second-order regression model and the optimal operating conditions for maximizing the electrogeneration of $H_2O_2$ with the lowest energy consumption.

1.2 Establishment of the best operation conditions.

Once the main parameters are optimized (pH and *j*), several tests are carried out to evaluate the effect of other process parameters on the SPEF pilot plant performance, such as water flow, air flow and different ionic strengths, in order to describe their influence on $H_2O_2$ electrogeneration.

***Task 2.*** Evaluation of the optimized electrochemical process for the removal of reference organic contaminants.

Preliminary tests are carried out with organic reference compounds (pyrimethanil and methomyl at 50 and 90 mg $L^{-1}$, each), which degradation behaviour by other advanced oxidation processes is well known, in order to assess the performance of the electrochemical process and its enhancement by solar energy. Experimental operation conditions will be those stablished by the previous optimization, by using $Na_2SO_4$ as supporting electrolyte. Parameters to be monitored through the experiments are: concentration of $H_2O_2$ and iron (total and dissolved), free chlorine, dissolved organic carbon and the organic compounds (analysed by HPLC-UV).

***Task 3.*** First approach to the combination of technologies, application of Nb-BDD electro-cells with carbon-PTFE GDE cathodes and NF membrane system for the degradation of OMCs contained in UWWTP effluents.

3.1 Development of a simulated NF retentate receipt.

A synthetic recipe of NF membrane retentate from the effluent of an UWWTP is developed according with previous characterizations reported on literature, which is used as water matrix for the removal of the target OMCs (pentachlorophenol, terbutryn, chlorphenvinfos and diclofenac).

3.2 Working at natural pH by studying the use of EDDS as iron complexing agent in electro-Fenton (EF) and SPEF processes.

Electrochemical treatments are applied at natural pH being crucial the use of an iron complexing agent to maintain it in solution. EDDS is selected for showing high biodegradability and stability in demineralized water at neutral pH as demonstrated in previous published works. The suitability of the complex formed by $Fe^{3+}$ and EDDS is evaluated under 1:2 ratio (0.1:0.2 mM), studying its stability in highly salted concentrated streams, its interaction with cations contained in the water matrix, as well as its behaviour during electro-oxidative processes.

3.3 OMCs removal in the SPEF pilot plant.

Different electrochemical processes assisted or not by solar energy, are evaluated for the removal of selected OMCs from the priority substances of the Directive 2013/39/EU: pentachlorophenol, terbutryn, chlorphenvinfos and diclofenac, at initial concentrations of 200 and 500 μg $L^{-1}$. Simulated NF retentate is used as water matrix.

***Task 4.*** Tertiary treatment of actual UWWTP effluents by the combination of NF system and electrochemical processes.

NF membrane system is applied as pre-concentration stage in a tertiary treatment line for the increase of OMCs concentration in the retentate stream as well as the reduction of the total volume to be treated, at the same time that a high quality permeate stream is produced, which could be directly reused for different purposes. In consequence, its combination with an electrochemical treatment envisages the reduction of the ohmic resistance with a subsequent decrease of the electrical cost related to the energy needed in the electrochemical treatment.

4.1 Combined technologies assessment by fortification of actual NF retentate with target OMCs.

Tests are carried out on an actual NF retentate from an UWWTP effluent, obtained in a pilot plant available at Plataforma Solar de Almería facilities (conformed by FilmTec NF90 2540 commercial NF membranes) and spiked with the selected OMCs (pentachlorophenol, terbutryn, chlorphenvinfos and diclofenac, at initial concentration of

100 µg $L^{-1}$). Electrochemical treatments: AO and EF, combined with solar energy (solar-assisted AO and SPEF) are evaluated in order to find the most suitable process according to the water matrix characteristics. Furthermore, the influence of the carbonates in the degradation process by electrochemical treatments is also addressed.

4.2 Combined technologies for the removal of OMCs contained in the actual NF retentate stream.

Effectiveness assessment of the most promising tertiary electrochemical treatment selected in the previous task will be studied for the elimination of OMCs actually present in the NF retentate stream. OMCs are detected and monitored by using liquid chromatography coupled to mass spectrometry.

***Task 5.*** Examination, diagnosis and degradation assessment of Carbon-PTFE GDE cathode.

5.1 Evolution study of $H_2O_2$ electrogenerated in the SPEF pilot plant.

The stability and robustness of carbon-PTFE cathodes is studied by monitoring the accumulated $H_2O_2$ electrogenerated after several tests carried out along the PhD Thesis. Their capacity to produce $H_2O_2$ and their suitability for EF and SPEF processes performance are also evaluated.

5.2 Cathodes cleaning procedure and evaluation of $H_2O_2$ electrogeneration capability recovery.

Disassembled of different pieces of the cell for a visual evaluation of physical changes observed on the cathode surface and the formation of salt inlays is planned. Removal of the inlays is performed by the cathode immersion in HCl solution 1:2 during 24 h. After cleaning procedure, the concentration of accumulated $H_2O_2$ electrogenerated is compared to the one attained when the cathode was new for the assessment of cleaning effectiveness for a possible cathode reuse.

5.3 SEM and X-ray analysis of cathode surface.

Cathode surface is studied after the cleaning procedure for analysing the loss of reactive surface provoked by the detachment of carbon-PTFE from the cloth support and by the possible remaining salt inlays. Detailed characterization of the cathode composition as well as the inlays will be tackled.

***Task 6***. Assessment of a photoelectrocatalytic process with innovative and newly developed $TiO_2$ nanotubes ($TiO_2$-NT) photo-anodes for the purification of fresh water at laboratory scale.

6.1 Manufacture of new $TiO_2$-NT photo-anodes at laboratory scale.

A titanium mesh is immersed in a specific electrolyte consisting on $NH_4F$ (0.3 wt%) in distilled water (3.0 vol%) and ethylene glycol (97 vol%). By applying a potential of 30 V during 3 h, the growing of $TiO_2$-NT over the entire surface of the mesh is promoted. Then the electrodes are assembled in a cell with a quartz window and an anode-anode-cathode configuration.

6.2 Definition of operation conditions for testing the electrocatalytic efficacy of the new developed cell with $TiO_2$-NT.

Best working potential is determined by scanning a range of potentials from 0.1 to 1.5 V till reaching the maximum photo-current when illuminating the photo-anodes with a UV-A lamp of 9 W at an irradiation of 50 W $m^{-2}$.

6.3 Evaluation of the new cathode effectiveness for OMCs and pathogens removal in natural water.

A comparison between OMCs degradation (terbutryn, chlorphenvinfos and diclofenac at 500 µg $L^{-1}$ each) and disinfection results (*E. coli* at $10^6$ CFU $mL^{-1}$) reached by the photoelectrocatalytic lab scale system using a counter cathode of Pt, and the possible improvement that could be obtained by replacing it by a carbon-based one able to electrogenerate $H_2O_2$ onsite is addressed. For this, tests will be carried out with OMCs and bacteria, following the degradation and inactivation rates along treatments.

6.4 Hole scavengers effect in disinfection by new lab scale photoelectrocatalytic system.

Methanol and acetate, well known hole scavengers, are added to the target natural water at 5 mM each aiming to check their influence in the photo-current achieved and in bacteria inactivation through the photoelectrocatalytic treatment.

***Task 7.*** Pre-treatment of complex industrial wastewaters by electrogenerated chlorine species using commercial DSA electrodes.

7.1 Characterization of industrial wastewaters: two different batches of landfill leachate.

A complete characterization of target industrial wastewaters will be carried out, addressing physicochemical parameters such as chemical oxygen and biological oxygen demands, dissolved organic carbon and concentration of ionic species. Toxicity and biodegradability are carried out by means of respirometry (oxygen uptake rate measurement) with active sludge from an UWWTP.

7.2 Landfill leachates treatment with a commercial device based on DSA electrolyzer.

Two different batches of landfill leachate are depurated applying the stand-alone electrolyzer until improving toxicity and biodegradability enough to allow a subsequent conventional biological treatment.

7.3 Commercial DSA electrolyzer assisted by solar energy.

DSA electrolyzer is combined with a solar CPC photo-reactor available at Plataforma Solar de Almería, in order to evaluate the benefits and/or disadvantages of the application of solar energy to the electrochemical process, aiming to reduce toxicity and increase biodegradability in a more efficient way.

To complete the feasibility study, landfill leachates treatment by commercial DSA electrolyzer, assisted and not by solar energy, was compared with solar photo-Fenton process.

# 2. Abstract

## Abstract

Nowadays society's lifestyle encourages a high rate of consumption of natural resources; many of them are non-renewable, meaning that an inadequate management will lead to a certain degree of scarcity in the medium to long term. The most illustrative example is water, used in almost any human activity, for human consumption, cleaning and domestic use or in industrial processes (even in energy production), either as cooling medium or directly intervening in the productive process, water is present. It was up to the 2000s that the Legislative Authorities were considering water no more than a commercial asset being the implementation of the Water Framework Directive (2000/60/CE) the inception to a mentality change towards water, considering it now more an heritage deserving protection and laying the foundations for the development of specific regulations that will establish minimum quality limits to be achieved prior to the discharge of the effluents into the environment.

Specifically, chemical industry undergone a strong development owed to a growing demand for new products to satisfy the needs of the consumers. The manufacture of drugs, personal care products, or pesticides and fertilizers to improve agricultural production has led to the appearance, development and deployment of new organic substances. These are usually toxic, non-biodegradable and highly recalcitrant, thus they are difficult to assimilate for microorganisms, being active in the environment for long periods of time and with unknown effects on the discharge ecosystems.

That situation motivates arisen, development and application of new highly oxidizing technologies, aiming the degradation of these emerging compounds and even, depending to their complexity, enhancing the biodegradability of the whole effluent. For this reason, electrochemical processes pose a versatile, useful and powerful tool since only by applying an electric current or potential on the electrodes it is able to generate oxidizing species that interacts with a broad spectra of contaminants, facilitating their removal.

Some electrochemical processes have been widely used at industrial scale. For example, electrocoagulation implies an advantage over the conventional coagulation-flocculation physicochemical process, since avoids the addition of chemical reagents by the use of sacrificial electrodes, generating a lower amount of sludge, and presenting higher efficiency in the colloids removal. On the other hand, electrodialysis, an electrically assisted membrane process, is able to separate the ions from an influent, yielding a high-

quality effluent of low ionic charge, being mainly applied in desalination processes aimed to produce drinking water.

In spite of involving great advantages such as an easy control of the process and therefore easy automatization, as well as the absence of external reagents, some electro-oxidative processes have not been evaluated further than at laboratory scale. In fact, most of the studies reported in the literature are focused in the development of new materials for electrodes manufacturing, to improve effectiveness and reduce costs associated to this technology. However, it must be highlighted that electrochlorination has been implemented on a larger scale due to the low cost of the electrodes.

The scarcity of studies facing these technologies under a realistic approach and for the purification of complex water matrices, has limited the possibilities of electro-oxidative systems from a commercial standpoint. It is important to note that from the ions species naturally contained in certain waters, a large amount and variety of oxidizing species can be generated, which entails an intrinsic improvement over the basic studies using a supporting electrolyte whose only function is to allow the transition of electrons. Furthermore, many of these electrogenerated species are photoactive, which means that just by irradiating the solution with ultraviolet light the generation of even more oxidizing species could be promoted, which results in an increase of the contaminants degradation rate. This has meant that the development, implementation, start-up and evaluation of these systems on a larger scale have not been also addressed in depth, hindering the scale-up of the electro-oxidative process.

In this context, the opportunity of this PhD Thesis arises bringing the study of electrochemical technology to a new level closer to reality. The application of electro-oxidative processes at pilot plant scale in actual wastewaters is addressed, assessing the operating conditions seeking to improve contaminants removal and water depuration. Combination of electro-oxidative systems with a natural and renewable energy source such as sunlight is also tackled.

The first objective addressed was characterization, start-up and optimization of the main operational parameters of a solar photoelectro-Fenton (SPEF) pilot plant able to treat up to 100 L of water developed and installed at Plataforma solar de Almería (PSA) (CIEMAT). The system consists of four electro-cells equipped with a niobium-supported boron doped diamond anode (Nb-BDD) and a carbon-polytetrafluoroethylene (carbon-PTFE) gas diffusion cathode (GDE) (Electro MP-Cells from ElectroCell). The cells are

connected in parallel to a recirculation tank and this, in turn, to a solar photo-reactor based on compound parabolic collectors (CPC) with 2 $m^{-2}$ of illuminated surface. Optimization of the main input variables, pH and current density (*j*), was carried out to maximize onsite $H_2O_2$ electrogeneration with the maximum current efficiency (CE). A central composite experimental design was defined, and after the completion of the 19 experiments proposed in the matrix, by means of the statistical analysis of the results, the adjustment model for $H_2O_2$ concentration was obtained: $[H_2O_2] = 2.19 - 0.31 \cdot pH + 0.81 \cdot j - 0.05 \cdot pH \cdot j + 0.15 \cdot pH^2 - 2.42 \times 10^{-3} \cdot j^2$, as well as for the CE percentage: $\%CE = 61.68 - 0.43 \cdot pH - 0.18 \cdot j - 0.0275 \cdot pH \cdot j$, and the corresponding response surface graphs. Finally, the model was validated, corroborating that, at pH 3 and applying 73.66 mA $cm^{-2}$, the maximum production of $H_2O_2$ is achieved (64.9 mg $min^{-1}$) with a CE associated of 89.3%. Once these parameters were established, the influence of the water and air flows, as well as the concentration of the electrolyte on the $H_2O_2$ electrogeneration was also studied, reaching the maximum applying a water flow of 5.6 L $min^{-1}$, an air flow of 10 L $min^{-1}$, and with 50 mM of $Na_2SO_4$. Afterwards, preliminary tests were developed assessing the efficiency in the removal of reference compounds, pyrimethanil and methomyl in a concentration of 50 mg $L^{-1}$ and 90 mg $L^{-1}$, respectively, by the application of the different oxidation processes that are able to be developed in the pilot plant system: anodic oxidation (AO), electro-Fenton (EF) and solar SPEF, having as supporting electrolyte a solution of $Na_2SO_4$ 50 mM. The highest degradation rates were attained by SPEF process: 55% of pyrimethanil and 50% of methomyl after only 5 minutes. This research was performed with the collaboration of Prof. Anastasios J. Karabelas and Dr. Konstantinos V. Plakas of the Chemical Processes and Energy Resources Institute of the Centre for Research and Technology-Hellas (Greece) in the framework of the European project SFERA-II at PSA facilities.

Second objective was focused on a real application of the previously optimized electrochemical pilot plant through its combination with a pre-treatment consisting of a nanofiltration (NF) membrane system. Urban wastewater treatment plant effluent was pre-treated for increasing the concentration of organic microcontaminants (OMCs) in the NF retentate stream, together with reducing the total volume to be treated in the tertiary electro-oxidation system. Also noteworthy is the increase in water salinity achieved after the NF system in the retentate, decreasing ohmic resistance and thus facilitating a subsequent tertiary treatment based on electro-oxidation. For studying the behavior of the SPEF system in highly saline and complex matrices, a recipe of simulated NF concentrate was developed from the characterization of concentrates previously reported in literature. Aiming to work at the effluent natural pH, avoiding the addition of

reagents for acidification and neutralization, the use of ethylenediamine-N,N'-disuccinic acid (EDDS) as an iron complexing agent in the electro-Fenton (EF) process was evaluated. It was also checked the stability of $Fe^{3+}$:EDDS complex in the EF process, which was degraded after 15 min of treatment, although iron did not precipitate completely until 30 min. Thereupon, the degradation of four OMCs was studied: pentachlorophenol, terbutryn, chlorfenvinphos and diclofenac (at 200 and 500 μg $L^{-1}$ of initial concentration each); by AO, EF, SPEF and solar-assisted AO at natural pH, using $Fe^{3+}$:EDDS (1:2) at 0.1:0.2 mM in EF and SPEF treatments.

When using simulated NF retentate, whose chloride concentration was 555 mg $L^{-1}$, the highest degradation of OMCs (500 μg $L^{-1}$ of initial concentration each) was obtained using SPEF reaching 85% of total contaminants removal. The reason is that chlorine species generated by solar-assisted AO were not enough to degrade OMCs (75% of total amount), despite the presence of lower organic matter in solution due to the absence of EDDS. On the other hand, EF process was discarded since no improvement was observed with respect to AO, consuming the hydroxyl radicals produced by the Fenton reaction in the degradation of the EDDS instead of the OMCs.

The evaluation of the SPEF system for the tertiary treatment of actual wastewater, was carried out by collecting effluent from the secondary treatment of El Ejido WWTP (in Almería, South-East of Spain), after its pre-treatment in the NF pilot plant installed at PSA until reducing the initial volume 4 times. The salinity of the effluent increased from 2.1 - 2.3 mS $cm^{-1}$ to 6.1 - 6.8 mS $cm^{-1}$, and the chloride concentration reached 1182 - 1960 mg $L^{-1}$. The concentrate was spiked with the four target OMCs (100 μg $L^{-1}$ each) and their degradation was studied by AO, SPEF (with the carbonates naturally contained in the concentrate and reducing them to 20 mg $L^{-1}$ to diminish the scavenger effect on hydroxyl radicals) and solar-assisted AO. The percentages of degradation of the sum of OMCs after 180 minutes of each applied treatment were 84% (AO), 69% (SPEF with carbonates), 75% (SPEF with low carbonates) and 84% (solar-assisted AO), respectively. In this occasion, the highest percentage of degradation with the lowest electricity consumption, 5.3 kWh $m^{-3}$, was obtained by solar-assisted AO, since the higher concentration of chlorides promoted a higher generation of active chlorine species. Finally, tertiary treatment by applying solar-assisted AO was chosen for the degradation of 44 OMCs actually contained in the secondary effluent of the WWTP and detected by LC-QqLIT-MS/MS, resulting in the elimination of 80% of the sum. This work was performed in collaboration with Prof. Ana Agüera and Dr. Ana Martínez-Piernas from CIESOL (mixed center CIEMAT-UAL) at the University of Almería.

After the experimental program conducted in the electrochemical pilot plant, which began with its start-up and optimization of operation parameters, it was considered to study and diagnose the state of the cathode surface of the cells used in those tests. While cathode usage hours increased, onsite production of $H_2O_2$ decreased progressively from 43 mg $L^{-1}$ of accumulated $H_2O_2$ in 30 min, in the first use of the cathode, to 1.5 mg $L^{-1}$ after several experiments. At the moment an important reduction of the $H_2O_2$ electrogenerated was observed, making impossible the effective development of EF and SPEF processes, the cell was disassembled and the autopsy of the cathode surface was carried out by means of scanning electron microscopy and X-rays in order to try to identify the main reasons for the contamination of the cathode and the consequent loss of efficiency. In the images obtained, a loss of the carbon-PTFE coating was detected as well as the formation of iron deposits, justifying the drop in $H_2O_2$ electrogenerated with the loss of the electrode active surface.

In the framework of the Marie Curie - ALICE project "AcceLerate Innovation in urban wastewater management for Climate change", H2020- MSCA-RISE, the PhD candidate carried out a research internship at the Nanotechnology and Integrated Bioengineering Centre (NIBEC) of the University of Ulster (UK), in collaboration with the Photocatalysis Research Team lead by Prof. John Anthony Byrne. The goal of this collaboration was the development and application of a laboratory-scale photoelectrocatalytic reactor for the simultaneous elimination of OMCs and pathogenic microorganisms in natural water. As a core part of the reactor, two nanotube photo-anodes of titanium dioxide were manufactured by anodizing a titanium mesh at 30 V for 3 h and then annealing it at 500°C to promote the anatase phase. The reactor consists of a 190 mL cell with a double photo-anode of titanium dioxide nanotubes illuminated by a 9 W UV-A lamp through a quartz window, with an applied irradiation of 50 W $m^{-2}$. The main objective was the simultaneous removal of OMCs (terbutryn, chlorfenvinphos and diclofenac at 500 µg $L^{-1}$ of initial concentration each) and pathogens (*E. coli* as reference bacteria at an initial concentration of 106 CFU $mL^{-1}$), at the same time that a possible improvement by replacing a counter cathode with no contribution to the degradation process (platinum-coated titanium) by a carbon-felt cathode able to electrogenerate $H_2O_2$, was evaluated. Assessing separately the degradation of OMCs and the inactivation of *E. coli*, when applying the photoelectrocatalytic process with platinum cathode, a clear improvement in the inactivation of bacteria was observed (2 Log reduction after 120 minutes of treatment), compared to the photo-catalytic process on its own (0.8 Log reduction in the same treatment time). However, degradation of OMCs remained at the same ratio;

around 70% of the sum after 60 min. Replacement of the platinum cathode by a carbon-felt cathode increased the efficiency of *E. coli* inactivation, reducing its concentration in 2.7 Log, although OMCs showed similar degradation percentages. When finally the degradation of OMCs was carried out simultaneously to the inactivation of bacteria by photoelectrocatalysis with carbon cathode, a significant increase in disinfection was observed, reaching the detection limit of the method through a reduction of 4.5 Log. This improvement could be attributed to the presence of methanol from the stock solution where OMCs were pre-dissolved, that acts as a hole scavenger increasing the photocurrent and getting oxidized so generating formaldehyde, a highly toxic substance for microorganisms (LC50 for *E. coli* = 1 mg $L^{-1}$). As a consequence of this outcome, the effect of hole scavengers presence in disinfection was evaluated, using acetate and methanol at a concentration of 5 mM. In both cases, as described in literature, an increase in the photocurrent was observed under their presence, observing also an increase in the rate of bacteria inactivation, which was greater in the case of methanol due to the generation of formaldehyde.

Finally, as a result of the strong collaboration between the PhD student and the Solar Water Treatment Unit with the electrochemical company DeNora built during transnational access program within SFERA-II project, the evaluation of a commercial electro-oxidation system specially designed for the abatement of chemical oxygen demand in industrial waters and supported by the action of active chlorine spices was carried out. Within the framework of this collaboration, and as part of the objectives developed in this PhD Thesis, the evaluation of a pilot plant equipped with a dimensionally stable anode cell (DSA) manufactured by DeNora was performed, combining it with a solar CPC photo-reactor (3.08 $m^2$), reaching a total capacity of 38 L, and with the aim of evaluating the possible improvement in efficiency of two batches of landfill leachates. These leachates were characterized by high organic loads (>2000 mg $L^{-1}$ of dissolved organic carbon (DOC)) and a high toxicity in one of the batches (53 % of inhibition on activated sludge) so the main purpose was to reduce the toxicity and increase the biodegradability enough for a subsequent combination with a conventional biological treatment (thus reducing the associated operation costs). First step was the treatment of two batches by solar photo-Fenton process, which required an excessive accumulated UV energy (142.2 kJ $L^{-1}$) to achieve only a 30% reduction of DOC in the first batch of leachate (diluted 1:1 with distilled water). In the second batch it was not possible to perform solar photo-Fenton treatment due to the large amount of foams generated, causing large oscillations of the DOC along the process. Later on, the two batches were treated by electro-oxidation, electro-oxidation by adding $H_2O_2$ and electro-

oxidation combined with solar radiation, being the second batch the one that showed the highest DOC and total nitrogen removal rates, 3.5 g DOC $kWh^{-1}$ and 18 g TN $kWh^{-1}$ in the first batch of leachate and 13.4 g DOC $kWh^{-1}$ and 45.2 g TN $kWh^{-1}$ in the second batch. After the application of electro-oxidation assisted by solar energy, a reduction on toxicity from 53% to 6% of inhibition, and a sufficient improvement of biodegradability were observed in both batches. This study corroborates the improvement caused by the application of sunlight to the electrochemical treatment of industrial wastewater, which may represent a step forward towards the application of these powerful oxidation systems, presenting themselves as a feasible, sustainable and green alternative to purely electrochemical treatments, with lower operation costs due to lower energy consumption.

# 3. Resumen

## Resumen

El ritmo de vida impuesto por la sociedad actual conlleva un alto consumo de recursos naturales, muchos de ellos no renovables, por lo que una gestión inadecuada puede producir una escasez de estos a medio o largo plazo. El caso más evidente es el del agua, que se utiliza tanto para consumo humano, en agua de bebida, aseo y labores domésticas, como en procesos industriales, ya sea como refrigerante o como parte del propio proceso de producción. Hasta el año 2000, este recurso ha sido considerado por las autoridades legislativas como un bien comercial, pero a partir de la implantación de la Directiva Marco de Agua (2000/60/EC) pasó a ser considerado como un patrimonio a proteger, sentando las bases para el desarrollo de una normativa más específica que establece unos límites mínimos de calidad a alcanzar previo a la descarga de efluentes en el medio ambiente.

Específicamente la industria química ha sufrido un fuerte desarrollo por la creciente demanda de nuevos productos que satisfagan las necesidades de los consumidores. La fabricación de fármacos, productos para el cuidado personal, o plaguicidas y fertilizantes para mejorar la producción agrícola, ha dado lugar a la aparición de nuevas sustancias orgánicas. Estas suelen ser tóxicas, no biodegradables y altamente recalcitrantes por lo que no son fácilmente asimilables por los microorganismos, permaneciendo por largos periodos de tiempo en el medio ambiente sin conocer los efectos que pueden generar en el ecosistema.

Por este motivo surge la necesidad de desarrollar y aplicar nuevas tecnologías altamente oxidantes, capaces de reaccionar con estos compuestos degradándolos o mineralizándolos e incluso, dependiendo de su complejidad, mejorando la biodegradabilidad del efluente. Para ello, los procesos electroquímicos suponen una herramienta útil versátil y potente ya que únicamente aplicando una corriente o potencial eléctricos sobre unos electrodos se pueden generar especies altamente oxidantes que interaccionen con esos contaminantes facilitando su eliminación.

Algunos de estos procesos electroquímicos han sido ampliamente utilizados a escala industrial. Por ejemplo, la electrocoagulación supone una ventaja respecto al proceso físico-químico convencional de coagulación-floculación, ya que utiliza un electrodo de sacrificio evitando la adición de reactivos, se genera menos lodo y es más efectivo en la eliminación de coloides. La electrodiálisis, un proceso de membrana asistido eléctricamente, es capaz de separar los iones de un influente generando un efluente de alta calidad con muy baja carga iónica siendo principalmente aplicado en procesos de desalación para la obtención de agua potable.

Pese a presentar importantes ventajas como la facilidad para controlar el proceso y, por tanto su fácil automatización, así como la ausencia de reactivos externos, algunos procesos electro-oxidativos aún no han sido evaluados más que a escala de laboratorio, centrando la mayoría de los estudios recogidos en la literatura en el desarrollo de nuevos materiales para la fabricación de electrodos para la mejora de la efectividad y la reducción de costes asociados a dicha tecnología. Sin embargo, la electro-cloración ha sido el único tratamiento implementado a mayor escala debido al bajo coste de los electrodos.

La escasez de estudios aplicando estas tecnologías en situaciones reales, para la purificación de aguas residuales complejas, ha limitado, desde el punto de vista comercial, las posibilidades de los sistemas electro-oxidativos. Es importante mencionar que, a partir de los diferentes iones presentes de forma natural en determinadas aguas, se pueden generar gran cantidad y variedad de especies oxidantes, lo que conlleva una mejora intrínseca en la eficacia del proceso con respecto a una solución salina cuya única función es permitir el tránsito de electrones. Además, muchas de esas especies electro-generadas son fotoactivas, lo que supone que tan sólo con irradiar con luz ultravioleta la solución, se pueden generar especies aún más oxidantes incrementando la tasa de degradación de los contaminantes. Esto ha provocado que el desarrollo, implementación, puesta en marcha y evaluación de estos sistemas a mayor escala tampoco haya sido abordado en profundidad, lo que dificulta su escalado y aplicación industrial.

En este contexto surge la motivación de la presente Tesis Doctoral, que aborda la aplicación de procesos oxidativos a escala planta piloto en aguas reales, además de estudiar las condiciones de operación que lleven a un incremento en la degradación de contaminantes y depuración de aguas, combinando el sistema electro-oxidativo con una fuente de luz natural y renovable como es la energía solar.

El primer objetivo abordado fue la puesta en marcha, caracterización y optimización de los principales parámetros de operación de una planta piloto de foto-electro-Fenton solar (SPEF siglas en inglés) con un volumen máximo de 100 L instalada en la Plataforma Solar de Almería (CIEMAT). El sistema está constituido por cuatro celdas comerciales equipadas con un ánodo de diamante dopado con boro soportado en niobio y un cátodo de difusión de gas de carbono-politetrafluoroetileno (Electro MP-Cells suministradas por ElectroCell). Las celdas están conectadas en paralelo a un tanque de recirculación y éste a su vez a un foto-reactor solar basado en captadores cilindro parabólico compuestos (CPC) con 2 $m^{-2}$ de superficie iluminada. Se llevó a cabo la optimización de

las principales variables de entrada del proceso: el pH y la densidad de corriente (*j*), para maximizar la electro-generación in situ de $H_2O_2$ con la máxima eficiencia en el empleo de la corriente eléctrica (CE). Se definió un diseño experimental central compuesto, de forma que tras la consecución de una matriz de 19 experimentos y a partir del análisis estadístico de los resultados se obtuvo el modelo de ajuste para la concentración de $H_2O_2$ generada directamente en el reactor: $[H_2O_2] = 2.19 - 0.31 \cdot pH + 0.81 \cdot j - 0.05 \cdot pH \cdot j + 0.15 \cdot pH^2 - 2.42 \times 10^{-3} \cdot j^2$, y para la CE, $\%CE = 61.68 - 0.43 \cdot pH - 0.18 \cdot j - 0.0275 \cdot pH \cdot j$, así como los gráficos de superficie de respuesta asociados. Finalmente se validó el modelo, corroborando que a pH 3 y aplicando 73.66 mA $cm^{-2}$ se logra la mayor producción de $H_2O_2$, 64.9 mg $min^{-1}$ con una eficiencia de la corriente aplicada del 89.3%. Una vez establecidos estos parámetros se estudió la influencia del caudal de agua, de aire y la concentración de electrolito en la electro-generación in situ de $H_2O_2$, alcanzando el máximo con un caudal de agua de 5.6 L $min^{-1}$, de 10 L $min^{-1}$ de aire, y una concentración de $Na_2SO_4$ de 50 mM. Posteriormente, se realizaron ensayos preliminares para la evaluación de la eficacia de eliminación de compuestos de referencia, concretamente pirimetanil y metomilo en una concentración de 50 mg $L^{-1}$ y 90 mg $L^{-1}$, respectivamente, mediante los diferentes procesos de electro-oxidación que podían llevarse a cabo en la planta piloto empleando como electrolito una solución 50 mM de $Na_2SO_4$, desde oxidación anódica (AO, siglas en inglés) hasta electro-foto-Fenton solar (SPEF, siglas en inglés), obteniéndose las mayores tasas de degradación con este último: 55% y 50% de pirimetanil y metomilo, respectivamente, en 5 minutos de tratamiento. Este trabajo se realizó con la colaboración del Prof. Anastasios J. Karabelas y el Dr. Konstantinos V. Plakas del Instituto de procesos químicos y recursos energéticos del Centro para la Investigación y Tecnología-Hellas (Grecia) en el marco del proyecto europeo de capacitación SFERA-II.

El segundo objetivo de esta Tesis Doctoral se centró en abordar la aplicación del sistema experimental a escala planta piloto previamente optimizado a un caso real mediante su combinación con un pre-tratamiento con membranas de nanofiltración (NF) del efluente de una Estación Depuradora de Aguas Residuales (EDAR). De esta manera se buscó aumentar la concentración de microcontaminantes orgánicos (OMCs, siglas en inglés) en la corriente de concentrado a la salida de la NF, a la vez que reducir el volumen total a tratar en el sistema terciario de electro-oxidación. Cabe destacar además el aumento en la salinidad del agua que se logra tras el sistema de NF en la corriente de concentrado, disminuyendo la resistencia óhmica y favoreciendo, por tanto, el tratamiento terciario posterior basado en electro-oxidación. Para estudiar el comportamiento del sistema de SPEF en matrices altamente salinas y complejas, se

desarrolló una receta de simulado de concentrado de NF a partir de la caracterización de concentrados previamente reportados en la literatura. Con el fin de trabajar al pH natural del agua, evitando la adición de reactivos para acidificar y volver a neutralizar, se evaluó el uso de ácido etilenediamina-N,N'-disuccínico (EDDS) como quelante del hierro en el proceso electro-Fenton (EF). A continuación, se estudió la degradación de cuatro OMCs: pentaclorofenol, terbutrina, clorfenvinfos y diclofenaco (a 200 y 500 µg $L^{-1}$ de concentración inicial cada uno); mediante AO, EF, SPEF y AO asistida por luz solar a pH natural, usando $Fe^{3+}$:EDDS (1:2) a una concentración 0.1:0.2 mM en los tratamientos EF y SPEF.

Cuando se empleó como matriz el agua simulada de concentrado de NF, con una concentración de cloruros de 555 mg $L^{-1}$, el mayor porcentaje de degradación de los OMCs (500 µg$L^{-1}$ de concentración inicial cada uno), se obtuvo mediante SPEF, alcanzando el 85% de eliminación del total. Esto se debe a que las especies oxidantes del cloro generadas mediante AO asistida por luz solar no fueron suficientes para degradar los OMCs (75% del total), pese a la presencia de menor materia orgánica en disolución debido a la ausencia de EDDS. Por otro lado, el proceso EF fue descartado ya que no se observó mejora con respecto a AO, consumiendo los radicales hidroxilo generados por la reacción Fenton en la degradación del EDDS.

Para la evaluación de este sistema de electro-oxidación en agua real, se recolectó efluente del tratamiento secundario de la EDAR de El Ejido y se pre-trató en el sistema piloto de NF disponible en la Plataforma Solar de Almería, hasta reducir el volumen inicial 4 veces (factor de concentración de 4). La salinidad del agua se incrementó de 2.1 - 2.3 mS $cm^{-1}$ a 6.1 - 6.8 mS $cm^{-1}$, con una concentración de cloruros final entre 1182 – 1960 mg $L^{-1}$. El concentrado generado fue fortificado con los cuatro OMCs evaluados en el trabajo previo con agua simulada (100 µg $L^{-1}$ de cada uno) y se estudió su degradación mediante AO, SPEF (con los carbonatos naturalmente contenidos en el concentrado y reduciéndolos a 20 mg $L^{-1}$ para disminuir la interacción con los radicales hidroxilo) y AO asistida por luz solar. Los porcentajes de degradación de la suma total de OMCs tras 180 minutos de tratamiento fueron 84%, 69%, 75% y 84%, respectivamente. En esta ocasión, el mayor porcentaje de degradación con el menor consumo eléctrico, 5.3 kWh $m^{-3}$, se obtuvo mediante AO asistida por luz solar, ya que la mayor concentración de cloruros promovió una mayor generación de especies activas del cloro. Finalmente, se escogió el tratamiento terciario mediante AO asistida por luz solar para la degradación de 44 OMCs realmente contenidos en el efluente secundario de la EDAR y detectados mediante LC-QqLIT-MS/MS, consiguiendo eliminar el 80% del

total. Este trabajo se llevó a cabo en colaboración con la Prof. Ana Agüera y la Dra. Ana Martínez-Piernas del CIESOL (centro mixto CIEMAT-UAL) en la Universidad de Almería.

Tras el programa experimental realizado en la planta piloto de electro-oxidación iniciando con su puesta en marcha y optimización de parámetros de operación, se consideró estudiar y diagnosticar el estado de la superficie de los cátodos de las celdas empleadas en dichos ensayos. A medida que las horas de uso del cátodo se incrementaron, la producción in situ de $H_2O_2$ sufrió un progresivo descenso, desde 43 mg $L^{-1}$ de $H_2O_2$ acumulado en 30 min, en el primer uso del cátodo, a 1.5 mg $L^{-1}$ en el peor de los casos. En el momento en el que se observó una importante reducción de la electrogeneración de $H_2O_2$ que imposibilitaba el correcto desarrollo de los procesos EF y SPEF, se procedió al des ensamblaje de la celda y se realizó la autopsia de la superficie del cátodo mediante microscopía electrónica de barrido y rayos X, con objeto de intentar discernir los motivos principales del ensuciamiento del mismo y la consiguiente pérdida de eficiencia. En las imágenes obtenidas se observó una pérdida del recubrimiento de carbono-politetrafluoroetileno además de la formación de depósitos de hierro, justificando la caída en electrogeneración de $H_2O_2$ con la pérdida de superficie activa del electrodo.

Como parte de las actividades recogidas en el proyecto Marie Curie - ALICE “AcceLerate Innovation in urban wastewater management for Climate changE”, H2020- MSCA-RISE, la doctoranda realizó una estancia de investigación en el Centro de Nanotecnología y Bioingeniería Integrada (NIBEC) de la Universidad de Ulster (Reino Unido), en colaboración con el grupo de Investigación en Fotocatálisis liderado por el Prof. John Anthony Byrne. El objetivo de dicha colaboración fue el desarrollo y aplicación de un reactor foto-electro-catalítico a escala de laboratorio, para la eliminación simultánea de OMCs y microorganismos patógenos en agua natural. Como parte fundamental del reactor, se fabricaron dos foto-ánodos de nanotubos de dióxido de titanio mediante la anodización de una malla de titanio a 30V durante 3h y su posterior recocido a 500°C para promover la fase anatasa. El reactor consiste en una celda de 190 mL con un doble foto-ánodo de nanotubos de dióxido de titanio iluminados por una lámpara ultravioleta de 9 W a través de una ventana de cuarzo, con una irradiación aplicada de 50 W $m^{-2}$. El objetivo del tratamiento fue la eliminación simultánea de OMCs (terbutrina, clorfenvinfos y diclofenaco a 500 µg $L^{-1}$ de concentración inicial cada uno) y patógenos (*E. coli* como bacteria de referencia en una concentración inicial de $10^6$ UFC $mL^{-1}$), evaluando además la posible mejora al sustituir un cátodo sin contribución en el proceso de degradación, titanio recubierto de platino, por uno de fieltro de carbono capaz de electrogenerar $H_2O_2$. Evaluando por separado la degradación de los OMCs e

inactivación de *E. coli*, en la aplicación del proceso foto-electro-catalítico con cátodo de platino se observa una clara mejora en la inactivación de la bacteria (2 Log de reducción tras 120 minutos de tratamiento), con respecto al proceso foto-catalítico sólo (0.8 Log de reducción en el mismo tiempo de tratamiento). Sin embargo, la degradación de OMCs se mantuvo en el mismo ratio, en torno al 70% del total tras 60 min. Al sustituir el cátodo de platino por uno de fieltro de carbono se incrementó la eficacia en la inactivación de *E. coli*, reduciendo su concentración en 2.7 Log, aunque los OMCs mostraron porcentajes de degradación similares. Cuando finalmente se llevó a cabo la degradación de OMCs de forma simultánea a la inactivación de bacterias mediante foto-electro-catálisis con cátodo de carbono, se observó un aumento significativo en la desinfección, alcanzando el límite de detección del método con una reducción de 4.5 Log. Esta mejora se debe a la presencia de metanol procedente de la solución en la que van pre-disueltos los OMCs, que actúa como neutralizador de huecos aumentando la fotocorriente y que además se oxida generando formaldehido, una sustancia altamente tóxica para los microorganismos ($LC_{50}$ for *E. coli* = 1 mg $L^{-1}$). Como consecuencia de este resultado, se evaluó el efecto de la presencia de sustancias neutralizadoras de huecos en la desinfección, utilizando para ello acetato y metanol en una concentración de 5 mM. En ambos casos, como está descrito en la literatura, se observó un aumento en la fotocorriente respecto a la alcanzada por el sistema en ausencia de ellos y, por lo tanto, se produjo un incremento en la tasa de inactivación de la bacteria siendo mayor en el caso del metanol por la generación de formaldehido.

Finalmente, y como resultado de la estrecha colaboración de la doctoranda y la Unidad de Tratamientos Solares del Agua en el proyecto SFERA-II con la empresa DeNora, se llevó a cabo la evaluación de un sistema comercial de electro-oxidación especialmente diseñado para la reducción de demanda química de oxígeno en aguas industriales y basado en la acción de las especias activas del cloro. En el marco de esta colaboración, y como parte de los objetivos desarrollados en esta Tesis Doctoral, se llevó a cabo la evaluación de una planta piloto equipada con una celda de ánodos dimensionalmente estables (DSA, siglas en inglés) procedente de DeNora, combinándola con un reactor solar CPC, con una capacidad total de 38 L y con el objetivo de evaluar la posible mejora en la eficiencia del tratamiento de lixiviados de vertedero. Dichos lixiviados presentaban una alta carga orgánica (>2000 mg $L^{-1}$ de carbono orgánico disuelto (DOC)), siendo el objetivo del tratamiento disminuir su toxicidad e incrementar su biodegradabilidad para poder combinar finalmente con un posterior tratamiento biológico (logrando así reducir los costes de operación asociados). En primer lugar se llevó a cabo el tratamiento de los dos lotes de concentrado de lixiviados mediante foto-Fenton solar, observando una

necesidad de energía UV acumulada excesiva (142.2 kJ $L^{-1}$) para lograr sólo un 30% de reducción del carbono orgánico disuelto (DOC, siglas en inglés) en el primer lote de lixiviados (diluido 1:1 con agua destilada). En el segundo lote no fue posible llevar a cabo el tratamiento de foto-Fenton solar a causa de la gran cantidad de espumas generada, que provocó grandes oscilaciones del DOC imposibilitando su seguimiento. Posteriormente se trataron los lixiviados mediante electro-oxidación, electro-oxidación añadiendo $H_2O_2$ y electro-oxidación combinada con radiación solar, siendo este último el que mayores tasas de degradación de DOC y de nitrógeno total mostró, 3.5 g DOC $kWh^{-1}$ y 18 g TN $kWh^{-1}$ en el primer lote de lixiviado tratado y 13.4 g DOC $kWh^{-1}$ y 45.2 g TN $kWh^{-1}$ en el segundo lote. Con este tratamiento, el primer lote de lixiviados, que presentaba una toxicidad del 53% de inhibición en la tasa de consumo de oxígeno por parte de fangos activos de EDAR, disminuyó su toxicidad al 6% de inhibición, y en ambos lotes estudiados se incrementó su biodegradabilidad hasta valores adecuados para la posterior aplicación de un tratamiento biológico. Gracias a este estudio se corrobora la mejora que supone la aplicación de la luz solar a los tratamientos electroquímicos de aguas industriales, lo que puede significar un paso adelante hacia la aplicación de estos sistemas altamente oxidantes presentándose como alternativa viable, sostenible y verde, a los tratamientos puramente electroquímicos, suponiendo unos costes de explotación menores debido al menor consumo energético.

# 4. Publications

Applied Catalysis B: Environmental 242 (2019) 327–336

Contents lists available at ScienceDirect

Applied Catalysis B: Environmental

journal homepage: www.elsevier.com/locate/apcatb

# Optimization of electrocatalytic $H_2O_2$ production at pilot plant scale for solar-assisted water treatment

Irene Salmerón[a,b], Konstantinos V. Plakas[c], Ignasi Sirés[d], Isabel Oller[a,b,*], Manuel I. Maldonado[a,b], Anastasios J. Karabelas[c], Sixto Malato[a,b]

[a] Plataforma Solar de Almería-CIEMAT, Ctra Senés km 4, 04200, Tabernas, Almería, Spain
[b] CIESOL, Joint Centre of the University of Almería-CIEMAT, 04120, Almería, Spain
[c] Chemical Process and Energy Resources Institute, Centre for Research and Technology – Hellas (CERTH), 6th Km Charilaou-Thermi Road, Thermi, Thessaloniki, GR 57001, Greece
[d] Laboratori d'Electroquímica dels Materials i del Medi Ambient, Departament de Química Física, Facultat de Química, Universitat de Barcelona, Martí i Franquès 1-11, 08028, Barcelona, Spain

ARTICLE INFO

*Keywords:*
Boron-doped diamond
Gas-diffusion electrode
Hydrogen peroxide electrogeneration
Solar photoelectro-Fenton
Wastewater treatment

ABSTRACT

This manuscript summarizes the successful start-up and operation of a hybrid eco-engineered water treatment system, at pilot scale. The pilot unit, with 100 L capacity, has been devised for the efficient electrocatalytic production of $H_2O_2$ at an air-diffusion cathode, triggering the formation of $^{\cdot}OH$ from Fenton's reaction with added $Fe^{2+}$ catalyst. These radicals, in combination with those formed at a powerful boron-doped diamond (BDD) anode in an undivided cell, are used to degrade a mixture of model pesticides. The capability of the plant to produce $H_2O_2$ on site was initially optimized using an experimental design based on central composite design (CCD) coupled with response surface methodology (RSM). This aimed to evaluate the effect of key process parameters like current density ($j$) and solution pH. The influence of electrolyte concentration as well as liquid and air flow rates on $H_2O_2$ electrogeneration and current efficiency at optimized $j$ and pH was also assessed. The best operation conditions resulted in $H_2O_2$ mass production rate of 64.9 mg $min^{-1}$, 89.3% of current efficiency and 0.4 kWh $m^{-3}$ of energy consumption at short electrolysis time. Performance tests at optimum conditions were carried out with 75 L of a mixture of pesticides (pyrimethanil and methomyl) as a first step towards the elimination of organic contaminants by solar photoelectro-Fenton (SPEF) process. The combined action of homogeneous ($^{\cdot}OH$) and heterogeneous (BDD($^{\cdot}OH$)) catalysis along with photocatalysis (UV photons collected at a solar CPC photoreactor) allowed the removal of more than 50% of both pesticides in 5 min, confirming the fast regeneration of $Fe^{2+}$ catalyst through cathodic reduction and photo-Fenton reaction.

## 1. Introduction

The extraordinary development of chemicals manufacturing and their widespread use in all human activities is intimately associated with contamination of aquatic environment. Water quality monitoring programs underline the seriousness of the problem worldwide and highlight the potential hazards posed by mixtures of synthetic organic contaminants (SOCs) and their metabolites in surface water and groundwater [1–4]. Typically, SOCs include solvents, preservatives, pharmaceuticals and personal care products, lubricants, dyes or active substances for plant protection [5]. Among the latter, methomyl (MET) and pyrimethanil (PYR) are ubiquitous in intensive agriculture, which is worrisome since they are classified as persistent organic pollutants (POPs) [6] and are considered extremely toxic [7,8]. This issue has prompted the application of advanced oxidation processes (AOPs) for the fast and complete removal of SOCs from polluted water streams [9], based on the in situ production of hydroxyl radical ($^{\cdot}OH$) as main reactive oxygen species (ROS).

Fenton's reaction between ferrous ions ($Fe^{2+}$) and hydrogen peroxide ($H_2O_2$), so-called Fenton's reagent, is the most popular source of $^{\cdot}OH$ for practical applications [10]. As an upgraded approach, the electro-Fenton (EF) process allows overcoming two key limitations of the conventional chemical method [11–13]: (i) it ensures the continuous regeneration of $Fe^{2+}$ through cathodic reduction of $Fe^{3+}$, thus requiring a much lower amount of catalyst to perform the treatment, and (ii) it avoids the handling, storage and transportation of $H_2O_2$ produced industrially, since this reagent can be electrosynthesized on site through Reaction (1) by using appropriate cathode materials.

* Corresponding author.
*E-mail address:* isabel.oller@psa.es (I. Oller).

https://doi.org/10.1016/j.apcatb.2018.09.045
Received 12 June 2018; Received in revised form 11 September 2018; Accepted 15 September 2018
Available online 29 September 2018
0926-3373/ 

$$O_{2(g)} + 2H^+ + 2e^- \rightarrow H_2O_2 \quad (1)$$

Electrocatalytic $H_2O_2$ generation is becoming a hot topic because the combination of electrochemistry with new catalysts enables a more eco-friendly and less energy-intensive production of this commodity [14,15]. Several prospective electrocatalysts have been developed, with noble metals and metal alloys like Pd-Au, Pt-Hg and Pt/Pd-Hg as particularly prominent options [14,16,17]. Non-precious Co-based particles are very active promoters of Reaction (1) as well, at smaller cost [18]. Unfortunately, none of these catalysts is viable for large-scale water treatment due to their high cost and toxicity, which has fostered the investigation on inexpensive carbonaceous materials [14,19,20]. Unmodified carbon-based catalysts exhibit appealing characteristics as cathodes, such as non-toxicity and high stability, conductivity and durability. $H_2O_2$ production with such inexpensive materials is particularly interesting for developing small- or medium-size decentralized units where the chemical is generated on demand [21]. This can be achieved using graphite felt, reticulated vitreous carbon, activated carbon fiber or carbon nanotubes as cathode, completely immersed into the solution to generate $H_2O_2$ from dissolved $O_2$ [22–24]. However, much greater $H_2O_2$ concentrations are attained upon implementation of an air-chamber in the electrochemical reactor, since it allows continuous air-feeding through a hydrophobized carbon-based gas-diffusion electrode (GDE) [15,18,25–28]. Worth noting, the vast majority of studies on Fenton-based electrochemical AOPs (EAOPs) reporting data on $H_2O_2$ production at GDE have been carried out either at laboratory scale or in small pre-pilot plants of 2.5 L [29] and 5 L [30,31]. Only one work reported the use of a bigger plant with 25 L capacity, but it was mainly focused on aniline degradation [32].

Undivided electrochemical cells are preferred to perform all these studies on water treatment because the use of a separator would increase the cell voltage and hence, the energy consumption. In addition, in such cells, the combination of carbonaceous cathodes with electrocatalytic materials that promote the anodic production of heterogeneous hydroxyl radical enhances the performance of EF process. Boron-doped diamond (BDD) thin film on Si substrate is the best anode to oxidize $H_2O$ to physisorbed $^{\cdot}OH$ via Reaction (2) [11,13,33], owing to its large overpotential for $O_2$ evolution. However, Ti and Nb substrates are more suitable for plant-scale applications due to their much higher mechanical and chemical resistance.

$$BDD + H_2O \rightarrow BDD(^{\cdot}OH) + H^+ + e^- \quad (2)$$

The best performance among Fenton-based EAOPs for SOCs degradation is attained upon continuous irradiation of the treated solution with UV/Vis light. This is feasible employing a UVA lamp in photoelectro-Fenton (PEF) process [11,13], since it promotes: (i) a high regeneration rate of $Fe^{2+}$, with concomitant production of homogeneous $^{\cdot}OH$, from photoreduction of the main Fe(III) species at pH ~ 3.0 (Reaction (3)), (ii) the photodegradation of Fe(III)-carboxylate complexes formed as intermediates (Reaction (4)), and (iii) the direct photolysis of some pollutants and/or their oxidation by-products [11,34].

$$[Fe(OH)]^{2+} + h\nu \rightarrow Fe^{2+} + {}^{\cdot}OH \quad (3)$$

$$[Fe(OOCR)]^{2+} + h\nu \rightarrow Fe^{2+} + CO_2 + R^{\cdot} \quad (4)$$

In order to achieve the synergy between electrocatalytic and photolytic reactions at an affordable cost, UVA lamps have been lately replaced by direct sunlight irradiation, yielding the promising solar PEF (SPEF) process. Its great oxidation capability arises from: (i) the higher UV photon flux from sun if the solar collector design is adapted to the photoreactor, which upgrades the $^{\cdot}OH$ production, along with (ii) the additional illumination within the visible range ($\lambda > 400$ nm), promoting Reaction (3) (also active in the visible range) and accelerating the photolysis of refractory Fe(III)-carboxylate complexes (Reaction (4)) [34]. Very good degradation results by SPEF with GDE were obtained using a recirculation small pilot plant of 2.5-L capacity equipped with a flat-plate photoreactor [35–37], also employed to treat pesticides like mecoprop [35], diuron [38] or tebuthiuron and ametryn [39]. Replacement by a more efficient photoreactor based on compound parabolic collectors (CPC) could increase the efficiency of SPEF due to the greater photon flux supply to the solution. At present, CPC is the most popular photoreactor, as confirmed by its integration in most of the SPEF units for treating 2.2 L [40], 6 L [41], 8 L [42] and up to 10 L [43–48], which is the largest volume investigated so far.

Based on the excellent performance of SPEF at limited scale, a larger pilot plant has been developed for the treatment of SOCs by EAOPs with $H_2O_2$ electrogeneration. The system, with capacity to treat up to 100 L, consists of four undivided Nb-BDD/GDE filter-press cells coupled with a solar CPC, and has been installed and tested at Plataforma Solar de Almería (PSA), the largest European facility to test solar technologies. As a first step toward the treatment of real wastewater, this work is focused on the optimization of pilot plant main operation variables for the electrocatalytic $H_2O_2$ production, including current density ($j$), solution pH, liquid flow rate, air flow rate and electrolyte concentration. This was made with the aid of central composite design (CCD) coupled to response surface methodology (RSM). The plant was further validated by performing degradation trials under optimum conditions using a mixture of fungicide PYR and insecticide MET spiked into conductive water at high concentrations to simulate real agricultural wastewater. Note that these pesticides have only been studied before by AOPs like solar $TiO_2$ photocatalysis and solar photo-Fenton at pilot scale [6] and EF at lab scale [8].

## 2. Materials and methods

### 2.1. Chemicals

Heptahydrated ferrous sulfate (Sigma-Aldrich) used as catalyst and anhydrous sodium sulfate (Fluka) employed as background electrolyte were of analytical grade. PYR (IQV, AgroEvo, 98% purity) and MET (Aragonesas Agro, 99.5% purity) were of reagent grade and used without further purification. Mixtures of the two pesticides were prepared with deionized water (conductivity < 10 μS $cm^{-1}$, dissolved organic carbon (DOC) < 0.5 mg $L^{-1}$) and the electrolyte, and their pH was adjusted with analytical grade sulfuric acid (J.T. Baker). Organic solvents and other chemicals employed for HPLC analysis of the pesticides were of analytical grade from Sigma-Aldrich.

### 2.2. Pilot plant

Images of the filter-press type electrochemical cells and the CPC photoreactor, along with a schematic diagram of the pilot plant, are shown in Fig. 1. The plant consisted of four plate-and-frame electrochemical reactors (Electro MP-Cells from ElectroCell) coupled to a purpose-made solar CPC. Each cell contained an anode made of BDD thin film deposited on a niobium mesh (Nb-BDD) and a carbon-polytetrafluoroethylene (PTFE) GDE as the cathode, both with 0.01 $m^2$ effective area. The CPC photoreactor had a total illuminated area of 2 $m^2$, corresponding to an irradiated volume of 23 L. It was comprised of 10 borosilicate glass tubes (150 cm length × 4.5 cm inner diameter) mounted in an aluminum frame on a platform tilted 37° (PSA, 37 °N, 2.4 °W). The working volume was 25 L to carry out the optimization of $H_2O_2$ electrogeneration, and 75 L to perform the degradation experiments. The unit was equipped with two magnetic drive pumps (PAN World, 0.75 kW), one for pumping the solution from the feed tank (maximum capacity of 100 L) to the electrochemical cells, and the other for the liquid recirculation to and from the CPC. The GDE was fed with compressed air (ABAC air compressor, 1.5 kW) at a pressure and flow rate regulated with a back-pressure gauge and a flowmeter, respectively, in order to avoid the flooding of the air chamber. The experiments were made at constant $j$ using a Delta Electronika power supply (limited to 70 V and 22 A).

Global ultraviolet solar radiation ($UV_G$) was measured using a radiometer (Kipp & Zonen, model CUV 3) mounted on a platform tilted 37°, the

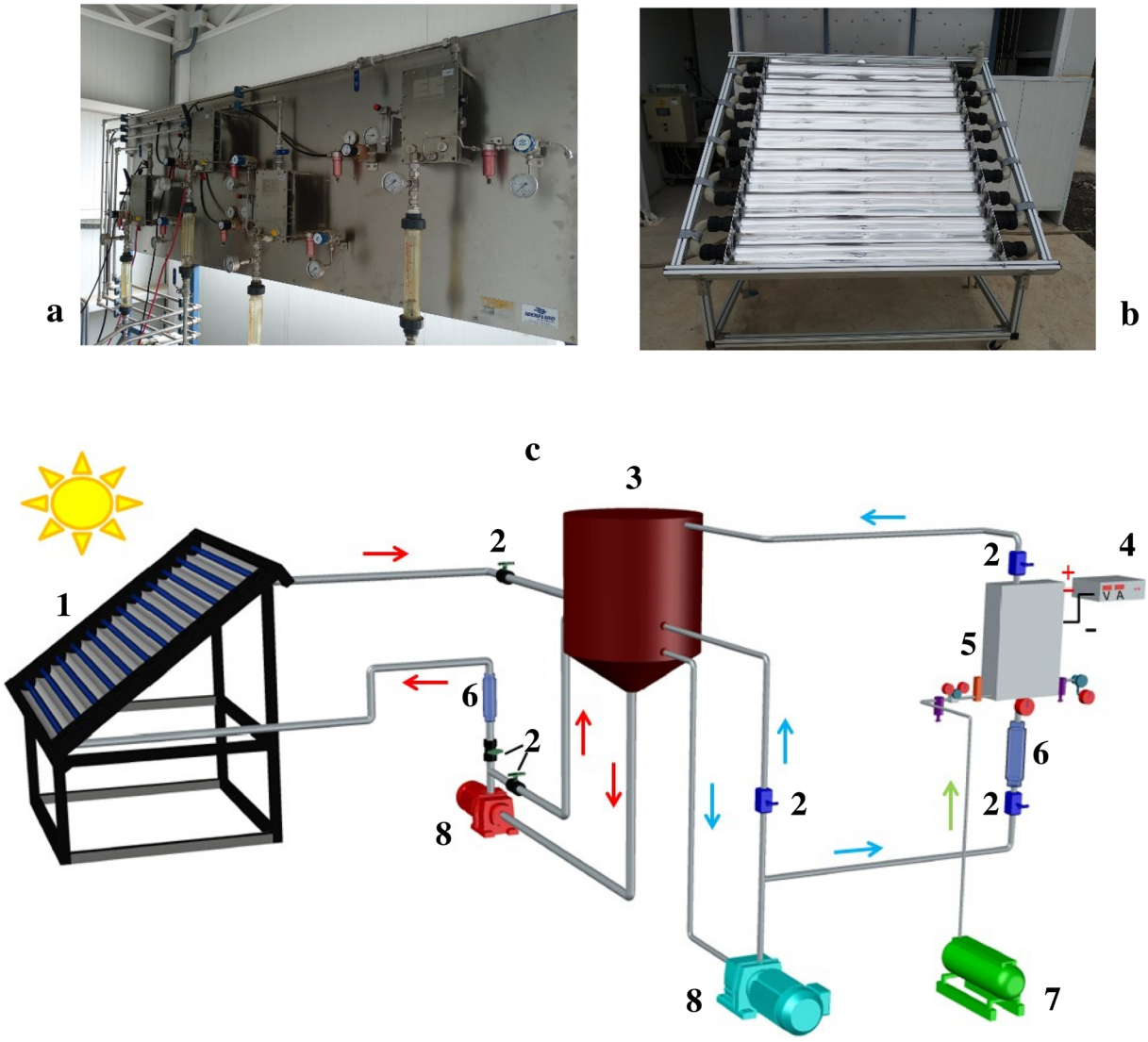


**Fig. 1.** Front view of (a) the four filter-press type electrochemical cells of the pilot unit, and (b) the CPC photoreactor. In (c), schematic diagram of the pilot unit equipped with one cell (examined in this work), showing: (1) CPC photoreactor, (2) valve, (3) feed tank, (4) power supply, (5) electrochemical reactor, (6) liquid flowmeter, (7) air compressor, (8) magnetic pump.

same angle as the photoreactor, which provided data in terms of incident irradiance ($W_{UV}\,m^{-2}$). This informs about the energy reaching any surface in the same position with regard to the sun. Eq. (5) allows combining the data from trials performed in different days, thus enabling comparison with results obtained in other photocatalytic experiments [49].

$$Q_{UV,n} = Q_{UV,n-1} + \Delta t_n \bullet \bar{UV}_{G,n} \bullet A_r \bullet V_T \quad (5)$$

where $Q_{UV}$ is the accumulated UV energy per unit of volume ($kJ\,L^{-1}$), $\bar{UV}_{G,n}$ (in $W\,m^{-2}$) is the average UV radiation measured during $\Delta t_n$ ($= t_n - t_{n-1}$), $A_r$ is the irradiated surface area ($2\,m^2$) and $V_T$ is the total volume treated in the pilot plant.

### 2.3. Experimental design

Experimental design by RSM was employed to optimize the in situ electrogeneration of $H_2O_2$. Trials were performed with one of the four identical electrochemical cells of the pilot, assuming that the resulting optimum conditions would be also valid for the other three cells. Two optimization criteria were considered: (a) maximization of the concentration of the produced $H_2O_2$, and (b) maximization of the current efficiency (CE, in percentage), defined as the ratio between the electricity consumed by the electrode reaction of interest and the total electricity supplied. CE can be calculated via Eq. (6), where *n* represents the stoichiometric number of electrons transferred in Reaction (1), F is the Faraday constant ($96{,}487\ C\ mol^{-1}$), $[H_2O_2]$ the concentration of $H_2O_2$ accumulated in bulk solution ($mg\ L^{-1}$), $V_T$ the volume of the treated solution (L), $M(H_2O_2)$ the molecular weight of $H_2O_2$ ($34\,g\,mol^{-1}$), and Q the charge consumed during the electrolysis (C).

$$\%\,CE = \frac{nF\,[H_2O_2]V_T}{1000\,M(H_2O_2)Q} \times 100 \quad (6)$$

RSM was first used to assess the relationship between response ($H_2O_2$ concentration or % CE) and two independent variables, namely the solution pH (factor A) and *j* (factor B), as well as to optimize the relevant conditions in order to predict the best value of responses. CCD, the most widely used approach of RSM and, more specifically, a face centered composite (FCC) design, was employed to determine the effect of the two variables. Design Expert® v.7.0.0 software (Stat-Ease Inc., USA) was used. Three levels between -1 and +1 were established for the two independent variables (Table 1). Ranges were chosen based on preliminary experiments (data not shown here), background knowledge, and some constraints arising from the cathodic $H_2O_2$ electrogeneration and the nature of the electrode materials. For example, the production of $H_2O_2$ is favored at acidic pH (Reaction (2)), whereas the use of GDE and BDD

**Table 1**
Experimental range and levels of independent variables.

| Variable | Factor | Units | Level and Range | | |
|---|---|---|---|---|---|
| | | | Low (-1) | Central (0) | High (+1) |
| pH | A | – | 3 | 5 | 7 |
| $j$ | B | mA cm$^{-2}$ | 30 | 65 | 100 |

anode limits the operation cell voltage to less than 25 V to prevent surface damage, which would cause the loss of electrocatalytic properties, and keep a reasonable CE [50]. This means that maximum current that can be applied is 10 A ($j$ = 100 mA cm$^{-2}$).

For the CCD, a $2^3$ full factorial design with 3 replicates at the center point (resulting in 19 experiments) was used to determine the optimum values of independent variables. These experiments were carried out by recirculating synthetic solutions of 50 mM $Na_2SO_4$ at a liquid flow rate of 4.4 L min$^{-1}$, and they were randomly performed to minimize the effect of systematic errors. Analysis of variance (ANOVA) of the data was performed to identify significant values (p-value < 0.05). The quality of the fit of polynomial model was expressed by the value of correlation coefficient ($R^2$). The main indicators demonstrating the significance and adequacy of the used model include the model F-value (Fisher variation ratio), probability value (Prob > F), and adequate precision. The optimal region of the independent variables was determined by plotting three-dimensional response surfaces of the independent and dependent variables. Additionally, numerical optimization of the independent variables was carried out using the same software.

A second set of experiments was carried out aiming to assess the effect of electrolyte concentration as well as liquid and air flow rates, under the optimum pH and $j$ conditions. The best operation conditions were finally applied to degrade mixtures of pesticides, in the absence or presence of iron catalyst. In SPEF, the pesticide solution was irradiated when circulating through the CPC photoreactor.

### 2.4. Instruments and analytical methods

The concentration of $H_2O_2$ accumulated during the electrolysis was determined by adding Ti(IV) oxysulfate to the sample and measuring the absorbance at 410 nm, according to DIN 38,409 H15. Iron concentration was measured by using 1,10-phenanthroline, following ISO 6332. In both cases, a Unicam UV/Vis UV2 spectrophotometer was employed. Dissolved organic carbon (DOC) was measured after sample filtration through a 0.22 μm Nylon filter, on a Shimadzu TOC-VCSN analyzer. The degradation rate of the two pesticides was monitored on a UPLC/UV Agilent Technologies Series 1200, equipped with a C-18 ZORBAX XDB C-18 analytical column. The column was kept at 30 °C and the injection volume was 50 μL. A linear gradient profile with water and acetonitrile (ACN) eluted at a flow rate of 1 mL min$^{-1}$ was established as follows: 0–4 min, isocratic at 85/15 (v/v) $H_2O$/ACN; 4–8 min, gradient from 85/15 to 20/80 (v/v); 8–15 min, isocratic at 85/15 (v/v). Re-equilibration time was 3 min. The UV signals for MET and PYR were monitored at the wavelength of their maximum absorption, 230 nm and 270 nm, respectively. For UPLC analyses, 9 mL of sample were filtered through a 0.22 μm PTFE syringe filter. Then, it was washed with 1 mL of UPLC grade ACN to extract any compound adsorbed on the filter. The pH of the treated solution was monitored by means of a Crison 25 pH-meter.

## 3. Results and discussion

### 3.1. Influence of independent experimental variables on the in situ $H_2O_2$ electrogeneration

The results obtained from the experimental design matrix including the two independent variables (pH, $j$) are shown in Table 2. The

**Table 2**
Design of experiments and results.

| Run | Independent variables | | Responses ($t$ = 5 min) | | Responses ($t$ = 30 min) | |
|---|---|---|---|---|---|---|
| | pH | $j$ (mA cm$^{-2}$) | [$H_2O_2$] (mg L$^{-1}$) | % CE | [$H_2O_2$] (mg L$^{-1}$) | % CE |
| 1 | 3 | 100 | 15.11 | 71.40 | 48.12 | 37.90 |
| 2 | 7 | 30 | 4.97 | 78.30 | 18.06 | 47.05 |
| 3 | 5 | 65 | 10.41 | 75.70 | 34.85 | 42.30 |
| 4 | 7 | 100 | 8.88 | 42.00 | 31.55 | 24.90 |
| 5 | 3 | 30 | 5.93 | 93.40 | 19.67 | 51.70 |
| 6 | 3 | 100 | 13.41 | 63.40 | 45.25 | 35.70 |
| 7 | 5 | 65 | 9.23 | 67.20 | 31.42 | 38.10 |
| 8 | 5 | 100 | 9.71 | 45.90 | 34.25 | 27.00 |
| 9 | 3 | 65 | 8.93 | 65.00 | 33.59 | 40.70 |
| 10 | 7 | 100 | 8.45 | 40.00 | 30.16 | 23.80 |
| 11 | 5 | 100 | 8.36 | 39.60 | 29.90 | 23.60 |
| 12 | 5 | 30 | 6.23 | 98.20 | 21.15 | 55.60 |
| 13 | 5 | 65 | 8.67 | 63.10 | 30.55 | 37.00 |
| 14 | 5 | 30 | 5.49 | 86.60 | 19.80 | 52.00 |
| 15 | 3 | 30 | 5.75 | 90.70 | 19.85 | 52.20 |
| 16 | 7 | 65 | 7.71 | 56.10 | 27.85 | 33.80 |
| 17 | 3 | 65 | 9.67 | 70.30 | 33.38 | 40.50 |
| 18 | 7 | 65 | 6.58 | 47.90 | 24.54 | 29.80 |
| 19 | 7 | 30 | 4.84 | 76.30 | 17.89 | 47.00 |

responses ($H_2O_2$ concentration and % CE) are presented at two electrolysis times, 5 and 30 min, corresponding to approximately one and five circulations of the initial feed solution volume (25 L) through the electrochemical cell, respectively. The average values of the two responses at 30 min are illustrated in Fig. 2a, whereas the changes in $H_2O_2$ mass production rate over the electrolysis time are depicted at constant pH = 3.0 (Fig. 2b) or $j$ = 100 mA cm$^{-2}$ (Fig. 2c).

As expected, a higher accumulation of $H_2O_2$ was found as the electrolyses were prolonged, although this occurred in concomitance with current efficiency decrease (Table 2). This is also confirmed from the profiles of the $H_2O_2$ production rates with time, since the highest values were attained at the beginning of the electrolyses until quasi-steady values were observed at longer times, regardless of the $j$ (Fig. 2b) or the pH (Fig. 2c) studied. According to Eq. (6), the gradual lower efficiency with electrolysis time is related to the reduced [$H_2O_2$]/$Q$ ratio as a result of nonlinear increase of the accumulated $H_2O_2$. This kind of behavior can be partly explained by the use of batch operation mode, since the $H_2O_2$ production rate at the air-diffusion cathode from Reaction (1) becomes equal to its decomposition rate by parasitic reactions that can take place in the cell. For example, the continuous recirculation of $H_2O_2$ accumulated in the solution may promote its electrochemical reduction at the cathode surface (Reaction (8)) and, to much lesser extent, its spontaneous disproportion in the bulk (Reaction (9)) [11].

$$H_2O_2 + 2H^+ + 2e^- \rightarrow 2H_2O \quad (8)$$

$$H_2O_2 \rightarrow ½\ O_{2(g)} + H_2O \quad (9)$$

Furthermore, considering that an undivided electrochemical reactor is employed, other additional parasitic reactions occur, as for example the oxidation of $H_2O_2$ to $O_2$ at the Nb-BDD anode surface via $HO_2^{\cdot}$ as an intermediate, according to the following reactions:

$$H_2O_2 \rightarrow HO_2^{\cdot} + H^+ + e^- \quad (10)$$

$$HO_2^{\cdot} \rightarrow O_{2(g)} + H^+ + e^- \quad (11)$$

In addition, it is worth mentioning that $H_2O_2$ decomposition is promoted as the solution pH becomes more alkaline, according to the following reaction:

$$H_2O_2 + OH^- \rightarrow H_2O + HO_2^- \quad (12)$$

As a consequence of these undesired reactions, the accumulated $H_2O_2$ concentration is always below the theoretical maximum. As explained

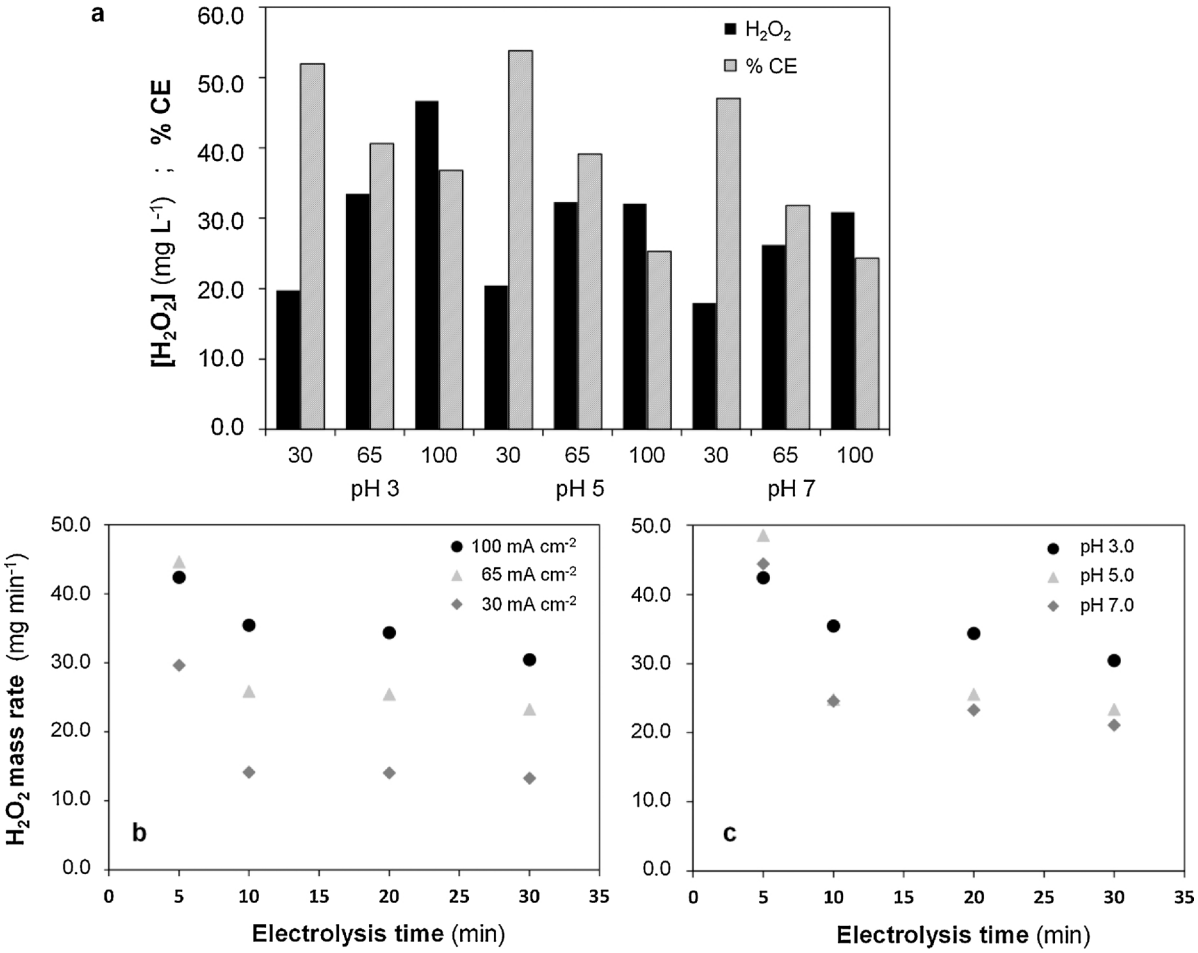


**Fig. 2.** (a) Accumulated $H_2O_2$ concentration and current efficiency (% CE) at different pH values and current densities ($j$). The values were obtained after 30 min of continuous recirculation of a 50 mM $Na_2SO_4$ solution at a liquid flow rate of 4.4 L $min^{-1}$ and air flow rate of 5 L $min^{-1}$. (b) $H_2O_2$ production rate as function of electrolysis time, at constant pH = 3.0 and various $j$ values. (c) $H_2O_2$ production rate as function of electrolysis time, at constant $j$ = 100 mA $cm^{-2}$ and varying pH.

in the Introduction, undivided reactors are the best choice for water treatment, but divided ones should be employed for industrial electrochemical $H_2O_2$ production. Note that similar trends for $H_2O_2$ accumulation have been reported by Brillas and co-workers, as shown during the electrolysis of $Na_2SO_4$ solutions in a similar batch filter-press BDD/GDE reactor at $j$ values between 50 and 150 mA $cm^{-2}$ [29].

In addition, Fig. 2b and c show that the maximum $H_2O_2$ production was achieved at 100 mA $cm^{-2}$ and pH 3.0. This agrees with the fact that a higher electron and proton supply promotes a faster $O_2$ reduction from Reaction (1).

### 3.2. Validation of the correlation models

With the aid of Design Expert software, the models that best correlated the responses and the independent variables shown in Table 2 were:

(i) Quadratic model:

$$[H_2O_2] = 2.19 - 0.31 \cdot pH + 0.81 \cdot j - 0.05 \cdot pH \cdot j + 0.15 \cdot pH^2 - 2.42 \times 10^{-3} \cdot j^2 \quad (12)$$

- Two-factor interaction model (2FI):

$$\% \text{ CE} = 61.68 - 0.43 \cdot pH - 0.18 \cdot j - 0.0275 \cdot pH \cdot j \quad (13)$$

Both models were validated by the analysis of variances (ANOVA), and the results are summarized in Table 3. The statistical significance was assessed by means of Fisher's test. The F-values calculated for the lack of fit of the quadratic and the 2FI models were 30.44 and 60.89, respectively, suggesting that they are satisfactory. Similar conclusions can be drawn from the low probability values (p-value) at a 95% confidence level (< 0.0001) for both models. The statistical significance of the two models is also verified from Fig. 3, since the actual values of the accumulated $H_2O_2$ concentration and current efficiency are randomly distributed around the mean of predicted values. Moreover, good linear correlations between the predicted and observed values for $H_2O_2$ concentration and % CE, with corresponding $R^2$ values of 0.932 and 0.924, were obtained.

According to the ANOVA analysis (Table 3), the effects of the independent variables (A-pH, B-$j$) were obvious and the effective order was $j$ > initial pH, whereas the interaction of the two variables (AB) was not obvious (p-value > 0.1). This can also be deduced from Fig. 2b and c, which show that the $H_2O_2$ production is more substantially affected by $j$ (Fig. 2b) rather than by solution pH, with the latter showing only a slight superiority at pH 3.0 as compared to neutral pH (Fig. 2c). This is important, since the adjustment of pH when treating wastewater complicates the process and increases the water salinity and the operation cost (for acidification and subsequent neutralization).

### 3.3. Optimization by response surface methodology

To better assess the effect of pH and $j$ on $H_2O_2$ production and current efficiency and identify their optimum values, 3D response

**Table 3**
ANOVA results for response surface of the Quadratic and 2FI models.

| Source | Sum of squares | Degree of freedom | Mean square | F-value | p-value | |
|---|---|---|---|---|---|---|
| *Quadratic model* | 1225.26 | 5 | 245.05 | 30.44 | < 0.0001 | significant |
| A-pH | 206.75 | 1 | 206.75 | 25.68 | 0.0002 | |
| B-*j* | 880.82 | 1 | 880.82 | 109.41 | < 0.0001 | |
| AB | 98.63 | 1 | 98.63 | 12.25 | 0.0039 | |
| $A^2$ | 1.56 | 1 | 1.56 | 0.19 | 0.6673 | |
| $B^2$ | 38.61 | 1 | 38.61 | 4.80 | 0.0474 | |
| Residual | 104.66 | 13 | 8.05 | | | |
| Lack of fit | 73.34 | 3 | 24.45 | 7.80 | 0.0056 | not significant |
| Pure error | 31.33 | 10 | 3.13 | | | |
| *2FI model* | 1723.02 | 3 | 574.34 | 60.89 | < 0.0001 | significant |
| A-pH | 228.38 | 1 | 228.38 | 24.21 | 0.0002 | |
| B-*j* | 1466.34 | 1 | 1466.34 | 155.45 | < 0.0001 | |
| AB | 28.31 | 1 | 28.31 | 3.00 | 0.1037 | |
| Residual | 141.49 | 15 | 9.43 | | | |
| Lack of fit | 102.41 | 5 | 20.48 | 5.24 | 0.0127 | not significant |
| Pure error | 39.08 | 10 | 3.91 | | | |

surfaces and contour maps were developed with the aid of Design Expert software. The response surface plot shown in Fig. 4 implies that the generation of $H_2O_2$ increases with $j$ at acidic pH values. On the other hand, the current efficiency (Fig. 5) decreases as $j$ is raised, regardless of the initial pH of the electrolyte solution. As explained above, this is attributed to the batch operation mode in an undivided cell configuration, which promotes the activation of detrimental side reactions. Four sets of optimum pH and $j$ values were proposed by the statistical software (Table 4), yielding maximum $H_2O_2$ production and current efficiency. Among the four solutions proposed, solution number 1, requiring electrolyte pH = 3.0 and $j$ = 73.66 mA $cm^{-2}$ (~74.0), was selected as the optimum one. Under these conditions, a set of experiments was conducted aiming to validate the two correlation models (Eqs. (12) and (13)) and to investigate the effect of other operation conditions like liquid and air flow rates, as well as electrolyte concentration. The main goal was to fully optimize the electrocatalytic $H_2O_2$ production at plant scale, eventually yielding the most effective (highest $H_2O_2$ production rate), efficient (maximum CE percentage) and profitable (lowest energy consumption) process at large scale.

The results of two replicate experiments under the aforementioned optimum conditions are summarized in Table 5. The relative errors were below 5% for both, $H_2O_2$ generation and % CE (3.69% and 4.38%, respectively), demonstrating the excellent fitting of the experimental results (actual values) with those predicted by the two models.

### 3.3.1. Effect of liquid flow rate

The feed flow rate is closely related to the hydraulic residence time (HRT) of the treated solution within the electrochemical cell. This is of great significance under continuous operation mode, where the feed solution is continuously treated and discharged. For batch operation, as is the case of the experiments carried out in this work, the recirculation flow rate does not necessarily match the HRT, but it rather affects the mixing and may create turbulent flow within the electrochemical cell. This, in turn, may intensify the mass transport induced by the higher local concentration of molecular oxygen dissolved in the aqueous phase. Indeed, when the flow rate was doubled (from 2.8 to 5.6 L $min^{-1}$), $H_2O_2$ production was gradually greater at each given time (Fig. 6b), finally increasing by 28.8% at 30 min (Fig. 6a, [$H_2O_2$] in mg $min^{-1}$). Current efficiency also increased in the same proportion, as a result of the higher $H_2O_2$ generation at similar charge consumption (note that energy consumption varied between 1.97 and 2.00 kWh $m^{-3}$ for all pilot runs) (Fig. 6a).

### 3.3.2. Effect of air flow rate

Large feeding of air or pure $O_2$ to the air chamber is often needed to counterbalance the existing pressure on the wet face of the GDE, thereby avoiding flooding that would stop the $H_2O_2$ production. If correctly adjusted, an increase in air flow rate may upgrade the $H_2O_2$ accumulation. As found for the pilot plant studied in this work, a rise in

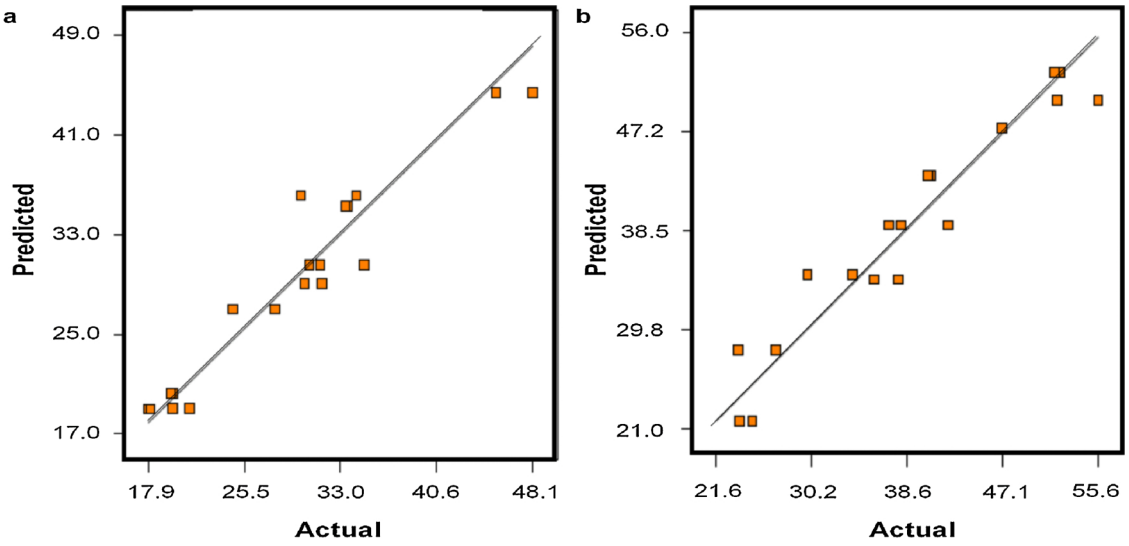


**Fig. 3.** Comparison of the actual results obtained experimentally regarding (a) $H_2O_2$ production and (b) current efficiency (in %), with those predicted via central composite design Eqs. (12) and (13), respectively.

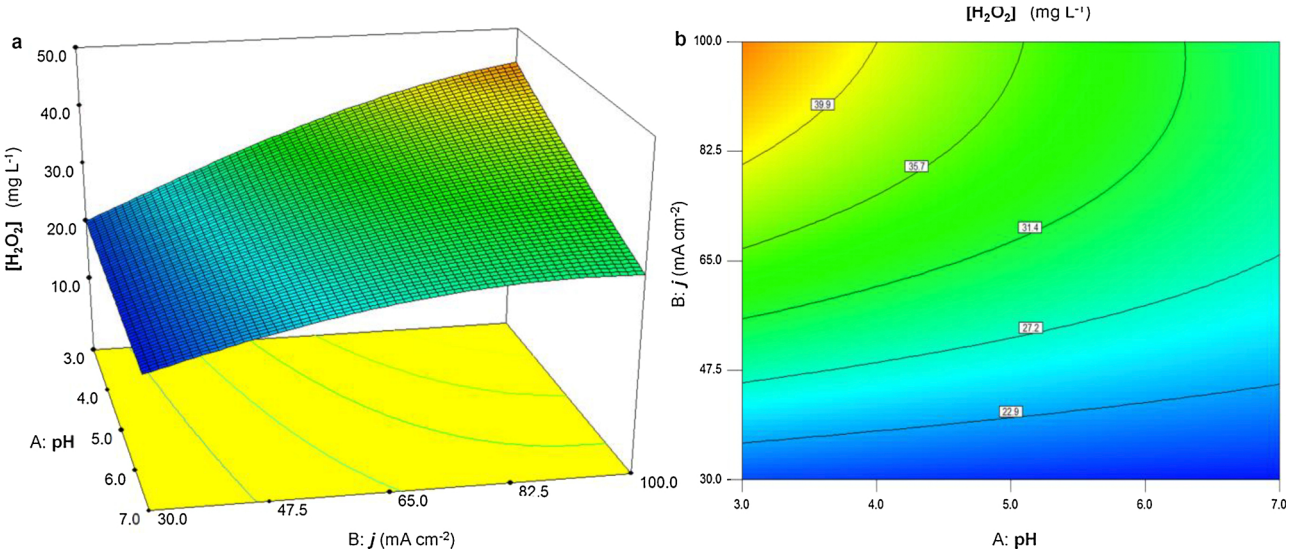


**Fig. 4.** (a) 3D surface plot and (b) contour plot for the $H_2O_2$ production as function of the initial pH (A) and current density (B). Experimental data correspond to 30-min electrolyses under continuous recirculation of a 50 mM $Na_2SO_4$ solution at liquid flow rate of 4.4 L $min^{-1}$ and air flow rate of 5 L $min^{-1}$.

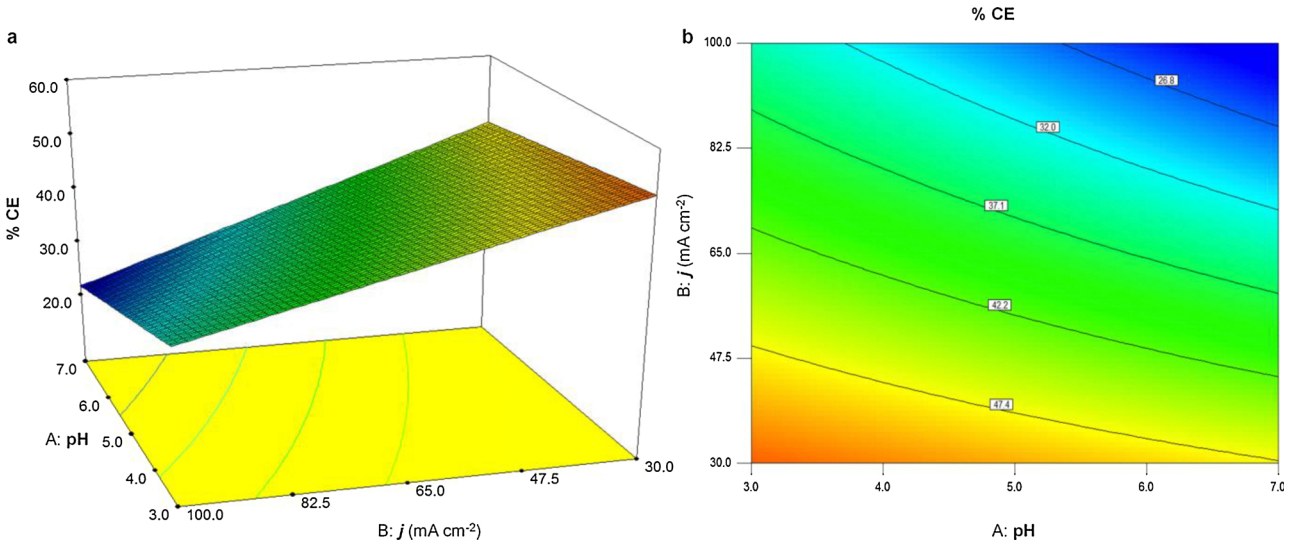


**Fig. 5.** (a) 3D surface plot and (b) contour plot for current efficiency (in %), as in Fig. 4.

**Table 4**
Optimum operation conditions proposed by Design Expert 7.0.0 software to attain maximum $H_2O_2$ concentration and current efficiency at 30 min of electrolysis.

| Test number | pH | $j$ (mA $cm^{-2}$) | [$H_2O_2$] (mg $L^{-1}$) | % CE | Desirability | |
|---|---|---|---|---|---|---|
| 1 | 3.00 | 73.66 | 38.0961 | 41.0744 | 0.604 | Selected |
| 2 | 3.00 | 74.16 | 38.2467 | 40.9437 | 0.604 | |
| 3 | 3.00 | 72.82 | 37.8392 | 41.2949 | 0.604 | |
| 4 | 3.00 | 70.00 | 36.9532 | 42.0343 | 0.603 | |

**Table 5**
Models validation under optimum conditions, with experimental data obtained after 30 min of electrolysis under continuous recirculation of 50 mM $Na_2SO_4$ solution at pH 3.0, 74 mA $cm^{-2}$, liquid flow rate of 3.3 L $min^{-1}$ and air flow rate of 5 L $min^{-1}$. Two independent runs were performed.

| | Run | | Average actual values | Predicted values | Relative error (%) |
|---|---|---|---|---|---|
| | a | b | | | |
| $H_2O_2$ (mg $L^{-1}$) | 35.51 | 38.07 | 36.79 | 38.20 | 3.69 |
| % CE | 37.80 | 40.60 | 39.20 | 40.99 | 4.38 |

the air flow rate from 2.5 and 5 L $min^{-1}$ to 10 L $min^{-1}$, resulted in an enhanced $H_2O_2$ production by 23.1% and 15.6% at 30 min, respectively (Fig. 7a and b). Moreover, the kinetics of $H_2O_2$ production was faster at the maximum air flow rate of 10 L $min^{-1}$ (Fig. 7b), with no negative effect on the corresponding energy consumption, which was similar at all air flow rates examined. This is interesting, since one might presume that an excessive air feeding could generate too many bubbles within the electrochemical reactor, thereby increasing the ohmic drop and also affecting the stability of the liquid flow rate, which did not occur.

Based on these results, as well as on the better performance of the plant at high electrolyte flow rates, it can be concluded that the combined increase of air and liquid flow rates may effectively enhance the fraction of oxygen consumed for $H_2O_2$ production (Reaction (1)) over the total amount of air fed. Indeed, under the optimum operation conditions, namely 50 mM $Na_2SO_4$ solution at pH 3.0 treated at 74 mA $cm^{-2}$, with liquid flow rate of 5.6 L $min^{-1}$ and air flow rate of 10 L $min^{-1}$, the highest $H_2O_2$ mass production rate and current efficiency were

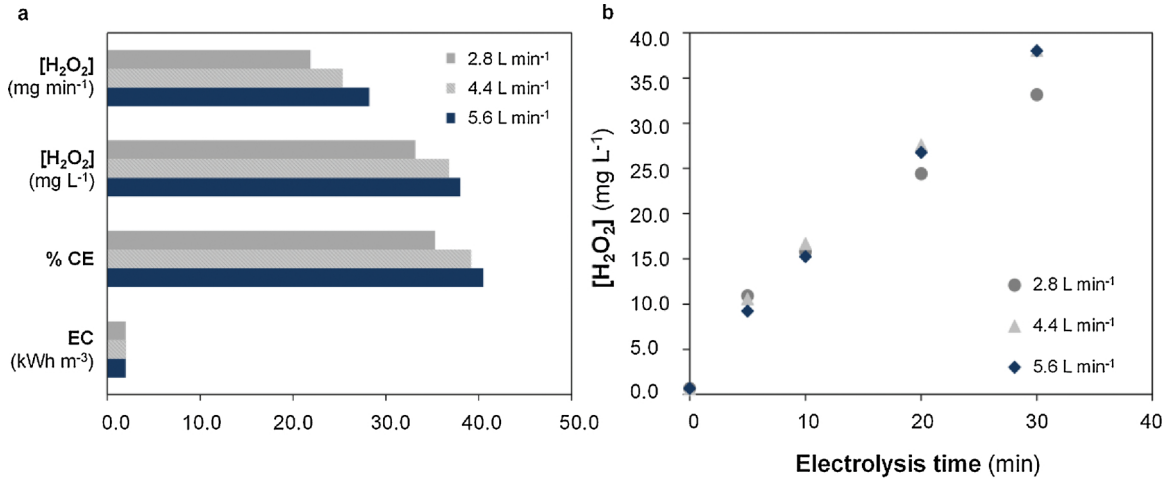


**Fig. 6.** (a) Effect of liquid flow rate on various process efficiency parameters, corresponding to 30-min electrolyses; (b) accumulated $H_2O_2$ as a function of electrolysis time, at three different liquid flow rates. Fixed parameters: 50 mM $Na_2SO_4$ at pH 3.0, $j$ = 74 mA $cm^{-2}$, air flow rate of 5 L $min^{-1}$.

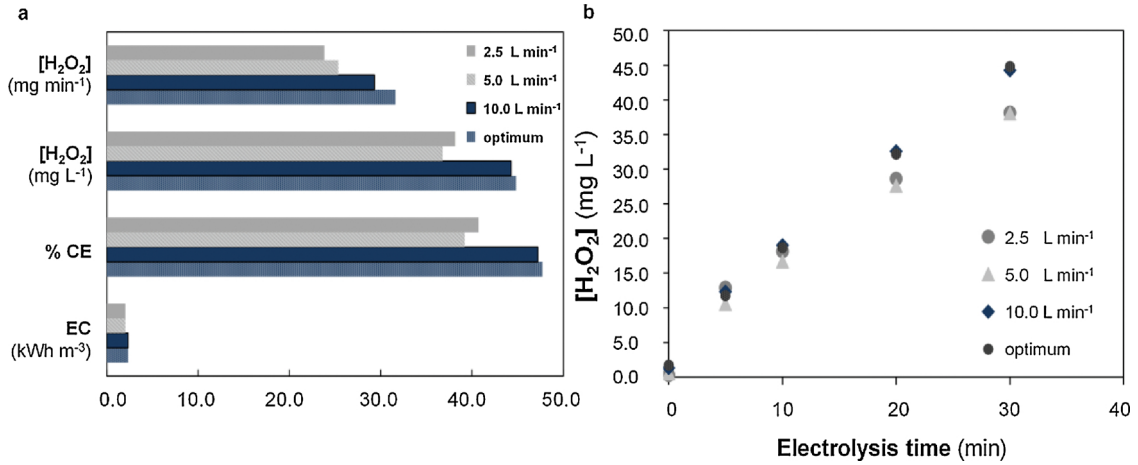


**Fig. 7.** (a) Effect of air flow rate on various process efficiency parameters, corresponding to 30-min electrolyses; (b) accumulated $H_2O_2$ as function of electrolysis time, at different air flow rates. Fixed parameters: 50 mM $Na_2SO_4$ at pH 3.0, $j$ = 74 mA $cm^{-2}$, liquid flow rate of 4.4 L $min^{-1}$. The optimum trial corresponds to the same conditions but using a liquid flow rate of 5.6 L $min^{-1}$ and air flow rate of 10 L $min^{-1}$.

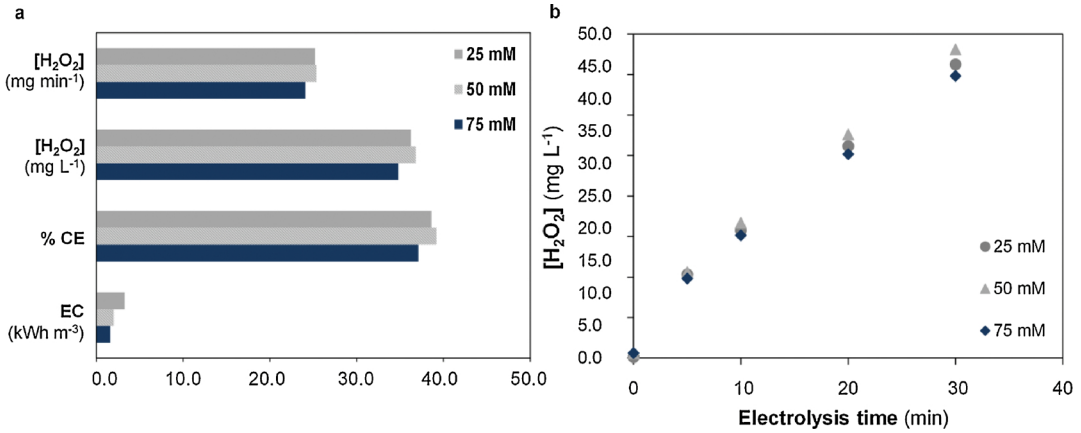


**Fig. 8.** (a) Effect of $Na_2SO_4$ molar concentration on various process efficiency parameters, corresponding to 30-min electrolyses; (b) accumulated $H_2O_2$ as a function of electrolysis time, at three different electrolyte concentrations. Fixed parameters: electrolyte solution at pH 3.0, $j$ = 74 mA $cm^{-2}$, liquid flow rate of 4.4 L $min^{-1}$ and air flow rate of 5 L $min^{-1}$.

obtained. In the first 5 min of electrolysis, these conditions led to $H_2O_2$ production with a mass rate of 64.9 mg $min^{-1}$, 89.3% current efficiency and energy consumption of 0.4 kWh $m^{-3}$. These values are among the best achieved with similar system configurations. For example, Flox et al. [29] reported a production rate of ca. 23 mg $min^{-1}$ at 30 min in 50 mM $Na_2SO_4$ at pH 3.0, 100 mA $cm^{-2}$ and liquid flow rate of 3 L $min^{-1}$, whereas Fig. 7a shows a higher $H_2O_2$ electrogeneration rate of 32 mg $min^{-1}$ at that time.

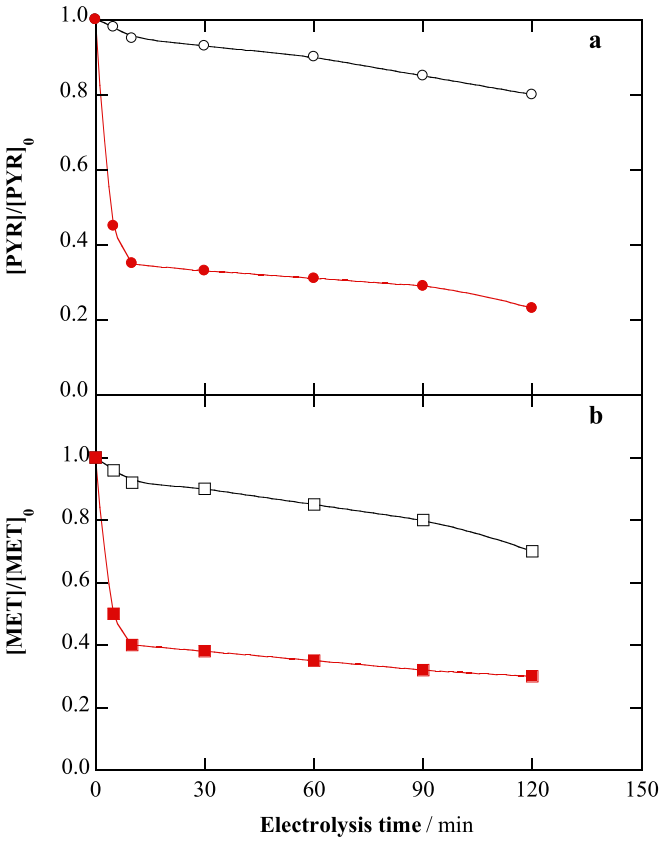


**Fig. 9.** Normalized concentration decays of pesticides (a) pyrimethanil (PYR) and (b) methomyl (MET) versus electrolysis time during the (○,□) electro-oxidation (EO) and (●,■) solar photoelectro-Fenton (SPEF) treatment of 75 L of mixtures of both pesticides (71 mg $L^{-1}$ DOC) in deionized water with 50 mM $Na_2SO_4$ at pH 3.0 using the pilot plant at $j$ = 74 mA $cm^{-2}$, liquid flow rate of 5.6 L $min^{-1}$ and air flow rate of 10 L $min^{-1}$. SPEF treatment was performed in the presence of 0.5 mM $Fe^{2+}$ as catalyst.

### 3.3.3. Effect of electrolyte concentration

Considering the rather small electrode gap (6 mm) between the anode and cathode in the electrochemical cell, it was assumed that the solution conductivity would not significantly affect the production of $H_2O_2$. Therefore, a set of experiments was made to determine the possible influence of electrolyte concentration. It was observed that, within the range of 25–75 mM of $Na_2SO_4$, which is equal to a solution conductivity range of 4.6–12.3 mS $cm^{-1}$, the accumulation of $H_2O_2$ was quite analogous, being only slightly higher in the case of 50 mM (Fig. 8). However, a rather substantial effect is observed regarding the energy consumption, since a higher conductivity led to a gradually lower consumption; i.e. 3.24, 2.00 and 1.61 kW h $m^{-3}$ at 25, 50 and 75 mM $Na_2SO_4$, respectively. This was expected, since the increase of electrolyte concentration causes a reduction of the ohmic resistance in the bulk solution, and accelerates the electron transfer, thus decreasing the overall charge consumption. From these findings, it can be concluded that the system would be more efficient at higher water conductivity. Therefore, future industrial application of this technology should focus on high conductivity wastewater or be coupled with membrane technologies for treating membrane concentrates.

### 3.4. Treatment of a mixture of pesticides

After the optimum operation conditions were determined for attaining the best balance between $H_2O_2$ production and current efficiency, the plant performance was validated by carrying out several tests to assess its capability to degrade a mixture of two model SOCs, namely PYR and MET, which were treated by sun-assisted AOPs like solar photo-Fenton [6,51]. All the assays were made with 75 L of mixtures of both pesticides in water with 50 mM $Na_2SO_4$ under optimized conditions: pH 3.0, 74 mA $cm^{-2}$ and air flow rate of 10 L $min^{-1}$.

First, a mixture containing 50 mg $L^{-1}$ PYR and 90 mg $L^{-1}$ MET (i.e., 71 mg $L^{-1}$ DOC) was treated by EO with electrogenerated $H_2O_2$. The influence of liquid flow rate (2.8, 4.4 and 5.6 L $min^{-1}$) was investigated, aiming to promote a larger oxidation of both organic contaminants either by increasing the HRT (at a lower flow rate) or by enhancing the mass transport of pollutants to the anode surface (at a higher flow rate). However, no significant effect of this parameter was found, which suggests that the amount of BDD(˙OH) produced via Reaction (2) at 74 mA $cm^{-2}$ was high enough to react with both pesticides regardless of the hydrodynamic conditions (within the studied range). Fig. 9a and b depict the normalized decays of PYR and MET concentrations at a liquid flow rate of 5.6 L $min^{-1}$, respectively. As can be seen, the degradation by EO-$H_2O_2$ was very slow, only attaining 20% and 30% of PYR and MET removal after 120 min. The larger degradation of MET could be explained by the greater electrocatalytic behavior of BDD with this pesticide as a result of a more favorable adsorption on its surface, thus reacting more quickly with physisorbed BDD(˙OH). At the end of the electrolysis, almost no mineralization was achieved in EO process, in agreement with the refractory nature of typical reaction by-products like carboxylic acids [10–13]. In all these trials, the energy consumption was around 10 kW h $m^{-3}$.

The same pesticides mixture was treated by EF, using the optimized parameters with liquid flow rate of 5.6 L $min^{-1}$, in the presence of different amounts of $Fe^{2+}$ as catalyst (not shown). After 120 min, a higher degradation percentage was reached for both pesticides, with up to 35% and 40% for PYR and MET, respectively. This demonstrates that the $H_2O_2$ produced under optimized conditions reacted with added $Fe^{2+}$ according to Fenton's reaction, yielding homogeneous ˙OH that enhanced the degradation because this radical acted concomitantly with BDD(˙OH). The former was confined into the reactor, whereas the latter radical was transported throughout the whole volume. In contrast, DOC abatement only attained 8% as maximum, which agrees with the high stability of Fe(III)-carboxylate complexes formed as intermediates [11]. Worth mentioning, a much larger mineralization was achieved working with a pesticide mixture that accounted for 20 mg $L^{-1}$ DOC, using 1.0 mM $Fe^{2+}$. In this case, 32% DOC removal was attained at 120 min. It is also important to note that the $Fe^{2+}$ concentration remained almost constant during all these EF trials, which confirms the capability of the cathode to regenerate it from Fe (III) reduction.

Finally, the mixtures with 71 mg $L^{-1}$ DOC were comparatively treated by SPEF using the best $Fe^{2+}$ concentration (i.e., 0.5 mM). In these experiments, required accumulated UV energy, $Q_{UV}$, was 7.1 kJ $L^{-1}$. As it can be observed in Fig. 9, 55% and 50% removal of PYR and MET was reached in only 5 min, which confirms the fast $Fe^{2+}$ photoregeneration with additional ˙OH production from Reaction (3). At longer time, the degradation was much slower, but ended in 77% and 70% removal, respectively, at 120 min. This is a much better performance as compared to EO and EF, which was further confirmed by DOC abatements higher than 15%, in agreement with the powerful action of UV/Vis photons on Fe(III)-carboxylate complexes according to Reaction (4).

## 4. Conclusions

The successful performance of the largest SPEF pilot plant existing to date has been demonstrated in this work. The core of the plant, the filter-press electrochemical reactor, is comprised of a Nb-BDD anode and a GDE as cathode. Optimization of main operation parameters has been carried out according to a thorough experimental design, in order to maximize the electrocatalytic $H_2O_2$ production with a high current efficiency. Optimum values obtained for the key parameters were: pH 3.0,

74 mA $cm^{-2}$, liquid flow rate of 5.6 L $min^{-1}$ and air flow rate of 10 L $min^{-1}$. Their application yielded a mass rate of up to 64.9 mg $H_2O_2$ $min^{-1}$, current efficiency of 89.3% and energy consumption of 0.4 kWh $m^{-3}$ during the first minutes. The SPEF treatment of 75 L of pesticides mixtures allowed the removal of more than 50% of each pesticide in only 5 min, whereupon further degradation as well as mineralization of by-products and their Fe(III) complexes became much slower but always superior to EO and EF treatments. Further optimization of the SPEF process for treating different kind of wastewater in the integrated pilot system is in progress.

## Acknowledgments

The authors wish to thank the EU funded SFERA-II project (7th Framework Programme, Grant Agreement n. 312,643), a Transnational Access program which aims at boosting scientific collaboration among the leading European institutions in solar concentration systems. Financial support from project CTQ2016-78616-R (AEI/FEDER, EU) is also acknowledged.

## References

[1] R. Loos, B.M. Gawlik, G. Locoro, E. Rimaviciute, S. Contini, G. Bidoglio, Environ. Pollut. 157 (2009) 561–568.
[2] The NORMAN Network, (2012) (Accessed 15 May 2018), http://www.norman-network.net/?q=Home.
[3] J.-Q. Jiang, Z. Zhou, V.K. Sharma, Microchem. J. 110 (2013) 292–300.
[4] B. Petrie, R. Barden, B. Kasprzyk-Hordern, Water Res. 72 (2015) 3–27.
[5] C. Postigo, D. Barceló, Sci. Total Environ. 503–504 (2015) 32–47.
[6] I. Oller, S. Malato, J.A. Sánchez-Pérez, M.I. Maldonado, R. Gassó, Catal. Today 129 (2007) 69–78.
[7] D.J.E. Costa, J.C.S. Santos, F.A.C. Sanches-Brandão, W.F. Ribeiro, G.R. Salazar-Banda, M.C.U. Araujo, J. Electroanal. Chem. 789 (2017) 100–107.
[8] M. Popescu, C. Sandu, E. Rosales, M. Pazos, G. Lazar, M.A. Sanromán, J. Electroanal. Chem. 808 (2018) 455–463.
[9] C. Comninellis, A. Kapałka, S. Malato, S.A. Parsons, I. Poulios, D. Mantzavinos, J. Chem. Technol. Biotechnol. 83 (2008) 769–776.
[10] M.A. Oturan, J.-J. Aaron, Crit. Rev. Environ. Sci. Technol. 44 (2014) 2577–2641.
[11] E. Brillas, I. Sirés, M.A. Oturan, Chem. Rev. 109 (2009) 6570–6631.
[12] L. Feng, E.D. van Hullebusch, M.A. Rodrigo, G. Esposito, M.A. Oturan, Chem. Eng. J. 228 (2013) 944–964.
[13] C.A. Martínez-Huitle, M.A. Rodrigo, I. Sirés, O. Scialdone, Chem. Rev. 115 (2015) 13362–13407.
[14] S. Chen, Z. Chen, S. Siahrostami, T.R. Kim, D. Nordlund, D. Sokaras, S. Nowak, J.W.F. To, D. Higgins, R. Sinclair, J.K. Nørskov, T.F. Jaramillo, Z. Bao, ACS Sustain. Chem. Eng. 6 (2018) 311–317.
[15] T. Pérez, G. Coria, I. Sirés, J.L. Nava, A.R. Uribe, J. Electroanal. Chem. 812 (2018) 54–58.
[16] S. Siahrostami, A. Verdaguer-Casadevall, M. Karamad, D. Deiana, P. Malacrida, B. Wickman, M. Escudero-Escribano, E.A. Paoli, R. Frydendal, T.W. Hansen, Ib Chorkendorff, I.E.L. Stephens, J. Rossmeisl, Nature Mater. 12 (2013) 1137–1143.
[17] E. Pizzutilo, O. Kasian, C.H. Choi, S. Cherevko, G.J. Hutchings, K.J.J. Mayrhofer, S.J. Freakley, Chem. Phys. Lett. 683 (2017) 436–442.
[18] C. Ridruejo, F. Alcaide, G. Álvarez, E. Brillas, I. Sirés, J. Electroanal. Chem. 808 (2018) 364–371.
[19] G.-L. Chai, Z. Hou, T. Ikeda, K. Terakura, J. Phys. Chem. C 121 (2017) 14524–14533.
[20] V. Čolić, S. Yang, Z. Révay, I.E.L. Stephens, Ib Chorkendorff, Electrochim. Acta 272 (2018) 192–202.
[21] S. Yang, A. Verdaguer-Casadevall, L. Arnarson, L. Silvioli, V. Čolić, R. Frydendal, J. Rossmeisl, Ib Chorkendorff, I.E.L. Stephens, ACS Catal. 8 (2018) 4064–4081.
[22] A. Dirany, I. Sirés, N. Oturan, A. Özcan, M.A. Oturan, Environ. Sci. Technol. 46 (2012) 4074–4082.
[23] M. Panizza, A. Dirany, I. Sirés, M. Haidar, N. Oturan, M.A. Oturan, J. Appl. Electrochem. 44 (2014) 1327–1335.
[24] G. Coria, T. Pérez, I. Sirés, J.L. Nava, J. Electroanal. Chem. 757 (2015) 225–229.
[25] K.V. Plakas, S.D. Sklari, D.A. Yiankakis, G.Th. Sideropoulos, V.T. Zaspalis, A.J. Karabelas, Water Res. 91 (2016) 183–194.
[26] A. Galia, S. Lanzalaco, M.A. Sabatino, C. Dispenza, O. Scialdone, I. Sirés, Electrochem. Commun. 62 (2016) 64–68.
[27] Z.G. Aguilar, E. Brillas, M. Salazar, J.L. Nava, I. Sirés, Appl. Catal. B: Environ. 206 (2017) 44–52.
[28] S. Lanzalaco, I. Sirés, M.A. Sabatino, C. Dispenza, O. Scialdone, A. Galia, Electrochim. Acta 246 (2017) 812–822.
[29] C. Flox, J.A. Garrido, R.M. Rodríguez, P.-L. Cabot, F. Centellas, C. Arias, E. Brillas, Catal. Today 129 (2007) 29–36.
[30] G.R. Agladze, G.S. Tsurtsumia, B.-I. Jung, J.-S. Kim, G. Gorelishvili, J. Appl. Electrochem. 37 (2007) 375–383.
[31] M. Giomo, A. Buso, P. Fier, G. Sandonà, B. Boye, G. Farnia, Electrochim. Acta 54 (2008) 808–815.
[32] E. Brillas, J. Casado, Chemosphere 47 (2002) 241–248.
[33] B. Chaplin, Environ. Sci.: Processes Impacts 16 (2014) 1182–1203.
[34] E. Brillas, J. Braz. Chem. Soc. 25 (2014) 393–417.
[35] C. Flox, P.L. Cabot, F. Centellas, J.A. Garrido, R.M. Rodríguez, C. Arias, E. Brillas, Appl. Catal. B: Environ. 75 (2007) 17–28.
[36] A. Thiam, I. Sirés, E. Brillas, Water Res. 81 (2015) 178–187.
[37] J.R. Steter, E. Brillas, I. Sirés, Appl. Catal. B: Environ. 224 (2018) 410–418.
[38] A.R.F. Pipi, I. Sirés, A.R. De Andrade, E. Brillas, Chemosphere 109 (2014) 49–55.
[39] F. Gozzi, I. Sirés, A. Thiam, S.C. de Oliveira, A. Machulek Jr., E. Brillas, Chem. Eng. J. 310 (2017) 503–513.
[40] F.C. Moreira, J. Soler, A. Fonseca, I. Saraiva, R.A.R. Boaventura, E. Brillas, V.J.P. Vilar, Appl. Catal. B: Environ. 182 (2016) 161–171.
[41] G. Coria, T. Pérez, I. Sirés, E. Brillas, J.L. Nava, Chemosphere 198 (2018) 174–181.
[42] C. Espinoza, J. Romero, L. Villegas, L. Cornejo-Ponce, R. Salazar, J. Hazard. Mater. 319 (2016) 24–33.
[43] L.C. Almeida, S. Garcia-Segura, N. Bocchi, E. Brillas, Appl. Catal. B: Environ. 103 (2011) 21–30.
[44] E. Isarain-Chávez, R.M. Rodríguez, P.L. Cabot, F. Centellas, C. Arias, J.A. Garrido, E. Brillas, Water Res. 45 (2011) 4119–4130.
[45] S. Garcia-Segura, E. Brillas, Electrochim. Acta 140 (2014) 384–395.
[46] V.S. Antonin, S. Garcia-Segura, M.C. Santos, E. Brillas, J. Electroanal. Chem. 747 (2015) 1–11.
[47] S. Garcia-Segura, E. Brillas, Appl. Catal. B: Environ. 181 (2016) 681–691.
[48] T. Pérez, I. Sirés, E. Brillas, J.L. Nava, Electrochim. Acta 228 (2017) 45–56.
[49] S. Malato, J. Blanco, A. Campos, J. Cáceres, C. Guillard, J.M. Herrmann, A.R. Fernández-Alba, Appl. Catal. B: Environ. 42 (2003) 349–357.
[50] M. Panizza, G. Cerisola, Chem. Rev. 109 (2009) 6541–6569.
[51] A. Zapata, T. Velegraki, J.A. Sánchez-Pérez, D. Mantzavinos, M.I. Maldonado, S. Malato, Appl. Catal. B: Environ. 88 (2009) 448–454.

Science of the Total Environment 705 (2020) 135831

Contents lists available at ScienceDirect

Science of the Total Environment

journal homepage: www.elsevier.com/locate/scitotenv

# Electro-oxidation process assisted by solar energy for the treatment of wastewater with high salinity

I. Salmerón, I. Oller *, S. Malato

*Plataforma Solar de Almería-CIEMAT, Carretera de Senés Km 4, 04200 Tabernas, Almería, Spain*
*CIESOL, Joint Centre of the University of Almería-CIEMAT, 04120 Almería, Spain*

## HIGHLIGHTS

- Solar-assisted electro-oxidative treatment enhanced wastewater biodegradability.
- Solar light promotes the formation of chlorine radicals from electrogenerated chlorine species.
- Combination of solar and electrochemical processes achieved substantial organic removal.
- Electro-oxidation is effective for removal of nitrogenated compounds.

## GRAPHICAL ABSTRACT

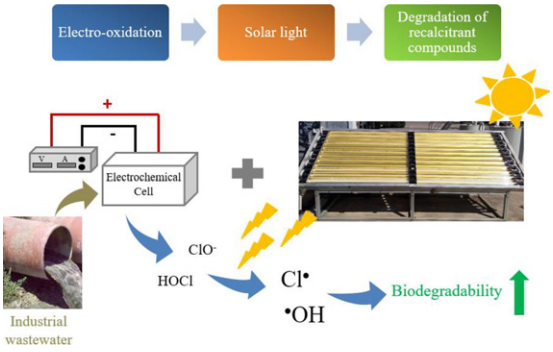


## ARTICLE INFO

*Article history:*
Received 23 October 2019
Received in revised form 27 November 2019
Accepted 27 November 2019
Available online 4 December 2019

Editor: Paola Verlicchi

*Keywords:*
Chlorine radical
Electro-oxidation
Nitrogen removal
Photochemistry
Water chemistry

## ABSTRACT

Industrial wastewaters characterized by its high content in organics and conductivity entails a challenge for conventional treatments due to its low biodegradability. Electro-oxidative processes have been successfully applied for the treatment of this kind of wastewaters achieving high organics and ammonia removal. The degradation process is executed mainly by electrochemically generated active chlorine species, as HClO and $ClO^-$ with $E^0 = 1.49$ V; and $E^0 = 0.89$ V, respectively. Under solar radiation, specifically at 313 nm, the formation of Cl• ($E^0 = 2.4$ V) from $ClO^-$ is promoted, improving the oxidizing capacity of the process. In this work the combination of an electrochemical device with a solar photo-reactor has been evaluated aiming to increase the degradation rate per $kWh^{-1}$. Two different complex industrial wastewaters were tested, achieving higher organics degradation when electrochemical treatment was assisted by solar light. Toxicity reduction was also assessed and biodegradability enhanced and allowing its ulterior lower-cost biological treatment.



## 1. Introduction

Wastewater with high content of organic matter and salts suppose a challenge to conventional depuration processes. Such complex wastewaters are normally toxic and/or contain bio-recalcitrant unknown contaminants. A good representative example is landfill leachate, which composition is complex and depends on several factors such as age, precipitation, seasonal weather variations, waste type and surrounding population (Kjeldsen et al., 2002). In general, its principal characteristics are high organic load and the presence of molecules with high molecular weight, as well as ammonia, heavy metals and

* Corresponding author.
*E-mail address:* isabel.oller@psa.es (I. Oller).

https://doi.org/10.1016/j.scitotenv.2019.135831
0048-9697/

chlorinated organic and inorganic salts (Renou et al., 2008; Wiszniowski et al., 2006), all granting them a highly toxic character, hampering a conventional treatment based on bioprocesses.

According to its age, landfill leachates are classified into two categories. Young leachates, a few years old, in which organic matter content is normally higher than 18 g $L^{-1}$ of Chemical Oxygen Demand (COD) and ammonium between 10 and 800 mg $L^{-1}$. Despite this, the $BOD_5$/COD ($BOD_5$, Biological Oxygen Demand in five days) ratio is generally higher than 0.6 evidencing the presence of biodegradable substances. Old leachates, with more than five years old, present a lower concentration of organics. With COD range usually between 100–500 mg $L^{-1}$ and 20–40 mg $L^{-1}$ of ammonium, but $BOD_5$/COD ratio normally lower than 0.3, evidencing that high biodegradable substances have been already degraded (Deng and Englehardt, 2007).

Given that conventional biological processes are very often unfeasible, especially for old leachates, alternative treatments based on Advanced Oxidation Processes (AOPs) have been widely studied and described in the literature reaching high COD degradation rates (Deng, 2009; Li et al., 2010; Primo et al., 2008; Wang et al., 2003) and/or increasing their biodegradability (de Morais and Zamora, 2005). Most efficient AOPs reported are photo-Fenton (Reactions 1 and 2) or ozonation processes attaining high mineralization rates but obtaining high concentration of ammonium at the end of the treatments due to the mineralization of the nitrogen included in the structure of organic contaminants.

$$Fe^{2+} + H_2O_2 \rightarrow Fe^{3+} + {}^{\cdot}OH + OH^- \quad (R.1)$$

$$Fe^{3+} + H_2O + h\nu \rightarrow Fe^{2+} + {}^{\cdot}OH + H^+ \quad (R.2)$$

In consequence, the effluent generated normally contains a very high concentration of ammonium unbalanced with the organic carbon available for a subsequent biological treatment. Therefore, alternative AOPs, showing a stronger oxidation effect based on other mechanisms apart from the hydroxyl radicals generation are required to obtain higher quality effluents.

Within the powerful advanced oxidation technologies, indirect electro-oxidation processes represent an effective alternative for the destruction of substances with high molecular weight and, specifically the elimination of COD as well as ammonium oxidation, considering it as an interesting technology specifically for the treatment of wastewaters with high conductivity (Bashir et al., 2013; Chiang et al., 1995; Turro et al., 2011)

Within these processes, organic load is degraded by strong oxidants as active chlorine species (ACS). ACS are generated from chloride present in water by an electron transfer to the anode (Reaction 3), which reacts with water producing hypochlorous acid (Martinez-Huitle and Brillas, 2009) (Reaction 4). According to the speciation of chlorine in water, equilibrium between hypochlorous acid and hypochlorite ion depends on the concentration and pH of the solution ($pK_a$ 7.55) (Sirés et al., 2014), following Reaction 5. Besides these active species, the chloride radical is generated by the direct oxidation at the anode (Reaction 6).

$$2Cl^- \rightarrow Cl_{2(aq)} + 2e^- \quad (R.3)$$

$$Cl_{2(aq)} + H_2O \rightarrow HClO + Cl^- + H^+ \quad (R.4)$$

$$HClO \leftrightarrow ClO^- + H^+ \quad (R.5)$$

$$Cl^- \rightarrow Cl^{\cdot} + e^- \quad (R.6)$$

These species have a redox potential sufficiently high to be able to efficiently degrade organics, $Cl_{2(aq)}$ $E^0 = 1.36$ V; HClO $E^0 = 1.49$ V; $ClO^-$ $E^0 = 0.89$ V and Cl• $E^0 = 2.4$ V (Armstrong et al., 2015).

Sunlight exposure of chlorine species could result in the chlorine and hydroxyl radicals' generation (see Table 1, $\lambda > 300$ nm). Although these radicals could be consumed by some scavengers present in solution, such as carbonate species and dissolved organic matter, a portion of them could react with the contaminants (Nowell and Hoigné, 1992) increasing the efficiency of the treatment.

This work studies the application of an electrolytic device based in ACS generation at pilot plant scale for the treatment of landfill leachate. Experiments include the assessment of some operational parameters' effect on the target wastewater remediation, such as the integration with a solar photo-reactor based on Compound Parabolic Collectors (CPC) aiming an increase of treatment efficiency accompanied of a reduction of related operating costs. Therefore, the main objective has been the evaluation of the efficiency of this combined system for the depuration of two landfill leachates, characterized by 2–3.2 g $L^{-1}$ of dissolved organic carbon (DOC), a high conductivity between 25 and 70 mS $cm^{-1}$ and till 4 g $L^{-1}$ of chloride. Toxicity and biodegradability analyses have been also carried out along the studied processes. The final main objective was not to achieve complete mineralization but to increase biodegradability of the effluent.

## 2. Experimental section

### 2.1. Wastewater characterization

Two different landfill leachates were studied (see Table 2). Although both are categorized as young leachates for its content of organics, there was evidence of maturity in leachate 1, with a lower COD value and higher toxicity. Both leachates were classified as non-biodegradable. It is important also to highlight the difference in turbidity between leachates, 35 NTU compared to 200–300 NTU.

### 2.2. Analysis

COD measurements were done by a COD Cell Test Spectroquant® by Merck. DOC and total nitrogen (TN) were monitored by using a Shimadzu TOC-VCSN analyzer after filtering the samples through 0.22 μm nylon filter from ASIMIO. Ions concentration was determined by ion chromatography (IC) by a Metrohm 850 Professional IC after sample filtration with the same filters. For anions determination, it was used a Metrosep A Supp 7150/4.0 column thermoregulated at 45 °C with 3.6 mM of sodium carbonate as eluent in a flow of 0.7 mL $min^{-1}$. For cations the column was a Metrosep C6 150/4.0 with a solution 1.7 mM nitric acid - 1.7 mM dipicolinic acid in a flow of 1.2 mL $min^{-1}$.

A CRISON 25 pH meter was used for measuring the pH continuously, which was always maintained above 3.5 through sodium hydroxide (J.T. Baker) addition to avoid the formation of toxic gaseous $Cl_2$. Conductivity was determined with a GLP 31 Conductimeter (from CRISON).

Iron concentration was measured spectrophotometrically by using 1,10-phenanthroline following ISO 6332. In the experiments done with the addition of hydrogen peroxide (30% in water from Chem-

**Table 1**
Reactions and quantum yield of photo-transformation of chlorine species at different wavelengths.
Modified from Nowell and Hoigné (1992).

| | Φ(λ) | | |
|---|---|---|---|
| | λ: 365 nm | 313 nm | 254 nm[a] |
| *Gaseous phase* | | | |
| $HOCl \rightarrow {}^{\bullet}OH + Cl^{\bullet}$ | | 1[b] | |
| *Aqueous phase* | | | |
| $ClO^- \rightarrow Cl^{\bullet} + O^- + O\ (^3P)$ | 0.28 | 0.075 | 0.074 |
| $ClO^- \rightarrow Cl^{\bullet} + O^- \rightarrow {}^{\bullet}OH$ | 0.08 | 0.127 | 0.278 |
| $ClO^- \rightarrow Cl^{\bullet} + O\ (^1D)$ | | 0.020 | 0.133 |

[a] Reactions at 254 nm are not possible under sunlight.
[b] At aprox 310 nm.

**Table 2**
Characterization of the landfill leachates studied.

| | Leachate 1 | Leachate 2 |
|---|---|---|
| pH | 7–8 | 7–8 |
| Conductivity (mS $cm^{-1}$) | 50–70 | 25–35 |
| Turbidity (NTU) | 35 | 200–300 |
| $Cl^-$ (g $L^{-1}$) | 6.4–8.2 | 4.5–5.2 |
| COD (g $L^{-1}$) | 8.1–8.4 | 8.8–11 |
| DOC (g $L^{-1}$) | 2–2.5 | 2–3.2 |
| TN (g $L^{-1}$) | 6–6.5 | 3.9–4.7 |
| Iron (mg $L^{-1}$) | 70–115 | 38–44 |
| Toxicity (activated sludge inhibition) | 53% | 0% |
| Total Solids (g $L^{-1}$) | 1.7 | <Detection limit |

Lab), its concentration was determined following DIN 38409 H15. Both iron and hydrogen peroxide were measured in a Unicam Uv/Vis UV2 spectrophotometer, at 510 nm and 410 nm, respectively.

Toxicity and biodegradability along the electro-oxidation treatment were analyzed with a SURCIS BM-Advanced Respirometer. This equipment allows studying the stimulation or inhibition rate in activated sludge coming from a municipal wastewater treatment plant (MWWTP) by direct contact with the sample. Toxicity analyses were performed by feeding 1 L of activated sludge with sodium acetate (0.5 g per gram of volatile solids) and, when the Oxygen Uptake Rate (OUR) was stable, putting in contact with 30 mL of the sample. The change in this parameter gives the percentage of inhibition related to the OUR of the activated sludge. Biodegradability of the samples was measured by adding 100 mL of sample to 900 mL of activated sludge. The system gives the biodegradable COD (CODb) which must be compared with the total COD of the sample. According to the protocol of the respirometer, when the ratio CODb/COD is higher than 0.2 the sample is considered slightly biodegradable and so a biological reactor could be adapted.

### 2.3. Experimental set-up

The electro-oxidative process was carried out by using a monopolar electrolyzer with a dimensionally stable electrode formed by five anodes with a total surface of 0.324 $m^2$ and fed by a power supply able to reach 110 A and 25 V maximum in direct current (DC). Considering the manufacturer's specifications for this type of water, a fixed current density was established in 25 mA $cm^{-2}$. Reactor configuration consists of an open tank that contains the submerged electrode generating in-situ the oxidants for the degradation of recalcitrant compounds. The reactor treats up to 15 L per batch.

The electrochemical device was connected to a solar photo-reactor based on CPC with a total illuminated area of 3.08 $m^2$ and an illuminated volume of 22 L formed by 24 borosilicate glass tubes (150 cm length × 3.2 cm diameter) mounted on a platform tilted 37°. The total volume of the whole combined system was 38 L (Fig. 1).

Electro-oxidation experiments, with only the electrolyzer or combining with the CPC reactor, were developed by adding the wastewater to the open tank; homogenize the total volume by recirculation and running the electrolyzer. Samples were taken every 2 h of treatment. Sodium hydroxide was added if pH dropped under 3.5 in order to avoid the formation of toxic gaseous $Cl_2$.

In the experiments with hydrogen peroxide, after solution homogenization, 600 mg $L^{-1}$ of hydrogen peroxide were added. Afterwards, the electrolyzer started to operate. Periodically hydrogen peroxide was added trying to maintain a stable concentration of 600 mg $L^{-1}$ throughout the experiment. As in the previous case, samples were taken every 2 h of treatment.

Photo-Fenton tests for comparison purposes were carried out by using the CPC photo-reactor alone. The operating conditions were pH 3 and an initial concentration of hydrogen peroxide of 1000 mg $L^{-1}$. The addition of iron was not necessary due to the high

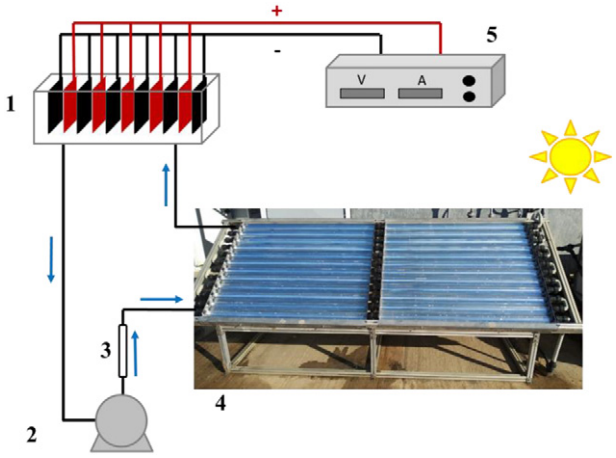


**Fig. 1.** Pilot plant scheme: (1) electrolyzer, (2) pump, (3) rotameter, (4) CPC, (5) power supply.

concentration present in the leachates. After 15 min of Fenton reaction (in dark), the CPC was uncovered starting the photo-Fenton process. Samples were taken every 15 min during the first hour and then every 30 min till reach 10 h of treatment. New additions of hydrogen peroxide were done with the aim of maintaining a concentration of above 500 mg $L^{-1}$ during the whole test.

The comparison between the different processes studied has been carried out by using Eq. (1), based on the relation between the degradation of DOC regarding to the energy required to reach it.

$$r_e = \Delta DOC/e \quad (1)$$

$r_e$ (g DOC $kWh^{-1}$) is the degradation rate, $\Delta DOC$ is the degradation of DOC (g DOC $m^{-3}$) along the treatment and $e$ is the electrical energy applied per volume treated (kWh $m^{-3}$). As well as for DOC, $r_e$ can be applied to compare efficiencies according to other parameters, such as TN.

Solar radiation collected in the CPC ($Q_{uv}$), is considered separately since it comes from a different energy source and so it is not included in Eq. (1). For avoiding confusions, the units for solar collected energy were kJ $L^{-1}$ instead of kWh $m^{-3}$ which corresponds to electrical consumption.

Solar ultraviolet radiation (UV) was measured by a global UV radiometer KIPP&ZONEN, model CUV 3 installed at Plataforma Solar de Almería (Spain) and tilted of 37° according to the local latitude, as the CPC. Eq. (2), allows the combination of the data from several days of experiments and their comparison with other tests (Malato et al., 2003).

$$Q_{UV,n} = Q_{UVn-1} + \Delta t_n \cdot \overline{UV}_{G,n} \cdot A_i/V_t ; \Delta t_n = t_n - t_{n-1} \quad (2)$$

where $Q_{UV,n}$ (kJ $L^{-1}$) is the accumulated UV energy per unit of volume, $\overline{UV}_{G,n}$ (W $m^{-2}$) is the average solar ultraviolet radiation ($\lambda < 400$ nm) measured between $t_n$ and $t_{n-1}$ being $n$ the number of sample, $A_i$ (3.08 $m^2$) is the irradiated surface and $V_t$ is the total volume.

## 3. Results and discussion

### 3.1. Preliminary solar photo-Fenton tests

As first approach to the treatment of the target wastewater, solar photo-Fenton test at pH 3, was carried out in order to compare with the results obtained when applying electro-oxidation alone or combined with the solar CPC photo-reactor.

Leachate 1 showed a strong dark color that hindered the transmission of photons inside the reactor tubes so, for oxidation studies it was diluted 1:1 with demineralized water in order to enhance the treatment itself. Moreover, due to the high organic load and the complexity of the

water, during the first stages of the treatment a large amount of foam was generated retaining DOC and TN, which, in turn, was re-dissolved in the water bulk during the treatment, causing oscillations in the parameters monitored (Fig. 2). TN was not degraded during the experiment and DOC started to decrease only after 75 kJ $L^{-1}$ of accumulated UV energy, approximately. Finally, after 10 h of treatment, with a $Q_{uv}$ of 142.2 kJ $L^{-1}$ and a $H_2O_2$ consumption of 3.3 g $L^{-1}$, almost 30% of mineralization (DOC abatement) was reached though TN did not change.

Since the organic load of leachate 2 was higher than 1, despite diluting it, the huge foam production made unfeasible the monitoring of DOC along the treatment. TN did not change during the treatment of leachate 2 by solar photo-Fenton at pH 3 (data not shown).

### 3.2. Electro-oxidative treatments

Electrochemical advanced oxidation processes (EAOPs) tested for the treatment of landfill leachates (without any dilution) were the electrolyzer alone, electrolyzer combined with solar treatment, and the electrolyzer with the addition of hydrogen peroxide (Fenton process using Fe content of leachate, see Table 2). The results obtained in each one of these processes, are summarized in Table 3, including those obtained with solar photo-Fenton treatment of leachate 1 (shown above).

Main difference between both leachates is their conductivity and TN (see Table 2). Electrical consumption when the electrolyzer was applied alone was higher in the treatment of leachate 1, as well as when combining with solar CPC. Even when solar energy assisting the electrolytic process, higher accumulated UV energy was required for leachate 1. These results confirm that the organic matter contained in younger leachate (leachate 2) was easier to degrade than the recalcitrant organics contained in the more mature leachate (leachate 1).

According to DOC elimination rate (g DOC $h^{-1}$), it can be observed, for both leachates, that the combination with the CPC photo-reactor did not implied an acceleration in DOC abatement. Regarding TN removal rate (g TN $h^{-1}$), for leachate 1 there was no enhancement when using the combined system, however leachate 2 showed an increase of 1.5 g TN $h^{-1}$ in its elimination.

When considering organics degradation rate as a function of the electrical energy applied, $r_e$, instead of treatment time, solar-assisted electrolytic processes entailed a clear improvement increasing the DOC and TN removal per applied kWh, evidencing that the application of solar radiation favors the formation of chlorine radicals, which provoked extra DOC and TN removal lower electrical consumption.

The potential benefits of hydrogen peroxide addition (Fenton process combined with electrolytic process) were studied by maintaining a hydrogen peroxide concentration of 600 mg $L^{-1}$ throughout the entire electrolytic process (Test $C_1$). Total amount of hydrogen peroxide consumed was 7.32 g $L^{-1}$. Despite adding a large amount of hydrogen peroxide, no remarkable improvement was obtained regarding any key parameter. This effect would be provoked by the fact that hydrogen peroxide was also oxidized in the anode generating hydroperoxyl radicals of lower oxidation potential, $E^0 = 1.06$ V (Buettner, 1993), following Reaction 7 but in turn it could be also consumed in the own anode by Reaction 8.

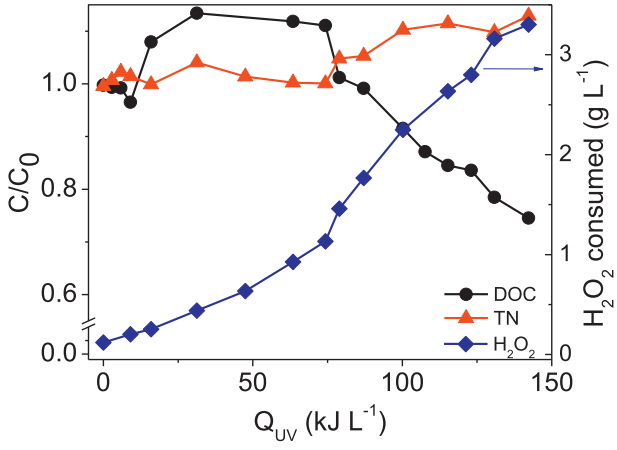


**Fig. 2.** Evolution of DOC, TN and hydrogen peroxide consumption along the solar photo-Fenton treatment.

**Table 3**
Summary of the results obtained in solar photo-Fenton, electrolytic treatment, electrolytic combined with solar treatment and electrolytic treatment with $H_2O_2$ applied to leachate 1 and 2.

| | P-$F_1$ | $A_1$ | $B_1$ | $C_1$ | $A_2$ | $B_2$ |
|---|---|---|---|---|---|---|
| $e$ (kWh $m^{-3}$) | – | 357 | 96.3 | 278 | 244 | 54.0 |
| $Q_{UV}$ (kJ $L^{-1}$) | 142 | – | 232 | – | – | 126 |
| DOC removal (g DOC $h^{-1}$) | 0.8 | 0.6 | 0.6 | 0.5 | 1.6 | 1.9 |
| TN removal (g TN $h^{-1}$) | 0 | 4.0 | 3.0 | 3.8 | 4.9 | 6.4 |
| $r_e$ DOC (g DOC $kWh^{-1}$) | – | 1.3 | 3.5 | 1.2 | 5.5 | 13.4 |
| $r_e$ TN (g TN $kWh^{-1}$) | – | 9.2 | 18.0 | 9.1 | 16.7 | 45.2 |
| $H_2O_2$ consumption (g $L^{-1}$) | 3.3 | – | – | 7.3 | – | – |

(P-F) solar photo-Fenton; (A) electrolyzer; (B) electrolyzer + solar CPC; (C) electrolyzer + $H_2O_2$ (1) leachate 1 (2) leachate 2.

$$H_2O_2 \rightarrow HO_2^{\cdot} + H^+ + e^- \quad (R.7)$$

$$HO_2^{\cdot} \rightarrow O_{2(g)} + H^+ + e^- \quad (R.8)$$

In view of the low efficient results obtained in $C_1$, it was decided not to test leachate 2 with the addition of hydrogen peroxide to the electrolytic process.

DOC and TN evolution along the studied processes are plotted in Fig. 3a and b, respectively. All cases showed a moderate DOC removal, being close to 50% for the best case. Higher and faster DOC removal were observed for leachate 2 (younger one) when applying both processes and with lower energy consumption when combining with the solar CPC. Conversely, TN removal showed the same behavior as DOC but reaching upper degradation (almost 100% in $A_2$ test). It is important to stress that one of the main advantages of applying an electrochemical system is the capacity of TN elimination compared with other processes based on the generation of hydroxyl radicals (such as photo-Fenton treatment) (Bejan et al., 2013). Elimination of TN is based on the reaction of generated ACS with ammonia that produced gaseous $N_2$ and chloride (Reaction 9).

$$2NH_4^+ + 3HClO \rightarrow N_2 + 3H_2O + 5H^+ + 3Cl^- \quad (R.9)$$

### 3.3. Chloride monitoring

From chloride present in leachates, ACS were generated having a crucial role in the degradation process. Fig. 4 shows the evolution of chloride, which in all cases decreased due to its continuous oxidation on the anode forming ACS. Part of them was not combined with organic matter, known as free available chlorine (FAC), and other part reacted with organics, and for instance, in the presence of nitrogenous species, chloramines could be produced provoking toxicity into the solution if they are not completely removed during the treatment.

In $A_1$ and $C_1$ tests the generation of oxidizing species was low, evidenced by the decrease of chlorides (Fig. 4), affecting the DOC degradation rate, being $r_e$ = 1.3 and 1.2 g DOC $kWh^{-1}$ for $A_1$ and $C_1$, respectively. $B_1$ treatment, that combined electrooxidation with solar CPC reactor, increased DOC degradation rate till $r_e = 3.5$ g DOC $kWh^{-1}$.

$A_2$ and $B_2$ treatments showed similar trends of chloride along the process, but $B_2$ showed higher DOC removal rate, being $r_e = 5.5$ and 13.4 g DOC $kWh^{-1}$ for $A_2$ and $B_2$, respectively. The higher degradation rates achieved in solar assisted treatments and similar chloride behavior confirmed the generation of oxidizing chlorine radicals from $ClO^-$ (see

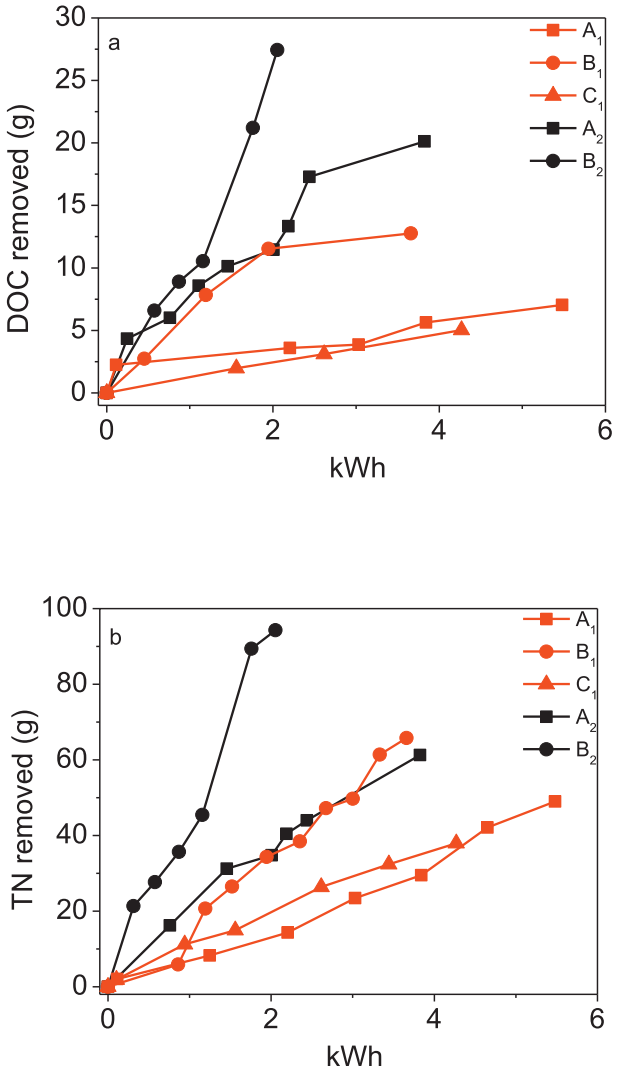


**Fig. 3.** (a) DOC and (b) TN evolution during the tested oxidation processes as function of the energy required: (A) electrolyzer; (B) electrolyzer + solar CPC; (C) electrolyzer + $H_2O_2$. (1) Leachate 1 and (2) leachate 2.

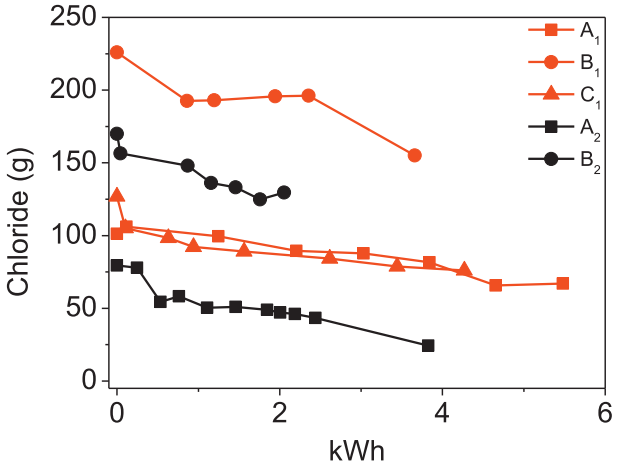


**Fig. 4.** Chloride evolution during the applied oxidation processes as function of the energy required: (A) electrolyzer; (B) electrolyzer + solar CPC; (C) electrolyzer + $H_2O_2$. (1) Leachate 1 and (2) leachate 2.

Table 1), so reducing the electric energy consumption in the electrolyzer, and, in consequence, also reducing the possible presence of chloramines.

### 3.4. Toxicity and biodegradability analysis

Evaluating the possibility of a subsequent application of a biological treatment after the electrochemical process in order to attain complete depuration of the target wastewater, both toxicity and biodegradability of partially treated leachates were monitored by means of respirometry assays using conventional activated sludge from a municipal wastewater treatment plant.

Toxicity tests showed absence of inhibition for raw leachate 2 but 53% of inhibition for leachate 1 (see Table 2). The treatment with electrolytic system combined or not with solar energy did not affect this parameter significantly for leachate 2. Nevertheless, positive effect was observed for leachate 1, in which the electrooxidation alone reduced inhibition till 6%, and when combined with CPC or with addition of hydrogen peroxide, toxicity was completely eliminated.

With respect to biodegradability results, for all the treatments tested the relation between $COD_b$ and COD finally attained values higher than 0.2, being exceptionally high in the case of $B_2$ test, in which a ratio of 0.75 was reached. Therefore, it was demonstrated that the tested electro-oxidative processes increased the biocompatibility of leachates, permitting a subsequent conventional aerobic biological system to achieve the complete treatment of the studied wastewater.

## 4. Conclusions

Solar photo-Fenton process has been demonstrated not to be suitable for the treatment of the landfill leachates under study, so Electrochemical Advanced Oxidation Processes has been tested with successful results as alternative for high salinity, high organic loaded and biorecalcitrant wastewaters, achieving both DOC and TN removal without the addition of any reagent.

Combination of electrolytic treatment with solar energy showed lower electrical consumption per volume of treated leachate compared with electrolytic treatment alone achieving biodegradability of the leachate with highest organic contents (leachate 2) with an electric consumption of 54 kWh $m^{-3}$ and a $Q_{UV}$ of 126 kJ $L^{-1}$ without the addition of any reagent. Generation of chlorine radicals from ACS present in water by solar radiation was corroborated, due to the increment in organics removal.

Toxicity and biodegradability were also improved by the combined oxidation processes, preventing, at least partially, the generation of chloramines making feasible the option of a subsequent biological treatment.

## Declaration of competing interest

The authors declare that they have no known competing financial interests or personal relationships that could have appeared to influence the work reported in this paper.

## Acknowledgements

The authors wish to thank the Spanish Ministerio de Ciencia, Innovación y Universidades for funding under the CalypSol Project (RTI2018-097997-B-C32).

## References

Armstrong, D.A., Huie, R.E., Koppenol, W.H., Lymar, S.V., Merényi, G., Neta, P., Ruscic, B., Stanbury, D.M., Steenken, S., Wardman, P., 2015. Standard electrode potentials involving radicals in aqueous solution: inorganic radicals (IUPAC technical report). Pure Appl. Chem. 87, 1139–1150.

Bashir, M.J.K., Aziz, H.A., Aziz, S.Q., Abu Amr, S.S., 2013. An overview of electro-oxidation processes performance in stabilized landfill leachate treatment. Desalin. Water Treat. 51, 2170–2184.
Bejan, D., Graham, T., Bunce, N.J., 2013. Chemical methods for the remediation of ammonia in poultry rearing facilities: a review. Biosyst. Eng. 115, 230–243.
Buettner, G.R., 1993. The pecking order of free radicals and antioxidants: lipid peroxidation, α-tocopherol, and ascorbate. Arch. Biochem. Biophys. 300, 535–543.
Chiang, L.-C., Chang, J.-E., Wen, T.-C., 1995. Indirect oxidation effect in electrochemical oxidation treatment of landfill leachate. Water Res. 29, 671–678.
de Morais, J.L., Zamora, P.P., 2005. Use of advanced oxidation processes to improve the biodegradability of mature landfill leachates. J. Hazard. Mater. 123, 181–186.
Deng, Y., 2009. Advanced oxidation processes (AOPs) for reduction of organic pollutants in landfill leachate: a review. Int. J. Environ. Waste Manag. 4, 366–384.
Deng, Y., Englehardt, J.D., 2007. Electrochemical oxidation for landfill leachate treatment. Waste Manag. 27, 380–388.
Kjeldsen, P., Barlaz, M.A., Rooker, A.P., Baun, A., Ledin, A., Christensen, T.H., 2002. Present and long-term composition of MSW landfill leachate: a review. Crit. Rev. Environ. Sci. Technol. 32, 297–336.
Li, W., Zhou, Q., Hua, T., 2010. Removal of organic matter from landfill leachate by advanced oxidation processes: a review. Int. J. Chem Eng. 2010, 1–10.
Malato, S., Blanco, J., Campos, A., Caceres, J., Guillard, C., Herrmann, J.M., Fernandez-Alba, A.R., 2003. Effect of operating parameters on the testing of new industrial titania catalysts at solar pilot plant scale. Appl. Catal. B Environ. 42, 349–357.
Martinez-Huitle, C.A., Brillas, E., 2009. Decontamination of wastewaters containing synthetic organic dyes by electrochemical methods: a general review. Appl. Catal. B Environ. 87, 105–145.
Nowell, L.H., Hoigné, J., 1992. Photolysis of aqueous chlorine at sunlight and ultraviolet wavelengths—II. Hydroxyl radical production. Water Res. 26, 599–605.
Primo, O., Rivero, M.J., Ortiz, I., 2008. Photo-Fenton process as an efficient alternative to the treatment of landfill leachates. J. Hazard. Mater. 153, 834–842.
Renou, S., Givaudan, J.G., Poulain, S., Dirassouyan, F., Moulin, P., 2008. Landfill leachate treatment: review and opportunity. J. Hazard. Mater. 150, 468–493.
Sirés, I., Brillas, E., Oturan, M.A., Rodrigo, M.A., Panizza, M., 2014. Electrochemical advanced oxidation processes: today and tomorrow. A review. Environ. Sci. Pollut. Res. 21, 8336–8367.
Turro, E., Giannis, A., Cossu, R., Gidarakos, E., Mantzavinos, D., Katsaounis, A., 2011. Electrochemical oxidation of stabilized landfill leachate on DSA electrodes. J. Hazard. Mater. 190, 460–465.
Wang, F., Smith, D.W., El-Din, M.G., 2003. Application of advanced oxidation methods for landfill leachate treatment - a review. J. Environ. Eng. Sci. 2, 413–427.
Wiszniowski, J., Robert, D., Surmacz-Gorska, J., Miksch, K., Weber, J.V., 2006. Landfill leachate treatment methods: a review. Environ. Chem. Lett. 4, 51–61.

Separation and Purification Technology

# Nanofiltration retentate treatment from urban wastewater secondary effluent by solar electrochemical oxidation processes

--Manuscript Draft--

| | |
|---|---|
| **Manuscript Number:** | SEPPUR-D-20-01148R1 |
| **Article Type:** | Full Length Article |
| **Section/Category:** | Advanced technologies in water and wastewater purification |
| **Keywords:** | Boron-doped diamond; electrochemistry; micropollutants; solar-assisted electrooxidation; wastewater regeneration |
| **Corresponding Author:** | ISABEL OLLER ALBEROLA<br>CIEMAT-PSA<br>TABERNAS, SPAIN |
| **First Author:** | Irene Salmerón |
| **Order of Authors:** | Irene Salmerón |
| | Gracia Rivas |
| | ISABEL OLLER ALBEROLA |
| | Ana Martínez-Piernas |
| | Ana Agüera |
| | Sixto Malato |
| **Abstract:** | Comparison of electrochemical processes at pilot plant scale for the elimination of organic microcontaminants (OMCs) in UWWTP secondary effluents pre-treated by nanofiltration ([Cl-] = 1100-2000 mg L-1) membranes have been addressed. Anodic oxidation (AO), solar-assisted AO, electro Fenton (EF) and solar photoelectron-Fenton (SPEF) processes have been evaluated by using, when required, ethylenediamine-N,N'-disuccinic acid (EDDS) as complexing agent to maintain iron in solution at natural pH. Target water was spiked with a mix solution of OMCs: pentachlorophenol, terbutryn, chlorfenvinphos and diclofenac format initial concentrations of 500 and 100 µg L-1, each. AO and EF processes obtained similar degradation rates as added EDDS competed with OMCs for oxidant species. SPEF and solar assisted AO showed that high chloride concentrations was a crucial factor since chlorine species generated by solar-assisted AO were enough for efficient OMCs removal avoiding the addition of EDDS. Degradation monitoring of OMCs contained in actual UWWTP effluents was carried out by LC-QqLIT-MS/MS. |
| **Suggested Reviewers:** | Ricardo Salazar<br>Universidad de Santiago de Chile<br>ricardo.salazar@usach.cl<br>Prof. Ricardo Salazar is a great expert in the application of advanced electrooxidation treatments for the elimination of contaminants. |
| | Ricardo Torres de Palma<br>Universidad de Antioquia<br>ricardo.torres@udea.edu.co<br>Ricardo Torres is a great expert in the topic of the aplicaction of electrooxidation systems combined with other technologies for the remediation of urban wastewater. |
| **Response to Reviewers:** | |

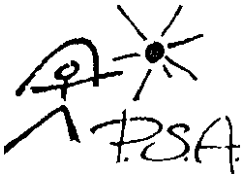

Plataforma Solar de Almería

Aptdo. 22

E-04200 Tabernas (Almería)

Tel.: 34-950387993 Fax.: 34-950 365015

e-mail: isabel.oller@psa.es

Tabernas, 7/29/2020

Dear Editor,

Please, find enclosed the revised manuscript according to reviewers´ suggestions: "Nanofiltration retentate treatment from urban wastewater secondary effluent by solar electrochemical oxidation processes" which co-authors are: Irene Salmerón, Gracia Rivas, Isabel Oller, Ana Martínez Piernas, Ana Agüera y Sisto Malato, to be published in *Separation and Purification Technology Journal*. Tables and Figures are included in the manuscript.

Supplementary information is also included at the end of the manuscript.

Thank you very much for considering this work to be published in this highly recognized journal.

Yours faithfully,

Corresponding author: Isabel Oller (isabel.oller@psa.es)

**Separation and Purification Technology (SEPPUR-D-20-01148)**

**Answers to the Editor and Reviewer comments:**

**Reviewer #1:** The authors provided an in depth field study of electrochemical treatment. With a great interest I started reading the article. Unfortunately the article is poorly written. Clarity is not there in entire manuscript? Abstract is dealing with urban wastewater treatment; introduction starts with industrial wastewater treatment. Several abbreviations in the manuscript, and all are confusing. For example, the authors used same abbreviations for advanced oxidation process and anodic oxidation. Whether the elctrochemical treatment methods used are of pilot scale? Language also needs to polished. Overall the article needs to be revised thoroughly. The manuscript can be submitted after revision.

**Answer:** We thank the reviewer for his/her comments. We have revised carefully the manuscript to avoid misunderstanding between "industrial and municipal WW treatment" as this work is focused on municipal wastewater tertiary treatment. Abbreviations have been also revised to avoid confusion from the reader´s side and are clearly stated in an abbreviations section in the first page of the Introduction. Specifically anodic oxidation is abbreviated as AO but Advanced Oxidation Processes by AOPs (which is internationally recognized in the scientific community). English style has been revised (not marked in the revised version).

**Reviewer #2:** This is an excellent paper which clear strengths are (i) treatment and larger scale, and (ii) treatment of real water samples. The manuscript presents a systematic and well-designed experimental plan to compare performance of anodic oxidation and Fenton-based electrochemical processes. The results are discussed with sound interpretations. The manuscript is of great quality and deserve publication. Some aspects that must be considered by the authors are described below"

**Answer:** We thank the reviewer for his/her comments.

1) "They can be applied before membranes with the aim of reducing fouling [6] or after them for the treatment of the rejection stream", and it can be used to prevent pore wetting (10.1016/j.chemosphere.2020.127214) which enhances the operational life of membranes.

**Answer:** Reviewer's suggestion has been included in the text as well as the new reference.

2) "strong oxidants such as HClO and ClO-, increasing the capacity to oxidize recalcitrant organic compounds" Note that these species are oxidants but not as stronger as hydroxyl radical. It is suggested to report the standard reduction potentials of these species and also to consider the electorgeneration of Cl* (a species formed during electrolysis with electrodes of high overpotential of oxygen evolution). Moreover, these aspects are discussed later on in the text in more detail, which make such statements redundant.

**Answer:** The sentence has been reformulated to avoid redundancies in the text. Oxidant potential of each one of the electrogenerated species that could appear in the system has been included in the text.

3) "i) inert surface regarding fouling," This statement is not correct. BDD electrodes can suffer biofouling and other classes of fouling, see (10.1016/j.elecom.2018.10.002). However, these electrodes have the capability of self-cleaning the surface through the oxidation of fouling.

**Answer:** The sentence has been corrected according to reviewer's suggestion and the reference included in the manuscript.

4) "efficient use of electrical energy" How so? What do the authors understand as high efficient use of electrical energy? Most of the time mineralization current efficiencies with BDD electrodes are around 5-10%. Or is that compared to other electrodes used in electrochemical oxidation?

**Answer:** In this case the efficiency in the use of electrical energy is related to other electrode materials. It has been specified in the text.

5) L59- Include the standard reduction potential of *OH for comparison with other species.

**Answer:** The standard potential of hydroxyl radicals has been included.

6) R3 should use the equilibrium arrow used for chemical equilibrium (two arrows one on top of the other).

**Answer:** It has been corrected as stated by the reviewer.

7) L83- It should be included the photodecarboxylation of iron-carboxylate complexes which increases the mineralization performance of the system.

**Answer:** Reactions of $Fe^{3+}$:EDDS photodecarboxylation have been included in introduction.

8) "An exhaustive review of the literature has evidenced a scarce number of works focused on the evaluation of solar-assisted electrochemical processes for the depuration of real and complex wastewater, finding only purely electrochemical processes" Indeed, the lack of such efforts may be misguiding research needs (10.1016/j.coelec.2020.03.001) and works on real water matrices are of the highest relevance to ensure successful translation of technology. Authors should re-emphasize this as one of the key points of this contribution.

**Answer:** We thank the reviewer for the observation and so we have included a sentence highlighting this issue in the introduction after the sentence mentioned by the reviewer. Suggested reference has been also included in the manuscript.

9) L103- Is not the organic chelant mineralized due to generation of *OH and other oxidants?

**Answer:** The complex degradation by electrogenerated oxidant species has been followed by HPLC (Fig. 3). However, mineralization of EDDS was not monitored.

10) What was the purity of the selected target OMCs?

**Answer:** Selected OMCs have analytical grade. It has been included in the text.

11) L146- What do the authors refer with x-hydrate? Are not usually hepta-hydrate salts?

**Answer:** The hepta-hydrated Iron(II) sulphate is commonly used at acidic pH as $Fe^{2+}$ source. In this study we worked at natural pH using $Fe^{3+}$:EDDS complex, thus we used the Iron(III) sulphate salt x-hydrated at 75% of purity, where x-hydrate means hydrated. It has been corrected in the manuscript to avoid misunderstandings.

12) Fig. 1a) will benefit of identifying the different elements in the pictures. Both figures should be clearly tagged as a) and b).

**Answer:** It has been corrected.

13) Effective are is referred to the geometric area or the true electroactive area?

**Answer:** Effective area is referred to the geometrical area of the electrodes. It has been corrected in the manuscript.

14) "EDDS is completely mineralized in a short time in the environment, whereas other similar complexing agents are only partially degraded" How short is short? Can the authors be more quantitative regarding the time of life of the complexing agent in the environment?

**Answer:** According to Schowanek et al (1997) who performed a study about EDDS degradation (doi:10.1016/S0045-6535(97)00082-9), in 28 days 99% of EDDS mineralization is achieved in soils with a dose of 1 mg of EDDS per kg of soil and 66% is attained in water with a dose of 0.1 mg/L. From our point of view this information is not specifically strategic for the correct understanding of the whole manuscript and it could maybe introduce excessive data and other reviewers have already stated the complexity of the manuscript regarding variability of technologies and operation conditions so we considered better not including this information on the manuscript but we have included the reference of Schowanek work. If the reviewer or Editor still consider this information strategic to be included in the manuscript we will do it.

15) L280-283: If the complex is only stable during 15 min and it is indicative that it is degraded by *OH. Does the complexing agent compete with OMCs? The scavenging effect can be highly meaningful specially considering the high difference in concentration between OMCs and complexing agent.

**Answer:** As the complexing agent is an organic substance, it is going to compete with OMCs for *OH, using them in mineralization process instead of OMCs degradation (we already had that discussion on the former manuscript). That's also the reason why we propose the use solar-assisted AO as an alternative for retentate depuration to avoid the requirement of EDDS. It has been specified clearly with little new text.

16) Does the addition of complexing agent increase cost of operation? How much complexing agent should be added in continuous operation to keep the EF system running? It is interesting as a proof of concept, but it does not seem a practical approach (not even for OMCs with high degradation rates). A brief discussion on that would be beneficial, especially when the simple electrochemical oxidation seems to behave competitively and simpler to be operated. This is somehow stated later on in the text, but seems to be far apart from the initial tests discussed in section 3.1.

**Answer:** Initially the addition of the commercial complexing agent EDDS would increase operation costs, though taking into account the wide variety of electrooxidation treatments tested in this work, a deep economic assessment considering other operating costs related to electricity consumption and not only reagents addition, jointly with infrastructure costs (from CPC photoreactor), should be carried out in a future work. Regarding the continuous addition of EDDS for keeping the EF running, it could be a good operation strategy as stated in the text (at the same initial concentration) though further experiments must be carried out. In addition, it would also appear the problem normally found with conventional Fenton compared to solar photo-Fenton, as recovery of iron (II) without sunlight would not occur. We thank the reviewer for calling our attention to this issues that will be highly interesting to tackle in a future work, but we think that including this kind of discussion in the present manuscript further than it is already in the text, will provoke confusion on the reader and it is not actually the scope of this work.

17) "So, despite the increasing in *OH production, oxidant species were mainly consumed in the mineralization process rather than in OMCs degradation, which was supported by the increase in the mineralization percentage till 31%." This statement is not clear. Do the authors refer to the fact that even though mineralization occurs the process is not efficient on the degradation of OMCs, because produced *OH is consumed by the complexing agent? Rephrasing of that section will increase clarity to the reader.

**Answer:** Reviewer is right in what we refer to. Sentence has been slightly modified to clarify the meaning.

18) "The production of oxidizing species was determined by the mass transfer on the electrode, being the same in both configurations, and so reaching lower concentrations in SPEF due to the higher working volume." The production of oxidizing species is determined by the electroactive surface area and the current applied. However, the relative concentration of ROS and other oxidants depends on the electrode area/volume ratio.

**Answer:** We agree with the reviewer and so the sentence has been corrected accordingly.

19) L346-347- Is photoelectron-Fenton instead of photo-Fenton.

**Answer:** It has been corrected

20) L371-372: Were different cathodes used to avoid in situ generation of H2O2? Operation of a GDE without air may result in the malfunction of the system due to the percolation of water into the gas chamber. This has to be clarified previously in the experimental section.

**Answer:** In AO and solar assisted AO experiments, to avoid $H_2O_2$ electrogeneration, the carbon-PTFE cloth was removed leaving the support as counter cathode. The aim was to study the stand-alone BDD anode oxidation power thus the air chamber has not any function in that process. This explanation has been added to the experimental section.

21) Seems that the main mechanism of degradation is by chlorine species. Is there any risk associated to the formation of disinfection by-products?

**Answer:** In the processes FAC was produced, thus considering the nature of BDD anodes as non-active electrodes, probably there were OH radicals available to react with that FAC producing chlorates and perchlorates which can increase water toxicity. In addition, such chlorates and perchlorates could react mainly with the organic content of actual MWWTP effluent pre-concentrated in the NF system and so producing disinfection by-products. Anyway and being conscious that their formation as well as a complete toxicity assessment must be considered for a future work, any related discussion has been included in the text to avoid misunderstanding from the reader. This is the first study carried out at pilot plant scale and with actual wastewater in which direct AO assisted or not by solar energy is compared with EF and SPEF with interesting and successful results.

22) Reports from Bergmann group highlight the formation of perchlorates due oxidation by BDD electrodes, which is themed as health risk. Did the authors observe any formation of these species?

**Answer:** Regarding formation of chlorates and FAC, they were measured in this work and so they have been included now in the manuscript as requested by the reviewer as well as the kinetic constant of chlorides generation along the AO of actual wastewater. Such parameters were measured in experiments carried out with SNR and 500 µg/L of each OMCs and with actual wastewater. Perchlorates were not measured. As stated in the previous comment of the reviewer, those substances are risky for health and so could be considered as a source of product contamination in agriculture when treated wastewater is reused in crops irrigation. A conclusion has been also included in this sense in the manuscript. Nevertheless, we consider that this is a wide enough study that deserves a specific work program, jointly with the generation of disinfection by-products and toxicity assessment. Not the scope of this first manuscript.

**Reviewer #3:** This paper reports an original and well-made work dealing with the electrochemical treatment of a real retentate by nanofriltration contaminated with four known organics. Typical treatments such as AO, EF, SPEF and Solar AO are made, with Fe(III)-EDDS as chelated iron catalyst in EF and PEF. It is demonstrated that Solar AO is the preferable treatment with a BDD anode. The organic contaminant of the wastewater were well determined. I recommend publication with attention to the following comments:

**Answer:** We thank the reviewer for his/her comments.

1) The following very recent review should be cited to emphasize the interest of SPEF for water treatment: E. Brillas, Chemosphere 250 (2020) 126198

**Answer:** The review has been included in the manuscript.

2) From experimental section one can conclude that a GDE electrode fed with air is always used. In such a case the processes are called AO with electrogenerated $H_2O_2$ (AO-$H_2O_2$) and Solar AO-$H_2O_2$.

**Answer:** In AO and solar assisted AO experiments any external addition of $H_2O_2$ was carried out and to avoid $H_2O_2$ electrogeneration, the carbon-PTFE cloth was removed leaving the support as counter cathode. It has been detailed in the experimental section.

3) L 280: Give, if possible, the reactions involved in Fe3+-EDDS decomposition. This complex is also destroyed by solar light, but this fact was not checked.

**Answer:** Reactions involved in $Fe^{3+}$:EDDS photodecomposition have been included in the introduction section and a study of $Fe^{3+}$:EDDS behaviour during EF processes in a supporting electrolyte has been also inserted. Effect of solar light on the complex degradation has been previously studied in other works, this is why only the stability and behaviour of the complex under high oxidant conditions in the electrooxidation system have been specifically studied in this work.

4) If experiments were replicated, the error bars have to be included in figures.

**Answer:** Replicas were not carried out in this work.

5) What is the final pH of the treatments checked.

**Answer:** pH change along the experiments was negligible, thus it has not included in the manuscript. Natural pH remained almost constant along treatments.

6) Why active chlorine was not measured in the solar treatments? This could help to understand the solar AO process.

**Answer:** FAC was not monitored for the first set of experiments (at 200µL of each OMC in SNR) as the main objective was to evaluate the behaviour of the system regarding mineralization and OMC removal. In the rest of experiments FAC was measured and data has been included in the manuscript as suggested by the reviewer.

7) It's a pity that COD and TOC decays were not measured during the experiments. These are important technological results to corroborate the beneficial of the solar treatments.

**Answer:** Though COD was not monitored along experiments, TOC (named as DOC when samples are filtered) has been measured in all the experiments and results discussed in the manuscript. As the reviewer suggests the monitoring of DOC allowed gave interesting results regarding mineralization and degree of competition with OMCs for hydroxyl radicals.

8) According to the explanations given, one can conclude that the SPEF process behaves as the Solar AO when all Fe3+ precipitates. Then, the superiority of the latter is due to the absence of additional EDDS that competes with the oxidation of organic pollutants. In this sense, it seems more apparent to use Fe(III)-oxalate complexes since they are completely photolyzed by sunlight.

**Answer:** The use of Fe (III)-oxalate would imply an enhancement regarding the EDDS as oxalate is photolyzed. However, in previous works (Huang et al 2012 https://doi.org/10.1016/j.jphotochem.2012.04.018) it has been demonstrated that its efficiency is lower than EDDS. In addition, and as stated by the previous reviewer, the addition of such complexing agents would also increase operation costs always.

9) The application of a high current density (7.5 A, for example) to a BDD anode in chloride medium originates chlorate and perchlorate ions. The concentration of these ions should be given.

**Answer:** Chlorates were measured in the final samples of experiments with SNR (500 µg/L of each OMC) and actual retentate from the effluent of MWWTP, so they have been included in the manuscript as suggested by the reviewer. Kinetic constant of chlorates generation along solar assisted AO of actual retentate of UWWTP effluent has been also calculated and included in the manuscript. Unfortunately perchlorates were not measured.

## Highlights

- OMCs removal by electrochemical processes enhance when combined with solar light.
- In EO, $Fe^{3+}$:EDDS keeps iron in solution during a short period of treatment time.
- At natural pH, chlorides are crucial for selecting the best electrochemical treatment.
- High amount of carbonates had non-scavenger effect on (solar) AO processes.

Graphical Abstract

Retentate

Nanofiltration

## Regeneration by Electro AOPs

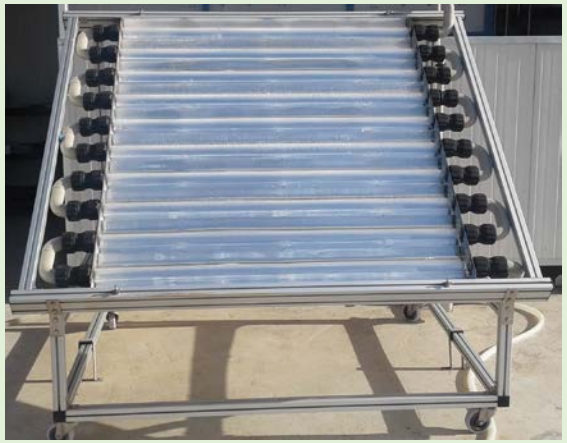

### Solar-assisted AO

$$ClO^- + H_2O + h\nu \rightarrow Cl^\bullet + {}^\bullet OH + OH^-$$

### SPEF Natural pH ❯ $Fe^{3+}$:EDDS

$$Fe^{2+} + H_2O_2 = Fe^{3+} + {}^\bullet OH + OH^-$$

$$[Fe(OH)]^{2+} + h\nu \rightarrow Fe^{2+} + {}^\bullet OH$$

# Nanofiltration retentate treatment from urban wastewater secondary effluent by solar electrochemical oxidation processes.

I. Salmerón[a,b], G. Rivas[a,b], I. Oller[a,b], A. Martínez-Piernas[b], A. Agüera[b], S. Malato[a,b].

[a]*Plataforma Solar de Almería-CIEMAT. Ctra Senés km 4, 04200 Tabernas (Almería), Spain.*

[b] *CIESOL, Joint Centre of the University of Almería-CIEMAT, 04120 Almería, Spain*

## Abstract

Comparison of electrochemical processes at pilot plant scale for the elimination of organic microcontaminants (OMCs) in UWWTP secondary effluents pre-treated by nanofiltration ([$Cl^-$] = 1100-2000 mg $L^{-1}$) membranes have been addressed. Anodic oxidation (AO), solar-assisted AO, electro Fenton (EF) and solar photoelectron-Fenton (SPEF) processes have been evaluated by using, when required, ethylenediamine-N,N'-disuccinic acid (EDDS) as complexing agent to maintain iron in solution at natural pH. Target water was spiked with a mix solution of OMCs: pentachlorophenol, terbutryn, chlorfenvinphos and diclofenac format initial concentrations of 500 and 100 μg $L^{-1}$, each. AO and EF processes obtained similar degradation rates as added EDDS competed with OMCs for oxidant species. SPEF and solar assisted AO showed that high chloride concentrations was a crucial factor since chlorine species generated by solar-assisted AO were enough for efficient OMCs removal avoiding the addition of EDDS. Degradation monitoring of OMCs contained in actual UWWTP effluents was carried out by LC-QqLIT-MS/MS.

**Keywords:** Boron-doped diamond, electrochemistry, micropollutants, solar-assisted electrooxidation, wastewater regeneration.

# 1. Introduction

The growth of chemical industry based on the development of products for personal care, pharmaceuticals or pesticides, involves the widespread in the environment of new recalcitrant substances unable to be removed by conventional secondary biological reactors in urban wastewater treatment plants (UWWTP). These substances are known as organic microcontaminants (OMCs), which, despite being in low concentrations, in the range of ng $L^{-1}$ - µg $L^{-1}$, can represent a serious concern to water bodies. Their direct impact on the ecosystem is still unknown and they can even affect humans due to their potential bioaccumulation. For this reason, the removal of OMCs is one of the main issues in wastewater regeneration, being crucial for the sustainability of modern chemical processes, the reuse of treated wastewater and the quality of water bodies.[1]

Separation processes have been widely applied on water regeneration. Nanofiltration (NF) or reverse osmosis commercial membranes have been applied for the removal of personal care products, drugs and pesticides from various water matrices [2] obtaining a very good quality permeate stream but also a retentate enriched with ions and OMCs [3-5]. Specifically, composite polyamide membranes exhibit greater rejection performance compared to other materials [2].

**Abbreviations**

ACS: Active chlorine species; AO: Advanced oxidation process; CVP: Chlorfenvinphos; DFC: Diclofenac; EDDS: Ethylenediamine-N,N'-disuccinic acid; EF: Electro-Fenton process; SPEF: Solar photoelectron-Fenton process; FAC: Free available chlorine; LC-QqLIT-MS/MS: Liquid chromatography coupled to a hybrid quadrupole/linear ion trap mass spectrometer; NF: Nanofiltration; OMCs: Organic Microcontaminants; PCP: Pentachlorophenol; SNR: Simulated nanofiltration retentate; TBT: Terbutryn; VRF: Volumen retention factor.

Electrochemical treatments can be considered as an interesting complement to membrane processes. They can be applied before membranes with the aim of reducing fouling [6] to prevent pore wetting enhancing the operational life of membranes [7] or after them for the treatment of the rejection streams. The main benefit when applied to the retentate is the reduction on the total volume to be treated, also involving an increase of OMCs concentration jointly with a decrease of the electrolyte ohmic resistance (increase of salinity), and so requiring lower cell voltage which would reduce the consumption of energy [8]. Accordingly, a higher concentration of ionic species in the retentate entails a higher electrogeneration of oxidants, increasing the capacity to remove recalcitrant organic compounds [9].

Regarding electrodes material, boron doped diamond (BDD) anodes present several characteristics that make them the most suitable for wastewater depuration: i) capability of self-cleaning through fouling oxidation [10], ii) high corrosion resistance, iii) stability up to high anodic potentials, iv) high oxygen evolution over-potential, involving high reactivity towards organics oxidation and v) higher efficient use of electrical energy regarding other electrode materials [9, 11, 12].

In the regeneration of high salinity wastewaters by BDD anodes, additionally to the generation of hydroxyl radicals ($^{\bullet}OH$) ($E^0$ = 2.8 V) at the anode surface, it is promoted the formation of a large number of oxidants in the bulk solution from dissolved ions. They are mainly active chlorine species (ACS) (hypochlorous acid and hypochlorite ion, $E^0$ = 1.49 V, $E^0$ = 0.86 V, respectively) and chloride radicals ($E^0$ = 2.4 V) from chlorides (reactions 1-4) [13], sulphate radicals ($E^0$ = 2.5 - 3.1 V) (reaction 5) [14], and even ozone ($E^0$ = 2.07 V) as product of low-saline water electrolysis (below 20 µS $cm^{-1}$) (reaction 6) [15, 16], increasing the oxidative treatment capacity. The formation of

oxidants in the bulk solution is limited by mass transfer as reactions are produced on the surface of the anode with limited contact area.

$$2Cl^- \rightarrow Cl_{2(aq)} + 2e^- \quad \text{(R.1)}$$

$$Cl_{2(aq)} + HO^- \rightarrow ClO^- + Cl^- + H^+ \quad \text{(R.2)}$$

$$HClO \rightleftarrows ClO^- + H^+ \quad \text{(R.3)}$$

$$Cl^- \rightarrow Cl^{\bullet} + e^- \quad \text{(R.4)}$$

$$SO_4^{2-} \rightarrow SO_4^{\bullet} + 2e^- \quad \text{(R.5)}$$

$$3H_2O \rightarrow O_3 + 6e^- + 6H^+ \quad \text{(R.6)}$$

The use of a gas diffusion electrode as cathode allows on-line $H_2O_2$ electrogeneration by $O_2$ reduction (reaction 7), so by adding iron, Fenton reactions are promoted and the process is known as electro-Fenton (EF) (reactions 8 & 9), producing an extra source of $^{\bullet}OH$ in the bulk solution [17, 18]. EF joined to the potentially great amount of oxidizing species generated in the anode, is considered as a powerful technology for the depuration of high saline waters as it was recently demonstrated by Tawabini et al. [19].

$$O_{2(g)} + 2H^+ + 2e^- \rightarrow H_2O_2 \quad \text{(R.7)}$$

$$Fe^{2+} + H_2O_2 \rightarrow Fe^{3+} + {}^{\bullet}OH + OH^- \quad \text{(R.8)}$$

$$Fe^{3+} + H_2O_2 \rightarrow Fe^{2+} + {}^{\bullet}{}_2OH + H^+ \quad \text{(R.9)}$$

Furthermore, this process can be improved by the application of solar light, regenerating iron (III) to iron (II) and so allowing to occur photo-Fenton process, which is known as solar photoelectro-Fenton (SPEF) (reaction 10). SPEF also promotes the formation of chlorine radicals from the ACS by radiation at 310 and 313 nm [20, 21] (reactions 11 and 12).

$$[Fe(OH)]^{2+} + h\nu \rightarrow Fe^{2+} + {}^{\bullet}OH \quad \text{(R.10)}$$

$$ClO^- + H_2O + h\nu \rightarrow Cl^{\bullet} + {}^{\bullet}OH + OH^- \quad \text{(R.11)}$$

$$HClO + h\nu \rightarrow Cl^{\bullet} + {}^{\bullet}OH \quad \text{(R.12)}$$

Working at neutral pH along EF and SPEF processes require the addition of a complexing agent to avoid iron precipitation. In this sense, EDDS is highly used as a safe and environmentally benign complexing agent in Fenton-like processes [22]. However, since $Fe^{3+}$:EDDS complex is photosensitive, its stability under photocatalytic processes is limited, being degraded till $Fe(OH)_3$ that immediately precipitates. A detailed study of $Fe^{3+}$:EDDS photodecarboxylation mechanism during solar photo-Fenton processes has been developed by Soriano-Molina et al.[23] which can be simplified in reactions 13-17[24].

$$Fe^{3+}\text{:EDDS} + h\nu \rightarrow [Fe^{3+}\text{:EDDS}]^* \quad \text{(R.13)}$$

$$[Fe^{3+}\text{:EDDS}]^* \rightarrow Fe^{2+}\text{:EDDS} + H^+ \quad \text{(R.14)}$$

$$Fe^{2+}\text{:EDDS} + H_2O_2 \rightarrow Fe^{3+}\text{:EDDS} + {}^{\bullet}OH + OH^- \quad \text{(R.15)}$$

$$Fe^{2+}\text{:EDDS} + \rightarrow Fe^{2+} + EDDS^{\,3-\bullet} \quad \text{(R.16)}$$

$$Fe^{2+} + H_2O_2 \rightarrow Fe(OH)_3 + {}^{\bullet}OH + OH^- \quad \text{(R.17)}$$

An exhaustive literature review has evidenced a scarce number of works focused on the evaluation of solar-assisted electrochemical processes for the depuration of real and complex wastewaters, finding only purely electrochemical processes [9, 25-27]. In consequence, it must be highlighted that one of the key strong points of the present study is the application of electrooxidation treatments not only at pilot plant scale but also to different actual wastewaters.

111 The present work addresses the comparison of different electrochemical treatments:
112 anodic oxidation (AO), EF, SPEF and AO assisted by solar energy, in order to find the
113 best alternative for the treatment of NF retentates. Two different water matrices were
114 evaluated: a synthetic retentate with medium content of chlorides (in the range of
115 550 mg $L^{-1}$, from natural water) and an actual wastewater with higher concentration of
116 chlorides (in the range of 1200-2000 mg $L^{-1}$, after NF pre-concentration of an UWWTP
117 effluent), spiked with a mix of four OMCs (pentachlorophenol, PCP; terbutryn, TBT;
118 chlorphenvinfos, CVP and diclofenac, DFC). All the processes were tested at natural
119 pH. In the case of EF and SPEF, iron was kept in solution at natural pH by the addition
120 of the commercial chelate Ethylenediamine-N,N'-disuccinic acid (EDDS) as iron
121 complexing agent [28]. Once the most suitable electrochemical treatment was selected,
122 an assay was carried out to verify the effectiveness of the process for the removal of
123 OMCs actually contained in the NF retentate of an UWWTP effluent. OMC degradation
124 was monitored by liquid chromatography coupled to a hybrid quadrupole/linear ion trap
125 mass spectrometer (LC-QqLIT-MS/MS).

126

127 ## 2. Materials and methods

128 ### *2.1 Water matrices*

129 #### *2.1.1 Simulated Nanofiltration Retentate*

130 A synthetic recipe of Simulated Nanofiltration Retentate (SNR) was developed
131 according to the composition described by Miralles-Cuevas et al. [29], of the retentate
132 obtained from a UWWTP effluent in El Ejido (Almería, Spain) operating in batch mode
133 after achieving a volume retention factor (VRF) of 4. This means reducing 4 times the
134 initial effluent volume, taking into account that NF membranes do not retain

135 monovalent ions. Maximum values for main ions were stablished as follows: 500 mg $L^{-1}$ of $Cl^-$, 1500 mg $L^{-1}$ of $SO_4^{2-}$, 1050 mg $L^{-1}$ of $Na^+$, 213 mg $L^{-1}$ of $Ca^{2+}$, 20 mg $L^{-1}$ of $NH_4^-$, 50 mg $L^{-1}$ of $Mg^{2+}$, 40 mg $L^{-1}$ of $K^+$ and 100 mg $L^{-1}$ of $NO_3^-$. To avoid a strong $^{\bullet}OH$ scavenger effect, inorganic carbon was established at 160 mg $L^{-1}$, which corresponds to the natural inorganic carbon found in the tap water at the Plataforma Solar de Almería (PSA), Spain.

141 According to these premises, SNR was formulated by using 82 mg $L^{-1}$ of $Ca(NO_3)_2$ (from Sigma-Aldrich), 1420 mg $L^{-1}$ of $Na_2SO_4$ (from Sigma-Aldrich), 87 mg $L^{-1}$ of $K_2SO_4$ (from Merck Millipore), 340 mg $L^{-1}$ of $CaSO_4$ (from Panreac), 497 mg $L^{-1}$ of NaCl (from Sigma-Aldrich), 66 mg $L^{-1}$ of $(NH_4)_2SO_4$ (from Merck Millipore) and 21 mg $L^{-1}$ of $Na_2HPO_4$ (from Panreac) dissolved in natural water. The final ionic composition of SNR and natural water are shown in Table SI-1 (see supplementary information).

148 *2.1.2 UWWTP effluent*

149 Actual UWWTP secondary effluent was collected from El Ejido (Almería, Spain) during the dry season, (April - July 2019). Before experimentation, wastewater was filtered through a 75 microns sand filter and two polypropylene wound filter cartridges of 25 and 5 microns, respectively. Most significant physicochemical measured parameters were: 2.1-2.3 mS $cm^{-2}$ of conductivity and COD between 17 and 50 mg $L^{-1}$. The rest of the effluent characterization is shown in Table SI-2 (see supplementary information).

156 *2.2 Chemicals*

157 Selected target OMCs were PCP, TBT, CVP and DFC (from Sigma-Aldrich, analytical grade). OMCs were previously dissolved in methanol in two stock solutions of 2.5 and

159 6.25 g $L^{-1}$ (of each OMCs), aiming to add to the experiments the similar amount of
160 dissolved organic carbon (DOC) coming from methanol, when working at low initial
161 concentrations, between 100 – 200 µg $L^{-1}$, or higher, 500 µg $L^{-1}$.

162 $Fe^{3+}$:EDDS complex, in a concentration rate of 0.1:0.2 mM, was prepared dissolving
163 iron (III) sulfate hydrate (~75% pure) from Panreac into acidified water (pH 2.8) in
164 darkness conditions. After this, the desired amount of EDDS (from Sigma-Aldrich) was
165 added stirring vigorously until the solution took a very intense yellow colour indicating
166 the proper formation of the complex.

167 *2.3 Analytical measurements*

168 A LAQUAact PH110 (HORIBA) portable pHmeter was used to monitor pH. Electric
169 conductivity was determined by a GLP 31 conductimeter from CRISON. DOC and
170 carbonates were measured by a TOC-VCSN analyser (Shimadzu), after filtering the
171 samples through 0.45 µm nylon filter from ASIMIO. Chemical Oxygen Demand (COD)
172 was measured by a Cell Test Spectroquant® from Merck.

173 Anion and cation concentrations were measured by ion chromatography (IC) in a
174 Metrohm 850 Professional IC after sample dilution (1:10 and 1:25, *v/v*) after filtration
175 through a 0.45 µm nylon filter from ASIMIO. For anions, it was used a Metrosep A
176 Supp 7 150/4.0 column thermoregulated at 45˚C with 3.6 mM of sodium carbonate as
177 eluent at 0.7 mL $min^{-1}$. For cations the column used was a Metrosep C6 150/4.0 with an
178 eluent solution of 1.7 mM nitric acid and 1.7 mM dipicolinic acid at1.2 mL $min^{-1}$.

179 Free available chlorine (FAC) was determined by the DPD Method 10069 from Hach,
180 using DPD powder pillows and measuring absorbance at 530 nm. Iron concentration
181 was measured following ISO 6332 and hydrogen peroxide following DIN 38409 H15,

182 at 510 nm and 410 nm, respectively. The spectrophotometer used for those analyses was
183 an Evolution 220 UV-Visible from Thermo Scientific.

184 Degradation of OMCs was monitored by a UPLC/UV Agilent Series 1200 system,
185 equipped with a reverse phase column ZORBAX Eclipse XDB-C18 (4.6 x 50 mm,
186 1.8 µm particle size, Agilent Technologies). Initial conditions of the method were 90/10
187 (*v/v*) ultrapure water with formic acid 25 mM and acetonitrile (ACN), achieving in
188 14 min 100% ACN at a flow rate of 1 mL $min^{-1}$. Inyection volume was 100µL. Sample
189 preparation before UPLC analysis consisted on a filtration step of 9 mL of the sample
190 through a 0.22 µm hydrofobic polytetrafluoroethylene (PTFE) membrane filter from
191 Millipore Millex. Then, the filter was flushed with 1 mL of ACN in order to extract any
192 absorbed compound. Analytical characteristics of the OMCs analyzed by UPLC/UV are
193 shown in Table SI-3 (see supplementary information).

194 $Fe^{3+}$:EDDS concentration was determined by a HPLC Agilent 1100 Series with a
195 reversed-phase column Luna C18 (150 x 3.00 mm, 5µm particle size), using an isocratic
196 method 95/5 (*v/v*) on buffer solution (2 mM tetrabutylammonium bisulfate - 15 mM
197 sodium formiate) and methanol. Inyection volume was 20 µL with a flow rate of 0.5 mL
198 $min^{-1}$. Maximun absortion of $Fe^{3+}$:EDDS occurs at 240 nm, and the limit of
199 quantification was 0.005 mM.

200 Evaluation of OMCs contained in actual UWWTP effluents was carried out by an LC
201 system (Agilent 1200 Series) coupled to a hybrid quadrupole-linear ion trap-mass
202 spectrometer (QqLIT-MS) 5500 QTRAP® from Sciex Instruments equipped with an
203 electrospray source (TurboIon Spray), operating in positive polarity. The analytical
204 column was a Kinetex C18 column (150 x 4.6 mm, 2.6-µm particle size; Phenomenex)
205 operated at a constant flow rate of 0.5 mL $min^{-1}$ and using an injection volume of 10 µL.

Eluent A was 0.1% formic acid in ultrapure water and eluent B was pure methanol. The analytical gradient was as follows: elution started with 20% B for 0.5 min, increased to 50% B within 3 min, and to 100% within 9.5 min, kept constant for 3.5 min and reduced to 20% B in 0.1 min. The total analysis run time was 13.1 min and the post-run equilibration time 6 min. The source settings were: ion spray voltage 5000 V; curtain gas 25 (arbitrary units); GS1 50 psi; GS2 40 psi; and 500 ºC. $N_2$ served as nebulizer, curtain and collision gas. Compounds were analysed by multiple reaction monitoring (MRM). To increase the sensitivity of the analytical method, the Schedule MRM™ algorithm was applied with a retention time window of 40 s per transition. The optimal MS/MS parameters for each compound are summarized in Table SI-4 (see supplementary information). Sciex Analyst version 1.6.2 software was used for data acquisition and processing. MultiQuant 3.0.1 software was used for quantification purposes.

### *2.4 Experimental Set-up*

#### *2.4.1 Preliminary $Fe^{3+}$:EDDS complex stability tests*

Stability of $Fe^{3+}$:EDDS in each tested water matrix was evaluated. Also the possible interactions with the highest positive charge ions were studied, as well as the oxidant effect of hypochlorite to $Fe^{3+}$:EDDS. Experiments were carried out in 1 L borosilicate stirring flasks in the dark. Water matrices used during the tests were demineralized water, demineralized water with 50 mM of $Na_2SO_4$ and SNR. For checking $Mg^{2+}$ and $Ca^{2+}$ effect, $MgSO_4$ and $CaSO_4$ were added in the concentration required to attain the same amount of divalent cations found in SNR, that is 247.6 mg $L^{-1}$ and 724.8 mg $L^{-1}$, respectively. Finally, hypochlorite effect was checked by adding 10 and 20 mg $L^{-1}$ (as NaClO) in demineralized water.

### *2.4.2 Nanofiltration pilot plant*

NF system (Fig. 1a and b) was composed by 400 L polypropylene feeding tank, 2.2 kW centrifugal pump (DP Pumps) with a frequency modulator and spiral-wound FILMTEC NF90-2540 membranes (2.6 $m^2$ of active area). Tests were carried out by adding the effluent to the feeding tank and passing the water through the membrane, recycling the retentate stream to the feeding tank and discarding the permeate stream. The system was operated in batch mode in order to reduce the total volume to be treated by subsequent electrooxidation processes. The feeding tank was periodically refilled to reduce 1 $m^3$ of UWWTP effluent to 250 L that is a VRF of 4. As NF pilot plant is controlled by a SCADA system, pressure, flow and conductivity of permeate and retentate streams were continuously monitored online.

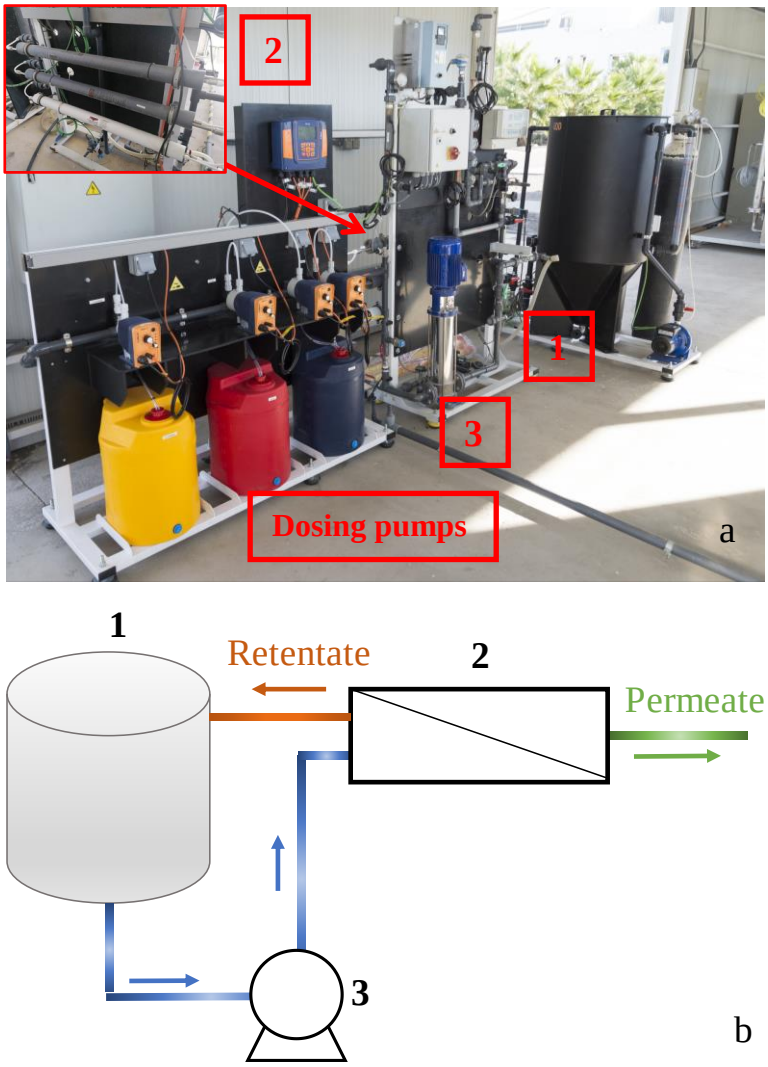


241
242 **Fig. 1**. a) NF pilot plant installed at Plataforma Solar de Almería. b) Scheme of the pilot
243 plant: 1) feeding tank, 2) NF membrane system, 3) centrifugal pump.

244

245 *2.4.3 Electrooxidation pilot plant*

246 Electrooxidation pilot plant consisted of an undivided electrochemical cell (Electro MP
247 Cell from ElectroCell) conformed by a boron-doped diamond film on a niobium mesh
248 substrate (Nb-BDD) as anode and a carbon-PTFE gas diffusion electrode (GDE) as
249 cathode, both with 0.010 $m^2$ geometrical area single-sides, separated by a 6 mm gap.
250 Carbon-PTFE GDE cathode was fed by compressed air (ABAC air compressor,

1.5 kW) at 10 L $min^{-1}$ and water flow rate in the cell was 300 L $h^{-1}$. When $H_2O_2$ electrogeneration was not necessary for AO and solar-assisted AO processes, carbon-PTEF cloth was removed using the support as counter cathode. Electrodes were connected to a Delta Electronika power supply (limited to 70 V and 22 A) that fed the cell fixing a constant current density (*j*) of 74 mA $cm^{-2}$, optimized by Salmerón et al.[30], in order to achieve the maximum $H_2O_2$ electrogeneration of 64.9 mg $H_2O_2$ $min^{-1}$ in the first 5 min with 50 mM of $Na_2SO_4$ as supporting electrolyte.

Electrochemical cell was coupled to a compound parabolic collector (CPC) photo-reactor, consisting of 10 borosilicate glass tubes mounted on an aluminium platform tilted 37º (PSA, 37º N, 2.4º W) with a total illuminated area of 2 $m^2$ and 23 L of illuminated volume. Working volume was 30 L in dark tests (AO and EF) and 75 L for solar-assisted electrochemical assays (solar-assisted AO and SPEF). Scheme of the solar-assisted electrooxidation pilot plant is shown in Fig. 2

Experiments were carried out by adding target wastewater (SNR or actual retentate stream) to the reservoir of the electrooxidation pilot plant. After that, OMCs from the stock solution were added, recirculating till their total homogenization and verifying their initial desired concentration. At that moment AO and solar assisted AO started, but in EF and SPEF assays, $Fe^{3+}$:EDDS was added after OMCs, homogenizing before starting the process.

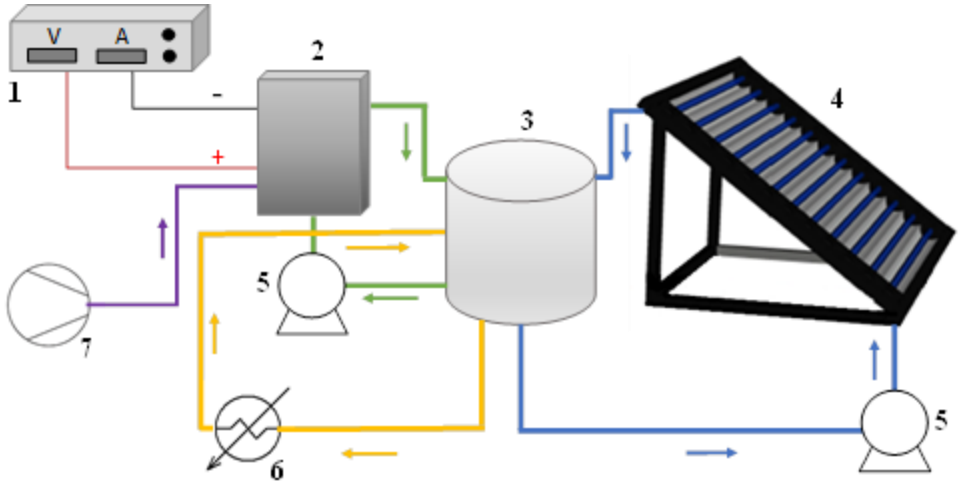


**Fig. 2**. Main components of the electrochemical pilot plant: 1) power supply, 2) ElectroCell with BDD anode and carbon-PTFE (GDE) cathode, 3) reservoir, 4) solar CPC photoreactor, 5) centrifugal pumps, 6) heat exchanger, 7) air compressor.

Temperature was always maintained between 25 and 35°C through a cooling coil connected to a heat exchanger.

Solar global ultraviolet radiation (UV) was measured with a CUV 3 UV radiometer from KIPP & ZONEN, installed at PSA and tilted 37° same as the CPC. Equation 1 allows the combination of the data from several days of experiment and their comparison with other tests [31].

$$Q_{UV,n} = Q_{UVn-1} + \Delta t_n \cdot \overline{UV}_{G,n} \cdot A_i/V_t\,; \quad \Delta t_n = t_n - t_{n-1} \qquad \text{(Eq.1)}$$

Where $Q_{UV,n}$ (kJ $L^{-1}$) is the accumulated UV energy per unit of volume, $\overline{UV}_{G,n}$ (W $m^{-2}$) is the average solar ultraviolet radiation (λ< 400 nm) measured between $t_n$ and $t_{n-1}$ being $n$ the number of sample, $A_i$ is the irradiated surface and $V_t$ is the total volume.

# 3 Results and discussion

## *3.1 Testing $Fe^{3+}$:EDDS stability*

EDDS is a structural isomer of ethylenediaminetetraacetic acid (EDTA) but more environmentally friendly, since it is not toxic and presents high biodegradability. EDDS is completely mineralized in a short time in the environment [32], whereas other similar complexing agents are only partially degraded [33, 34]. In fact, this advantage has made EDDS one of the most studied complexing agents to keep iron in solution at neutral pH, so enhancing the production of $^{\bullet}OH$, and therefore the degradation of OMCs [35].

As determined by Klamerth et al. 2012 [36], $Fe^{3+}$:EDDS molar ratio of 1:2 is the optimal in terms of degradation and energy consumption. This ratio was successfully used by Miralles-Cuevas et al. 2014 [37] in a complex water matrix (real NF retentate with a VRF of 4), for the degradation of a mix of OMCs in a concentration range of 47-63 µg $L^{-1}$, each and achieving 95% removal of the sum of OMCs in 86 min with a requirement of accumulated UV energy of 21.1 kJ $L^{-1}$.$Fe^{3+}$:EDDS behaviour during EF treatment by using 50 mM $Na_2SO_4$ solution as supporting electrolyte has been described elsewhere [38]. Nevertheless, to check the suitability of $Fe^{3+}$:EDDS for different electrochemical processes in a highly complex water, an EF assay was carried out with SNR as water matrix at natural pH. $Fe^{3+}$:EDDS was completely degraded in 15 min despite iron continued in solution for 30 min (Fig. 3), which can be explained by the presence of oxidized species of Fe:EDDS [39].

To evaluate the possible interaction with the highest positive charge ions contained in SNR, the stability of $Fe^{3+}$:EDDS was tested in the dark by using SNR and demineralized water containing $Na_2SO_4$ (50mM), $MgSO_4$ (247.6 mg $L^{-1}$) and $CaSO_4$

309 (724.8 mg $L^{-1}$). Fig. 3 shows, as expected, that the concentration of the complex
310 remained constant in all cases.

311 As hypochlorite was going to be generated during electrochemical processes (taking
312 into account the characterization of SNR, as well as UWWTP effluent), it was necessary
313 to determine $Fe^{3+}$:EDDS degradation caused by this oxidant, demonstrating that with 10
314 and 20 mg $L^{-1}$ of hypochlorite, $Fe^{3+}$:EDDS kept stable during at least one hour (data not
315 shown).

316 After these preliminary tests, it was also determined that the use of this complex in
317 electrochemical processes would be suitable for OMCs degradation with higher
318 degradation rates. However, it must be stressed that, for the most recalcitrant
319 compounds, the complex would have to be added continuously as it was degraded in 15
320 min, which would not be pertinent as a continuous addition of organic matter would
321 scavenge OMCs degradation.

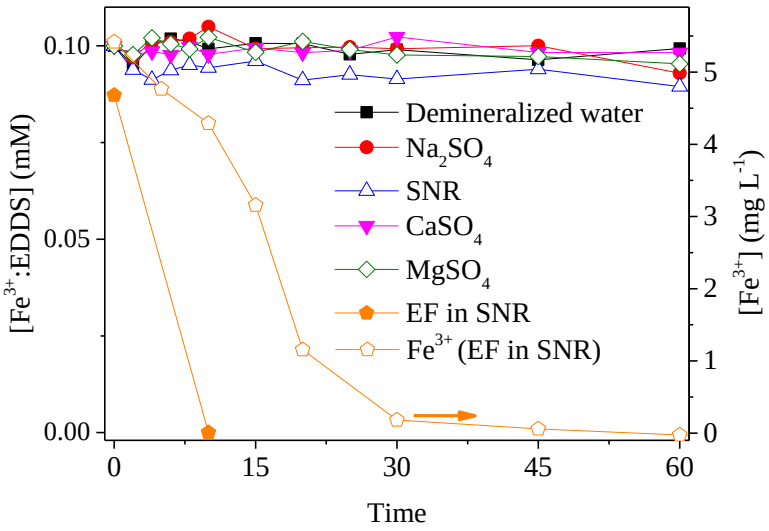

322

323 **Fig. 3.** Evolution of $Fe^{3+}$:EDDS in different water matrices and during EF processes in
324 SNR matrix. Evolution of dissolved iron during EF treatment is also plotted.

325 *3.2 Electrochemical oxidation of microcontaminants contained in simulated*
326 *nanofiltration retentate*

327 As a first approach, AO, EF and SPEF, were tested for the degradation of 200 μg $L^{-1}$ of
328 each selected OMC (PCP, TBT, CVP and DFC) in SNR (Fig. 4a). AO assays were
329 developed as reference, achieving the removal of 83% of the total amount of OMCs by
330 applying 13.9 kWh $m^{-3}$. The organic content, coming from the methanol of the OMC
331 stock solution simulated the organic carbon of a real MWWTP effluent (around 24 mg
332 $L^{-1}$) and was slightly mineralised (15% of DOC removal). In the case of EF treatment,
333 88% of the total OMCs were degraded with slightly higher energy consumption
334 (15.6 kWh $m^{-3}$), showing similar trend as AO. The addition of $Fe^{3+}$:EDDS in the EF
335 treatment implied a theoretical increase of 24 mg $L^{-1}$ of the organic carbon (52 mg $L^{-1}$ of
336 total initial DOC). So, despite the increasing in •OH production, oxidant species were
337 mainly consumed in the mineralization process of EDDS rather than in OMCs
338 degradation, which was demonstrated by the increase in the mineralization percentage
339 till 31%. Similar results were obtained by Huang et al. 2012 [35], in which 2,2-bis-(4-
340 hydroxyphenyl)propane (BPA) degradation by photo-Fenton was inhibited when the
341 concentration of the complex increased from 0.2 to 0.4 mM, evidencing the role of
342 EDDS as a competitor of OMCs for the •OH.

343 Moreover, in EF treatment, only 2.91 mg $L^{-1}$ of iron remained dissolved after 15 min,
344 being totally precipitated after 30 min. From the moment there was no iron in solution,
345 the degradation process proceeded only through the anode action (mainly physisorbed
346 •OH and ACS)

347 Since the EF treatment did not achieve a substantial improvement in the degradation of
348 OMCs compared with AO but entailed the addition of reagents that would imply an

increase in operating costs, it was discarded as an alternative for the NF retentate treatment.

In SPEF process (EF combined with a CPC photoreactor), the volume of water to be treated was much higher (75 L) than in AO or EF (30 L), while electrodes surface remained constant. The production of oxidizing species was determined by the electroactive surface area and the current applied, being the same in both configurations. However, the relative concentration of oxidants depends on the electrode area/volume ratio so lower concentrations in SPEF were reached due to the higher working volume. For such reason, despite the initial concentration of OMCs was the same, in terms of mass, the amount was much higher in SPEF than in AO or EF.

In SPEF, $Fe^{3+}$:EDDS was also required for maintaining iron in solution at neutral pH. Despite the increase in the mass of OMCs, it was shown an improvement in the degradation rate mostly at the beginning of the treatment, due to the oxidation of iron (II) to iron (III) that allowed photo-Fenton process occurred. Dissolved iron (5.5 mg $L^{-1}$) remained till 15 min of treatment, showing slow precipitation till 75 min, thus the degradation process went on for the generation of oxidizing species in the anode and for the solar promoted species. 14 kJ $L^{-1}$ of accumulated UV energy were required for the 88% elimination of the sum of OMCs.

Along SPEF process the generation of $H_2O_2$ (Reaction 7) never exceeded an accumulated value of 2.3 mg $L^{-1}$, which supposed an important limitation in the SPEF process. In consequence, an additional SPEF test was carried out by adding 10 mg $L^{-1}$ of $H_2O_2$ extra at the beginning of the test. In such a case, OMCs degradation rate increased greatly, verifying the limitation provoked by the lower ratio between electrode surface and total volume in SPEF compared to AO. Dissolved iron was totally precipitated after

30 min but at that time 80% of OMC removal was achieved. At the end of the treatment 96% of OMCs were removed with lower electrical energy consumption (5.9 kWh $m^{-3}$) and an accumulated solar UV energy of 8.8 kJ $L^{-1}$.

Considering the fast removal obtained when the initial concentration of each OMC was 200 µg $L^{-1}$, it was decided to increase it to 500 µg $L^{-1}$ for a better monitoring of the operating parameters (Fig. 4b). In this case, AO achieved 70% of OMCs removal in 30 min consuming 2.3 kWh $m^{-3}$ of energy (28 mg $L^{-1}$ of FAC and 11 mg $L^{-1}$ of chlorates). From that point, degradation rate decreased and 82% of OMC degradation was attained after consuming 15 kWh $m^{-3}$ accompanied by an increase of FAC till 71 mg $L^{-1}$ and chlorates till 55 mg $L^{-1}$. When SPEF was applied, the removal rate increased significantly, attaining 85% OMC removal with the requirement of 5.9 kWh $m^{-3}$ of electric consumption and 10.5 kJ $L^{-1}$ of $Q_{UV}$ after 180 min of treatment. In this experiment, iron showed the same trend as in previous SPEF test (without adding extra amount of $H_2O_2$), remaining after 15 min in solution at a concentration of 4.8 mg $L^{-1}$ and precipitating completely after 60 min. At that moment, the treatment went ahead by the action of other oxidant species (ACS among them considering SNR characterization) generated by the anode and assisted by solar energy, keeping the FAC stable between 22 and 31 mg $L^{-1}$ until 120 min (chlorates concentration was 17 mg $L^{-1}$), when 80% of OMC removal was reached.

From this point, FAC started to increase till 71 mg $L^{-1}$ at 180 min achieving 26 mg $L^{-1}$ of chlorates. This means that the degradation promoted by ACS stopped at 120 min and from that point instead of reacting with organics; they were accumulated in the solution as FAC.

In view of the results obtained by SPEF, the excess of FAC produced and inefficiently used at the end of the treatment, it was considered to test solar-assisted AO (without the addition of iron nor the in-situ generation of $H_2O_2$) in order to evaluate the effect of solar energy on the electrogenerated species and the oxidants produced avoiding the addition of EDDS which competes with OMCs for $^{\bullet}OH$.

In solar-assisted AO, chlorides concentration (550-565 mg $L^{-1}$ in SNR) has a crucial role as precursors of ACS. 76% of OMCs were degraded after an energy consumption of 5.9 kWh $m^{-3}$ and an accumulated UV energy of $Q_{UV}$ of 11.6 kJ $L^{-1}$. FAC showed similar behaviour as in SPEF, being constant (17 – 26 mg $L^{-1}$) till 150 min and increasing till 85 mg $L^{-1}$ after 180 min of treatment. As well as FAC, chlorates also showed same trend: 22 mg $L^{-1}$ at 150 min and 26 mg $L^{-1}$ at 180 min. Therefore, generated ACS and $Cl^{\bullet}$ in this specific wastewater were not enough to completely degrade the sum of OMCs, evidencing the crucial role of $^{\bullet}OH$ in SPEF.

(a)

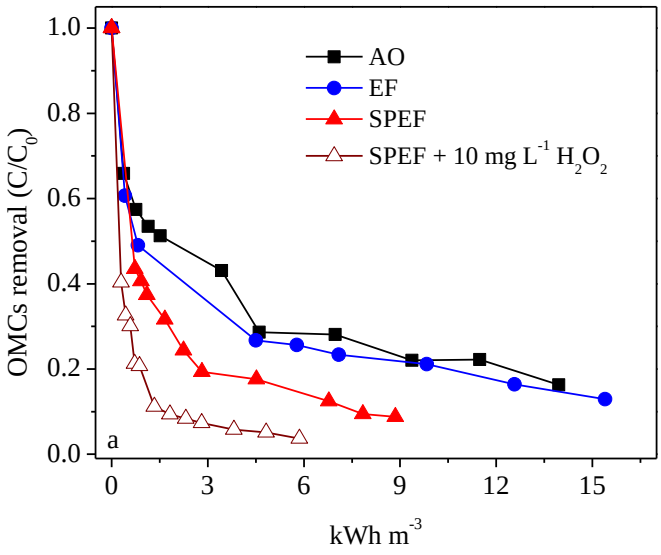


(b)

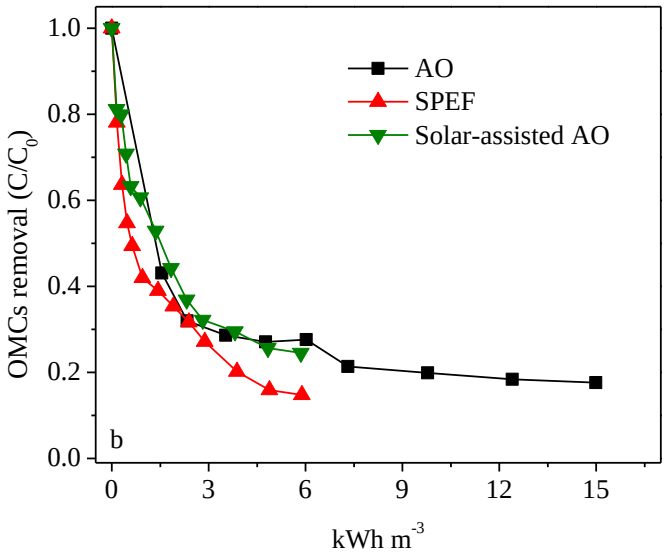


409

410 **Fig. 4.** Removal of the sum of OMCs (PCP, TBT, CVP and DFC) in SNR by using different
411 electroxidation processes. a) OMCs initial concentration of 200 µg $L^{-1}$, each b) initial
412 concentration of 500 µg $L^{-1}$, each.

413

### *3.3 Actual Nanofiltration Retentate treatment by electrochemical oxidation processes*

Several batches (1 $m^3$ each) were taken from the UWWTP secondary effluent of El Ejido (Almería) and introduced in the NF system (till attaining VRF of 4). Permeate stream generated contained only some monovalent ions that passed across the membrane (DOC below 2 mg $L^{-1}$ and carbonates below 25 mg $L^{-1}$), thus the conductivity kept under 100 µS $cm^{-1}$ during the most of the NF process and below 200 µS $cm^{-1}$ at the end due to the operation in batch mode. In such operation mode, retentate stream was recirculated into the feeding tank to reduce the total volume of final retentate and increase its conductivity for obtaining a better efficiency of the electrochemical processes. Table 1 shows its main physicochemical characteristics.

**Table 1.** Characterization of the retentate obtained in the NF plant from the UWWTP effluent.

| | | | |
|---|---|---|---|
| **Conductivity (mS $cm^{-1}$)** | 6.1 - 6.8 | **$SO_4^-$ (mg $L^{-1}$)** | 386 - 660 |
| **NTU** | 9 – 45 | **$Na^+$ (mg $L^{-1}$)** | 747 - 787 |
| **pH** | 8 - 8.6 | **$Ca^{2+}$ (mg $L^{-1}$)** | 259 - 273 |
| **DOC (mg $L^{-1}$)** | 31 – 42 | **$NH_4^+$ (mg $L^{-1}$)** | 46 - 76 |
| **COD (mg $L^{-1}$)** | 103 – 190 | **$Mg^{2+}$ (mg $L^{-1}$)** | 197 - 209 |
| **$HCO_3^-$ (mg $L^{-1}$)** | 1010 – 1316 | **$K^+$ (mg $L^{-1}$)** | 62 - 71 |
| **$Cl^-$ (mg $L^{-1}$)** | 1182 – 1960 | **$NO_3^-$ (mg $L^{-1}$)** | 25 - 27 |

Commonly, actual concentration of OMCs in UWWTP effluents is very low reaching, at most, tens of µg $L^{-1}$ as found in Luo et al. 2014 [40]. For this reason, in actual NF retentate experiments, the spiked concentration of OMCs was 100 µg $L^{-1}$ each (PCP, TBT, CVP and DFC), trying to address a more realistic approach jointly with a direct analysis by UPLC/UV.

From the physicochemical characterization of NF retentate it must be highlighted the presence of a high concentration of carbonates, which are well known scavengers of hydroxyl radicals in Fenton and photo-Fenton processes [41]. Nevertheless, their influence in electro-oxidative processes has not been defined, yet. In order to investigate this matter, each electrochemical treatment has been carried out with the natural hydrogen carbonate present in the retentate stream (> 1000 mg $L^{-1}$), but also lowering it till 20 mg $L^{-1}$ by adding acid and purging with air.

Results from AO (Fig. 5) showed exactly the same trend of OMC degradation in high and low hydrogen carbonate concentration, achieving 84% and 83%, respectively. About DOC elimination, it was attained 9% and 12% in the presence of high and low concentration of hydrogen carbonate, respectively, remaining at the end of the treatment 17 mg $L^{-1}$ and 4 mg $L^{-1}$ of FAC, and 47 and 42 mg $L^{-1}$ of chlorates. In both cases results are similar, and the slight difference found can be explained due to the recalcitrant character of the organic matter contained in the different water batches used, that despite achieved higher concentration of oxidizing species, they were not able to degrade the organic content. Therefore, in our study carbonates had no substantial effect on AO or any scavenger effect on ACS and $Cl^{\bullet}$.

This is consistent with what Xiong et al., [42] described in their study of propranolol degradation with UV-LED/chlorine system testing hydrogen carbonate concentrations till 840 mg $L^{-1}$ (10 mM) without finding a remarkable difference in removal rates.

Regarding SPEF, retentate with high concentration of hydrogen carbonate showed 69% of OMC degradation applying 5.1 kWh $m^{-3}$and requiring 14.2 kJ $L^{-1}$ of accumulated UV energy. At lower concentration of hydrogen carbonate, with the same electrical consumption (5.2 kWh $m^{-3}$) and even lower $Q_{UV}$ (10.8 kJ $L^{-1}$), higher OMC degradation

457 was reached (75%) and thus it can be said that carbonates had a slight effect on SPEF.
458 DOC degradation was 17% in both cases, and final FAC was extremely low, 1.1 mg $L^{-1}$
459 and 0.7 mg $L^{-1}$ under both operating conditions, which means that most of the oxidant
460 species were consumed by the organic load. Regarding chlorates, concentration reached
461 24 mg $L^{-1}$ and 16 mg $L^{-1}$ for both high and low hydrogen carbonates content,
462 respectively, showing a possible quencher effect in chlorates due to the presence of
463 carbonates in the solution.

464 Inasmuch AO process was not affected by carbonates concentration, a solar-assisted AO
465 test was developed with the retentate at natural (high) hydrogen carbonate
466 concentration. With 5.3 kWh $m^{-3}$ and 13.8 kJ $L^{-1}$ of accumulated UV energy, 84% of
467 OMC removal was achieved, higher than in all previous experiments. FAC reached was
468 3.9 mg $L^{-1}$ slightly higher than in SPEF with the same water matrix even with a lower
469 DOC removal of 9%. Probably provoked by the higher recalcitrant character of organic
470 matter contained in the actual water matrix itself used in AO and solar-assisted AO in
471 regard with the easy mineralization of EDDS used in SPEF. Chlorates measured at the
472 end of the process were 30 mg $L^{-1}$, in the same range of previous solar-assisted
473 treatments (solar-assisted AO and SPEF).

474 In electrochemical treatments, chloride is the precursor of ACS and $Cl^{\bullet}$, thus higher
475 concentration of chloride pose higher electro-generation of ACS. As described by Shu
476 et al. [21], higher concentration of ACS increased in solar processes and resulted in
477 higher radicals generation (reactions 11 and 12), enhancing OMC degradation rates.
478 Consequently, actual NF retentate with high concentration of chloride (See table 1),
479 showed electro-generation of higher amount of oxidants, enough to degrade OMCs,
480 avoiding the addition of any reagent and therefore, simplifying the process. In

consequence, solar-assisted AO was selected as the best alternative for the treatment of NF retentates.

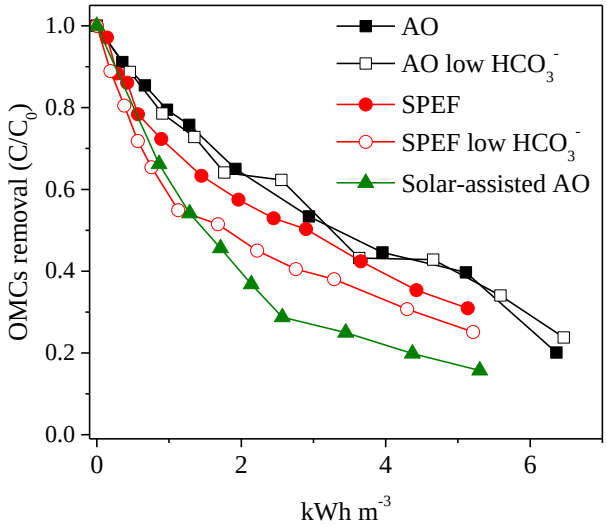


**Fig. 5.** Removal of the sum of OMCs (each one spiked at 100 µg $L^{-1}$) in actual NF retentate.

Finally, the effectiveness of solar-assisted AO was tested under complete actual conditions. A new batch of the secondary UWWTP effluent was introduced into the NF system, collecting the retentate (VRF 4) stream without reducing hydrogen carbonate concentration. Actual degradation of the OMCs contained in the retentate was monitored by using LC-QqLIT-MS/MS. A summary of the results is shown in Table 2. Detailed degradation of all OMCs contained in the actual effluent during electrochemical treatment, as well as their removal percentage, is shown in Table SI-5 (see supplementary information).

**Table 2.** Evolution of most relevant OMCs (> 250 ng $L^{-1}$) detected by LC-QqLIT-MS/MS in the UWWTP effluent, as well as their final removal percentage. NF retentate and their concentration after solar-assisted AO.

| | OMCs | El Ejido UWWTP effluent (ng $L^{-1}$) | Nanofiltration Retentate (VRF 4) (ng $L^{-1}$) | After solar-assisted AO (ng $L^{-1}$) | Removal (%) in solar-assisted AO |
|---|---|---|---|---|---|
| 1 | 4FAA | 7440 | 28360 | 780 | 97 |
| 2 | 4AAA | 3660 | 14350 | 360 | 98 |
| 3 | Gabapentin | 3250 | 12385 | 2730 | 78 |
| 4 | Carbamazepine | 1945 | 7070 | 3940 | 44 |
| 5 | Iminostilbene | 1500 | 5775 | 3410 | 41 |
| 6 | 4AA | 1170 | 4580 | ND | >99 |
| 7 | Imidacloprid | 1200 | 4525 | 2090 | 54 |
| 8 | Sulpiride | 1045 | 4060 | 13 | >99 |
| 9 | Venlafaxine | 750 | 2930 | ND | >99 |
| 10 | Levofloxacin | 490 | 1930 | ND | >99 |
| 11 | Cetirizine | 435 | 1690 | 1030 | 39 |
| 12 | Telmisartan | 420 | 1590 | 1275 | 20 |
| 13 | Irbesartan | 400 | 1550 | 905 | 42 |
| 14 | Diatrizoic acid | 380 | 1460 | 690 | 53 |
| 15 | OMCs < 250 ng $L^{-1}$ | 1960 | 7500 | 1730 | 77 |

*ND: Non detected

Up to forty-four OMCs were detected in UWWTP effluent, highlighting the presence of 4FAA, 4AAA, (dipyrone metabolites) and gabapentin (antiepileptic) which were found in the highest concentrations, 7440, 3660 and 3250 ng $L^{-1}$, respectively. Eleven OMCs were detected at relevant concentrations between 300 and 2000 ng $L^{-1}$ as carbamazepine, iminostilbene and others (see Table 2). The rest of OMCs were detected at lower concentrations (< 250 ng $L^{-1}$), being mainly pharmaceuticals as naproxen, diazepam, propanolol or flecainide.

After NF treatment, 99040 ng $L^{-1}$ of total OMCs were found in the retentate stream. After 90 min of solar-assisted AO application to the retentate, with 2.7 kWh $m^{-3}$ of electric consumption and a $Q_{UV}$ of 4.2 kJ $L^{-1}$, fourteen OMCs were substantially

509 degraded (>99%): 4AA, lincomicin, fenofibric acid, indomethacin, naproxen,
510 propranolol, dimethoate, erythromycin, metronidazole, sulfathiazole, trimethoprim,
511 levofloxacin, alfuzosin, domperidone, propafenone, memantine and trazodone. At that
512 point, DOC removal was 9% and measured FAC was only 2.6 mg $L^{-1}$, indicating the
513 high oxidation activity of the process.

514 At the end of the treatment, 80% of the total amount of OMCs detected in the NF
515 retentate was eliminated (Fig. 6). Energy consumption at the end of the treatment was
516 5.5 kWh $m^{-3}$ and the required accumulated UV energy was 11.5 kJ $L^{-1}$. Final DOC
517 removal was similar to previous cases, 19%, and FAC was 8.8 mg $L^{-1}$. This increase in
518 FAC, from 2.6 to 8.8 mg $L^{-1}$ at the end of the process, means that ACS was not able to
519 efficiently react with the organic compounds still remaining in NF retentate, much more
520 recalcitrant to oxidation than initial organics, after suffering several oxidation steps (but
521 not mineralized). As it was observed in previous tests, chlorates are generated
522 continuously regardless OMC removal, so the kinetic constant of chlorates generation
523 was calculated: $1.47 \pm 0.02$ ($10^{-1}$ $min^{-1}$) ($R^2 = 0.996$).

524 Despite being among the pollutants with an important presence (> 250 ng $L^{-1}$), it is
525 remarkable the low removal of telmisartan (20%). Same applies to other compounds
526 such as carbamazepine or iminostilbene, two tricyclic compounds that despite being
527 detected at higher concentrations than other OMCs (> 1.5 μg $L^{-1}$), showed higher
528 stability being only able to reach degradation rates lower that 50%.

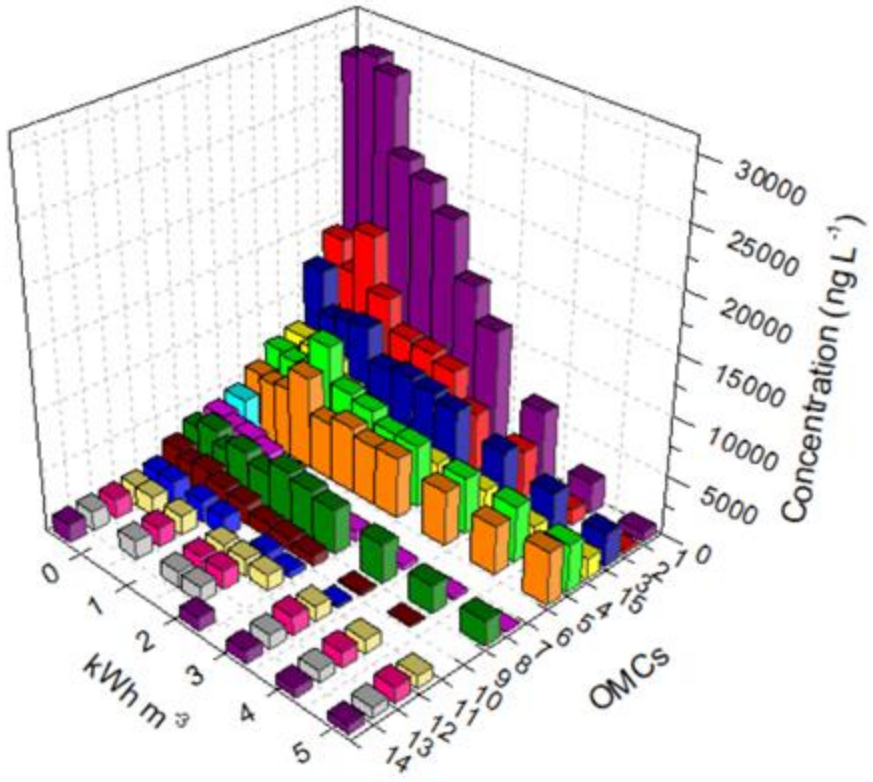


529

530 **Fig. 6.** Removal of the OMCs contained in actual NF retentate from UWWTP effluent
531 during solar-assisted AO treatment.

532

533 ## Conclusions

534 It has been demonstrated that the combination of an electrochemical device with a solar
535 CPC reactor entails an enhancement in OMC removal percentages regarding pure
536 electrooxidative processes, due to the generation of higher amount of oxidative species.

537 EDDS has been a useful tool to keep iron in solution in solar-assisted processes but
538 taking into consideration that it is only effective during the first part of the treatment
539 due to its degradation by the electrochemical process itself.

If the effluent contains a high concentration of chloride, the use of $Fe^{3+}$:EDDS could be avoided as only with solar-assisted AO enough oxidant species can be generated for the complete degradation of OMCs

The complete combined process, nanofiltration and solar-assisted electrooxidation, was successfully applied for the removal of OMCs of an actual UWWTP effluent, reaching high degradation for most of them and 80% of elimination of the total amount. On the contrary, it is important to stress that this process is not effective for DOC removal.

Finally it important to mention that the measurement of high concentrations of chlorates at the end of the electrochemical treatments, makes necessary the performance of risk and health assessment studies before considering the reuse of treated wastewater for crops irrigation.

## Acknowledgements

The authors wish to thank the Spanish Ministry of Science, Innovation and Universities (MCIU), AEI and FEDER for funding under the CalypSol Project (Reference: RTI2018-097997-B-C32).

## References

[1] M. Patel, R. Kumar, K. Kishor, T. Mlsna, C.U. Pittman, Jr., D. Mohan, Pharmaceuticals of Emerging Concern in Aquatic Systems: Chemistry, Occurrence, Effects, and Removal Methods, Chem. Rev., 119 (2019) 3510-3673.

[2] K.V. Plakas, A.J. Karabelas, Removal of pesticides from water by NF and RO membranes — A review, Desalination, 287 (2012) 255-265.

561 [3] C. Fonseca Couto, L.C. Lange, M.C. Santos Amaral, A critical review on membrane
562 separation processes applied to remove pharmaceutically active compounds from water
563 and wastewater, J. Water Process Eng., 26 (2018) 156-175.
564 [4] R. Rienzie, S. Ramanayaka, N.M. Adassooriya, Nanotechnology applications for the
565 removal of environmental contaminants from pharmaceuticals and personal care
566 products, in: M. Prasad, M. Vithanage, A. Kapley (Eds.) Pharmaceuticals and Personal
567 Care Products: Waste Management and Treatment Technology, 2019, pp. 279-296.
568 [5] J. Heo, S. Kim, N. Her, C.M. Park, M. Yu, Y. Yoon, Removal of contaminants of
569 emerging concern by FO, RO, and UF membranes in water and wastewater, in: A.
570 Hernandez-Maldonado, L. Blaney (Eds.) Contaminants of Emerging Concern in Water
571 and Wastewater, 2020, pp. 139-176.
572 [6] R. Gonzalez-Olmos, A. Penadés, G. Garcia, Electro-oxidation as efficient
573 pretreatment to minimize the membrane fouling in water reuse processes, J. Membr.
574 Sci., 552 (2018) 124-131.
575 [7] K. Rajwade, A.C. Barrios, S. Garcia-Segura, F. Perreault, Pore wetting in membrane
576 distillation treatment of municipal wastewater desalination brine and its mitigation by
577 foam fractionation, Chemosphere, 257 (2020) 127214.
578 [8] A. Soriano, D. Gorri, L.T. Biegler, A. Urtiaga, An optimization model for the
579 treatment of perfluorocarboxylic acids considering membrane preconcentration and
580 BDD electrooxidation, Water Res., 164 (2019) 114954.
581 [9] G. Perez, A.R. Fernandez-Alba, A.M. Urtiaga, I. Ortiz, Electro-oxidation of reverse
582 osmosis concentrates generated in tertiary water treatment, Water Res., 44 (2010) 2763-
583 2772.

584 [10] D. Rice, P. Westerhoff, F. Perreault, S. Garcia-Segura, Electrochemical self-
585 cleaning anodic surfaces for biofouling control during water treatment, Electrochem.
586 Commun., 96 (2018) 83-87.
587 [11] M. Panizza, Importance of electrode material in the electrochemical treatment of
588 wastewater containing organic pollutants, in: C. Comninellis, G. Chen (Eds.)
589 Electrochemistry for the Environment, Springer, 2010, pp. 25-54.
590 [12] Y. He, H. Lin, Z. Guo, W. Zhang, H. Li, W. Huang, Recent developments and
591 advances in boron-doped diamond electrodes for electrochemical oxidation of organic
592 pollutants, Sep. Purif. Technol., 212 (2019) 802-821.
593 [13] E. Mostafa, P. Reinsberg, S. Garcia-Segura, H. Baltruschat, Chlorine species
594 evolution during electrochlorination on boron-doped diamond anodes: In-situ
595 electrogeneration of $Cl_2$ , $Cl_2O$ and $ClO_2$, Electrochim. Acta, 281 (2018) 831-840.
596 [14] A. Farhat, J. Keller, S. Tait, J. Radjenovic, Oxidative capacitance of sulfate-based
597 boron-doped diamond electrochemical system, Electrochem. Commun., 89 (2018) 14-
598 18.
599 [15] M.E.H. Bergmann, Drinking water disinfection by in-line electrolysis: Product and
600 inorganic by-product formation, in: C. Comninellis, G. Chen (Eds.) Electrochemistry
601 for the Environment, Springer, 2010, pp. 163-204.
602 [16] Y. Meas, L.A. Godinez, E. Bustos, Ozone Generation Using Boron- Doped
603 Diamond Electrodes, in: E. Brillas, C.A. Martínez- Huitle (Eds.) Synthetic Diamond
604 Films: Preparation, Electrochemistry, Characterization, and Applications, Wiley Online
605 Library, 2011, pp. 311-331.
606 [17] E. Brillas, I. Sirés, M.A. Oturan, Electro-Fenton process and related
607 electrochemical technologies based on Fenton's reaction chemistry, Chem. Rev., 109
608 (2009) 6570-6631.

609 [18] E. Brillas, A review on the photoelectro-Fenton process as efficient
610 electrochemical advanced oxidation for wastewater remediation. Treatment with UV
611 light, sunlight, and coupling with conventional and other photo-assisted advanced
612 technologies, Chemosphere, 250 (2020) 126198.
613 [19] B.S. Tawabini, K.V. Plakas, M. Fraim, E. Safi, T. Oyehan, A.J. Karabelas,
614 Assessing the efficiency of a pilot-scale GDE/BDD electrochemical system in removing
615 phenol from high salinity waters, Chemosphere, 239 (2020) 124714.
616 [20] L.H. Nowell, J. Hoigné, Photolysis of aqueous chlorine at sunlight and ultraviolet
617 wavelengths—II. Hydroxyl radical production, Water Res., 26 (1992) 599-605.
618 [21] Z. Shu, C. Li, M. Belosevic, J.R. Bolton, M.G. El-Din, Application of a solar
619 UV/chlorine advanced oxidation process to oil sands process-affected water
620 remediation, Environ. Sci. Technol., 48 (2014) 9692-9701.
621 [22] W. Huang, M. Brigante, F. Wu, C. Mousty, K. Hanna, G. Mailhot, Assessment of
622 the Fe(III)-EDDS complex in Fenton-like processes: from the radical formation to the
623 degradation of bisphenol A, Environ. Sci. Technol., 47 (2013) 1952-1959.
624 [23] P. Soriano-Molina, J.L. García Sánchez, O.M. Alfano, L.O. Conte, S. Malato, J.A.
625 Sánchez Pérez, Mechanistic modeling of solar photo-Fenton process with $Fe^{3+}$-EDDS at
626 neutral pH, Appl Catal B-Environ., 233 (2018) 234-242.
627 [24] P. Soriano-Molina, P. Plaza-Bolaños, A. Lorenzo, A. Agüera, J.L. García Sánchez,
628 S. Malato, J.A. Sánchez Pérez, Assessment of solar raceway pond reactors for removal
629 of contaminants of emerging concern by photo-Fenton at circumneutral pH from very
630 different municipal wastewater effluents, Chem. Eng. J., 366 (2019) 141-149.
631 [25] A.Y. Bagastyo, D.J. Batstone, I. Kristiana, W. Gernjak, C. Joll, J. Radjenovic,
632 Electrochemical oxidation of reverse osmosis concentrate on boron-doped diamond
633 anodes at circumneutral and acidic pH, Water Res., 46 (2012) 6104-6112.

[26] A. Soriano, D. Gorri, A. Urtiaga, Efficient treatment of perfluorohexanoic acid by nanofiltration followed by electrochemical degradation of the NF concentrate, Water Res., 112 (2017) 147-156.

[27] S. Garcia-Segura, A.B. Nienhauser, A.S. Fajardo, R. Bansal, C.L. Coonrod, J.D. Fortner, M. Marcos-Hernández, T. Rogers, D. Villagran, M.S. Wong, P. Westerhoff, Disparities between experimental and environmental conditions: Research steps toward making electrochemical water treatment a reality, Curr. Opin. in Electrochem., 22 (2020) 9-16.

[28] L. Clarizia, D. Russo, I. Di Somma, R. Marotta, R. Andreozzi, Homogeneous photo-Fenton processes at near neutral pH: A review, Appl Catal B-Environ., 209 (2017) 358-371.

[29] S. Miralles-Cuevas, I. Oller, J.A.S. Perez, S. Malato, Removal of pharmaceuticals from MWTP effluent by nanofiltration and solar photo-Fenton using two different iron complexes at neutral pH, Water Res., 64 (2014) 23-31.

[30] I. Salmerón, K.V. Plakas, I. Sirés, I. Oller, M.I. Maldonado, A.J. Karabelas, S. Malato, Optimization of electrocatalytic $H_2O_2$ production at pilot plant scale for solar-assisted water treatment, Appl Catal B-Environ., 242 (2019) 327-336.

[31] S. Malato, J. Blanco, A. Campos, J. Caceres, C. Guillard, J.M. Herrmann, A.R. Fernandez-Alba, Effect of operating parameters on the testing of new industrial titania catalysts at solar pilot plant scale, Appl. Catal. B-Environ., 42 (2003) 349-357.

[32] D. Schowanek, T.C.J. Feijtel, C.M. Perkins, F.A. Hartman, T.W. Federle, R.J. Larson, Biodegradation of [S, S],[R, R] and mixed stereoisomers of ethylene diamine disuccinic acid (EDDS), a transition metal chelator, Chemosphere, 34 (1997) 2375-2391.

[33] E. Cuervo Lumbaque, D. Salmoria Araújo, T. Moreira Klein, E.R. Lopes Tiburtius, J. Argüello, C. Sirtori, Solar photo-Fenton-like process at neutral pH: Fe(III)-EDDS complex formation and optimization of experimental conditions for degradation of pharmaceuticals, Catal. Today, 328 (2019) 259-266.

[34] M. Orama, H. Hyvönen, H. Saarinen, R. Aksela, Complexation of [S,S] and mixed stereoisomers of N,N′-ethylenediaminedisuccinic acid (EDDS) with Fe(III), Cu(II), Zn(II) and Mn(II) ions in aqueous solution, J. Chem. Soc., Dalton Trans., (2002) 4644-4648.

[35] W. Huang, M. Brigante, F. Wu, K. Hanna, G. Mailhot, Development of a new homogenous photo-Fenton process using Fe(III)-EDDS complexes, J. Photoch. Photobio. A., 239 (2012) 17-23.

[36] N. Klamerth, S. Malato, A. Aguera, A. Fernandez-Alba, G. Mailhot, Treatment of municipal wastewater treatment plant effluents with modified photo-Fenton as a tertiary treatment for the degradation of micro pollutants and disinfection, Environ. Sci. Technol., 46 (2012) 2885-2892.

[37] S. Miralles-Cuevas, F. Audino, I. Oller, R. Sánchez-Moreno, J.A.S. Pérez, S. Malato, Pharmaceuticals removal from natural water by nanofiltration combined with advanced tertiary treatments (solar photo-Fenton, photo-Fenton-like Fe (III)–EDDS complex and ozonation), Sep. Purif. Technol., 122 (2014) 515-522.

[38] Z. Ye, E. Brillas, F. Centellas, P.L. Cabot, I. Sirés, Electro-Fenton process at mild pH using Fe(III)-EDDS as soluble catalyst and carbon felt as cathode, Appl Catal B-Environ., 257 (2019).

[39] P. Soriano-Molina, J.L. García Sánchez, S. Malato, L.A. Pérez-Estrada, J.A. Sánchez Pérez, Effect of volumetric rate of photon absorption on the kinetics of

682 micropollutant removal by solar photo-Fenton with $Fe^{3+}$-EDDS at neutral pH, Chem.
683 Eng. J., 331 (2018) 84-92.
684 [40] Y. Luo, W. Guo, H.H. Ngo, L.D. Nghiem, F.I. Hai, J. Zhang, S. Liang, X.C. Wang,
685 A review on the occurrence of micropollutants in the aquatic environment and their fate
686 and removal during wastewater treatment, Sci. Total Environ., 473-474 (2014) 619-641.
687 [41] N. Klamerth, N. Miranda, S. Malato, A. Agüera, A.R. Fernández-Alba, M.I.
688 Maldonado, J.M. Coronado, Degradation of emerging contaminants at low
689 concentrations in MWTPs effluents with mild solar photo-Fenton and $TiO_2$, Catal.
690 Today, 144 (2009) 124-130.
691 [42] R. Xiong, Z. Lu, Q. Tang, X. Huang, H. Ruan, W. Jiang, Y. Chen, Z. Liu, J. Kang,
692 D. Liu, UV-LED/chlorine degradation of propranolol in water: Degradation pathway
693 and product toxicity, Chemosphere, 248 (2020).
694
695
696
697
698
699
700
701
702
703

# Supplementary Information

**Table SI-1.** Ionic composition of SNR and Natural water

| | Natural water (mg $L^{-1}$) | SNR (mg $L^{-1}$) |
|---|---|---|
| $HCO_3^-$ | 813 | 813 |
| Cl- | 254 | 555 |
| $SO_4^{2-}$ | 169 | 1465 |
| $Na^+$ | 389 | 1050 |
| $Ca^{2+}$ | 73 | 213 |
| $NH_4^+$ | 0 | 18 |
| $Mg^{2+}$ | 50 | 50 |
| $K^+$ | 7.3 | 46 |
| $NO_3^-$ | 11 | 73 |
| $HPO4^{2-}$ | 0 | 14 |

**Table SI-2.** Characterization of UWWTP secondary effluent from El Ejido (Almería, Spain)

| | UWWTP effluent |
|---|---|
| Conductivity (mS $cm^{-1}$) | 2.1 - 2.3 |
| NTU | 3.1 - 5.9 |
| pH | 7.4 - 7.7 |
| DOC | 11 - 12 |
| COD | 17 - 50 |
| $HCO_3^-$ (mg $L^{-1}$) | 264 - 440 |
| $Cl^-$ (mg $L^{-1}$) | 423 - 460 |
| $SO_4^-$ (mg $L^{-1}$) | 127 - 140 |
| $Na^+$ (mg $L^{-1}$) | 254 - 264 |
| $Ca^{2+}$ (mg $L^{-1}$) | 96 - 105 |
| $NH_4^+$ (mg $L^{-1}$) | 22 - 35 |
| $Mg^{2+}$ (mg $L^{-1}$) | 66 -67 |
| $K^+$ (mg $L^{-1}$) | 23 - 25 |
| $NO_3^-$ (mg $L^{-1}$) | 12 - 31 |

709 **Table SI-3.** Retention time, limit of quantification (LOQ) and maximum absorption wavelength
710 of studied OMCs under UPLC-UV analysis.

| OMCs | Retention time (min) | LOQ (μg $L^{-1}$) | Maximum absorption (λ) |
|---|---|---|---|
| PCP | 10.4 | 10 | 220 nm |
| TBT | 7.7 | 10 | 230 nm |
| CFV | 10.9 | 10 | 240 nm |
| DFC | 9.6 | 10 | 285 nm |

711

712 **Table SI-4**. Optimal LC-QqLIT-MS/MS conditions for OMCs multi-residue analysis.

| Compound | Rt (min) | Precursor ion | Quantifier/ qualifyer | DP[a] (V) | EP[b] (V) | CE[c] (eV) | CXP[d] (V) |
|---|---|---|---|---|---|---|---|
| 10,11 - Dihydrocarbamazepine | 9.31 | 239.3 | 194.1 | 66 | 12 | 32 | 10 |
| | | | 180.2 | 150 | 10 | 47 | 11 |
| 4 -AA | 5.3 | 204.2 | 56.2 | 45 | 5 | 30 | 2 |
| | | | 159.2 | 45 | 5 | 16 | 2 |
| 4 -AAA | 6.62 | 246.2 | 228.1 | 46 | 5 | 18 | 2 |
| | | | 83.1 | 46 | 5 | 40 | 2 |
| 4 -DAA | 5.1 | 232.2 | 113.2 | 48 | 5 | 17 | 2 |
| | | | 111.2 | 48 | 5 | 21 | 2 |
| 4 -FAA | 6.54 | 232.2 | 214.2 | 60 | 5 | 18 | 2 |
| | | | 77 | 60 | 5 | 50 | 2 |
| 4 -MAA | 4.75 | 218.2 | 56.1 | 35 | 5 | 30 | 2 |
| | | | 97.2 | 35 | 5 | 16 | 2 |
| 9-Acridinecarboxilic acid | 11.63 | 224.2 | 196 | 63 | 12 | 36 | 11 |
| | | | 167.2 | 63 | 12 | 54 | 11 |
| | | | 180 | 63 | 12 | 42 | 10 |
| Acetaminophen | 5.8 | 152.1 | 110.1 | 40 | 5 | 20 | 2 |
| | | | 64.8 | 40 | 5 | 45 | 2 |
| Acetamiprid | 7.84 | 223 | 126 | 100 | 10 | 30 | 4 |
| | | | 128 | 50 | 13 | 25 | 7 |
| Acetanilide | 8 | 136 | 94 | 70 | 10 | 24 | 15 |
| | | | 77 | 70 | 11 | 40 | 10 |
| Alfuzosin | 7.17 | 390.3 | 235.1 | 50 | 12 | 40 | 12 |
| | | | 156.1 | 50 | 12 | 37 | 10 |
| Amitriptyline | 8.8 | 278.4 | 91.2 | 30 | 5 | 35 | 2 |
| | | | 233.1 | 30 | 5 | 22 | 2 |
| Amoxicilin | 4.91 | 366.1 | 114 | 70 | 12 | 30 | 19 |
| | | | 208 | 70 | 12 | 13 | 8 |
| | | | 349.1 | 70 | 6 | 18 | 11 |

| Compound | Rt (min) | Precursor ion | Quantifier/ qualifyer | DP[a] (V) | EP[b] (V) | CE[c] (eV) | CXP[d] (V) |
|---|---|---|---|---|---|---|---|
| Antipyrine | 7.41 | 189.2 | 77.1 | 48 | 5 | 51 | 2 |
| | | | 104.1 | 48 | 5 | 32 | 2 |
| Atenolol | 3.41 | 267.3 | 145.2 | 70 | 5 | 35 | 2 |
| | | | 190.2 | 70 | 5 | 27 | 2 |
| Atrazine | 9.93 | 216 | 174 | 100 | 13 | 25 | 10 |
| | | | 176 | 40 | 8 | 25 | 10 |
| Azithromycin | 7.07 | 749.5 | 83.1 | 50 | 11 | 110 | 20 |
| | | | 591.4 | 50 | 12 | 40 | 13 |
| | | | 573.3 | 50 | 8 | 47 | 14 |
| Azoxystrobin | 9.93 | 404.1 | 372.2 | 100 | 10 | 20 | 10 |
| | | | 329 | 56 | 10 | 42 | 6 |
| Betamethasone | 9.76 | 393.3 | 373.1 | 70 | 10 | 13 | 20 |
| | | | 355 | 70 | 11 | 18 | 20 |
| | | | 147 | 70 | 10 | 39 | 15 |
| Buprofezin | 11.69 | 306 | 201 | 20 | 11 | 17 | 5 |
| | | | 116 | 20 | 13 | 22 | 6 |
| | | | 106 | 20 | 13 | 40 | 6 |
| C13 Caffeine | 6.95 | 198.1 | 140.1 | 40 | 5 | 30 | 2 |
| | | | 112.2 | 40 | 5 | 35 | 2 |
| C13 -Phenacetin | 8.68 | 181.3 | 110.3 | 150 | 10 | 47 | 11 |
| | | | 139.3 | 150 | 10 | 47 | 11 |
| Caffeine | 6.95 | 195 | 138 | 20 | 4 | 27 | 4 |
| | | | 110 | 20 | 5 | 31 | 13 |
| | | | 123 | 20 | 5 | 45 | 5 |
| Carbamazepine | 9.38 | 237.2 | 194.3 | 80 | 5 | 25 | 2 |
| | | | 192.1 | 80 | 5 | 35 | 2 |
| Carbendazim | 6.15 | 192.3 | 160.1 | 100 | 10 | 27 | 4 |
| | | | 132.2 | 100 | 10 | 41 | 4 |
| Cefalexin | 6.43 | 348 | 158.1 | 60 | 12 | 13 | 8 |
| | | | 174.1 | 60 | 11 | 20 | 11 |
| | | | 106.1 | 150 | 10 | 47 | 11 |
| Cefotaxime | 6.76 | 456.1 | 324.1 | 40 | 5 | 15 | 3 |
| | | | 396.1 | 40 | 5 | 10 | 2 |
| | | | 241.3 | 40 | 5 | 20 | 2 |
| Cetirizine | 9.31 | 389.4 | 201 | 48 | 12 | 30 | 12 |
| | | | 166.2 | 48 | 12 | 55 | 8 |
| Chlorfenvinphos | 10.95 | 359.1 | 99 | 60 | 10 | 50 | 6 |
| | | | 155 | 100 | 8 | 18 | 10 |
| Chlorpyriphos | 12.19 | 352 | 97 | 55 | 10 | 55 | 7 |
| | | | 197.9 | 96 | 10 | 26 | 6 |
| Chlortetracycline | 7.37 | 479.2 | 444 | 100 | 9 | 31 | 10 |
| | | | 462 | 100 | 9 | 24 | 11 |
| Ciprofloxacin | 6.47 | 332.2 | 314.3 | 50 | 5 | 25 | 2 |
| | | | 231.2 | 50 | 5 | 48 | 2 |

| Compound | Rt (min) | Precursor ion | Quantifier/ qualifyer | DP[a] (V) | EP[b] (V) | CE[c] (eV) | CXP[d] (V) |
|---|---|---|---|---|---|---|---|
| Citalopram | 7.88 | 325.3 | 109.1 | 100 | 5 | 30 | 2 |
| | | | 262.1 | 100 | 5 | 25 | 2 |
| Clarithromycin | 8.87 | 748.4 | 158.4 | 45 | 5 | 35 | 2 |
| | | | 590.4 | 45 | 5 | 26 | 2 |
| Clindamycin | 7.88 | 425.2 | 126.1 | 80 | 11 | 35 | 7 |
| | | | 377.1 | 80 | 12 | 28 | 9 |
| Clomipramine | 9.05 | 315.2 | 86.1 | 40 | 5 | 27 | 2 |
| | | | 58.1 | 40 | 5 | 60 | 2 |
| Clotrimazole | 9.06 | 344.9 | 277.3 | 30 | 5 | 15 | 2 |
| | | | 165 | 30 | 5 | 43 | 2 |
| Cotinine | 3 | 177 | 80 | 45 | 5 | 36 | 2 |
| | | | 98 | 45 | 5 | 26 | 2 |
| Cyclophosphamide | 8.67 | 261.2 | 140 | 40 | 12 | 23 | 12 |
| | | | 233.2 | 40 | 8 | 30 | 8 |
| | | | 106 | 40 | 8 | 25 | 6 |
| Cyprodinil | 10.83 | 226 | 77 | 120 | 12 | 63 | 9 |
| | | | 93 | 120 | 12 | 80 | 9 |
| D10-Carbamazepine | 9.37 | 247.2 | 204.3 | 150 | 10 | 47 | 11 |
| | | | 202.1 | 150 | 10 | 47 | 11 |
| Danofloxacin | 6.48 | 358.2 | 340.2 | 100 | 8 | 31 | 12 |
| | | | 314.3 | 100 | 8 | 26 | 11 |
| Dextromethorphan | 8.1 | 272.4 | 215.1 | 150 | 10 | 47 | 11 |
| | | | 171.1 | 150 | 10 | 47 | 11 |
| | | | 173 | 150 | 10 | 47 | 11 |
| Diatrizoic acid | 5.03 | 632 | 361 | 80 | 9 | 35 | 8 |
| | | | 233.1 | 80 | 8 | 55 | 12 |
| Diazepam | 10.37 | 285.2 | 193.2 | 100 | 12 | 42 | 10 |
| | | | 154.2 | 100 | 12 | 36 | 10 |
| Difloxacin | 6.67 | 400.3 | 299 | 70 | 8 | 42 | 17 |
| | | | 356 | 70 | 8 | 30 | 20 |
| Dimethoate | 7.96 | 230 | 199.1 | 100 | 10 | 13 | 4 |
| | | | 125.1 | 100 | 10 | 28 | 4 |
| | | | 171 | 50 | 7 | 19 | 9 |
| Dimethomorph | 10.32 | 388 | 301 | 100 | 10 | 30 | 8 |
| | | | 165 | 100 | 10 | 45 | 8 |
| | | | 303 | 130 | 10 | 29 | 7 |
| Diphenhydramine | 8.01 | 256.4 | 167.2 | 40 | 12 | 21 | 9 |
| | | | 152 | 40 | 12 | 50 | 7 |
| Diuron | 10.04 | 233 | 72 | 60 | 7 | 50 | 12 |
| | | | 72 | 110 | 6 | 36 | 10 |
| Domperidone | 7.56 | 426.2 | 175 | 37 | 12 | 35 | 10 |
| | | | 147.1 | 37 | 11 | 55 | 7 |
| Donepezil | 7.51 | 380.4 | 91 | 65 | 12 | 63 | 9 |
| | | | 151.1 | 65 | 14 | 40 | 8 |

| Compound | Rt (min) | Precursor ion | Quantifier/ qualifyer | DP[a] (V) | EP[b] (V) | CE[c] (eV) | CXP[d] (V) |
|---|---|---|---|---|---|---|---|
| Doxycycline | 7.98 | 445.3 | 428.2 | 90 | 10 | 28 | 9 |
| | | | 410.2 | 90 | 10 | 34 | 10 |
| | | | 154.1 | 90 | 10 | 39 | 10 |
| EDDP | 7.96 | 278.6 | 234 | 30 | 11 | 42 | 14 |
| | | | 249.2 | 30 | 12 | 31 | 12 |
| Enrofloxacin | 6.48 | 360.3 | 245.2 | 80 | 10 | 37 | 10 |
| | | | 316.2 | 80 | 10 | 27 | 12 |
| Eprosartan | 8.01 | 425.2 | 135.1 | 79 | 11 | 47 | 9 |
| | | | 207.1 | 79 | 12 | 35 | 10 |
| | | | 163.2 | 79 | 10 | 44 | 5 |
| Erithromicyn | 8.45 | 734.6 | 158.3 | 58 | 5 | 40 | 2 |
| | | | 576.5 | 58 | 5 | 28 | 2 |
| Famotidine | 3.42 | 338 | 189.3 | 25 | 5 | 24 | 2 |
| | | | 259.4 | 25 | 5 | 15 | 2 |
| Fenhexamid | 10.51 | 302 | 97 | 80 | 14 | 30 | 12 |
| | | | 55 | 80 | 8 | 60 | 7 |
| Fenofibrate | 11.87 | 361.2 | 233.1 | 60 | 5 | 25 | 2 |
| | | | 139.1 | 60 | 5 | 35 | 2 |
| Fenofibric acid | 10.98 | 319.1 | 233.1 | 65 | 5 | 22 | 2 |
| | | | 139.1 | 65 | 5 | 42 | 2 |
| Flecainide | 7.84 | 415.2 | 301 | 48 | 12 | 49 | 7 |
| | | | 398.1 | 48 | 12 | 35 | 9 |
| | | | 98 | 48 | 12 | 36 | 15 |
| Flumequine | 9.38 | 262.3 | 244.08 | 50 | 5 | 21 | 14 |
| | | | 202.3 | 50 | 5 | 41 | 12 |
| Fluoxetine | 8.73 | 310.3 | 44.2 | 30 | 5 | 25 | 2 |
| | | | 148.2 | 30 | 5 | 10 | 2 |
| Gabapentin | 5.96 | 172.4 | 154.1 | 50 | 9 | 18 | 9 |
| | | | 137.2 | 50 | 9 | 22 | 7 |
| Ifosfamide | 8.49 | 261.1 | 91.9 | 60 | 5 | 33 | 2 |
| | | | 154.3 | 60 | 5 | 29 | 2 |
| Imazalil | 8.54 | 297 | 159 | 80 | 12 | 31 | 8 |
| | | | 255 | 80 | 12 | 25 | 7 |
| Imazalil d6 | 8.54 | 302.1 | 159 | 60 | 10 | 32 | 4 |
| | | | 203 | 60 | 10 | 26 | 4 |
| | | | 255.1 | 60 | 10 | 26 | 4 |
| Imidacloprid | 7.45 | 256.1 | 175.1 | 100 | 10 | 27 | 4 |
| | | | 209.2 | 100 | 10 | 25 | 4 |
| Iminostilbene | 9.31 | 194 | 179 | 150 | 10 | 47 | 11 |
| | | | 167 | 150 | 10 | 47 | 11 |
| | | | 152 | 150 | 10 | 47 | 11 |
| Indomethacin | 10.91 | 358.2 | 139.1 | 50 | 5 | 25 | 2 |
| | | | 174.3 | 50 | 5 | 15 | 2 |
| Irbesartan | 9.82 | 429.3 | 207 | 55 | 12 | 34 | 5 |

| Compound | Rt (min) | Precursor ion | Quantifier/ qualifyer | DP[a] (V) | EP[b] (V) | CE[c] (eV) | CXP[d] (V) |
|---|---|---|---|---|---|---|---|
| | | | 195 | 55 | 12 | 32 | 14 |
| Isoproturon | 9.88 | 207 | 72 | 60 | 8 | 25 | 12 |
| | | | 165 | 60 | 8 | 20 | 10 |
| Josamycin | 8.77 | 828.6 | 174.2 | 54 | 12 | 46 | 13 |
| | | | 229.1 | 54 | 11 | 43 | 11 |
| | | | 600.2 | 54 | 11 | 37 | 14 |
| Ketolorac | 9.76 | 256.2 | 105.1 | 70 | 5 | 25 | 2 |
| | | | 178.1 | 70 | 5 | 34 | 2 |
| Ketoprofen | 10.03 | 255.2 | 105.1 | 47 | 5 | 33 | 2 |
| | | | 209.2 | 47 | 5 | 16 | 2 |
| Labetalol | 7.45 | 329.1 | 162.1 | 32 | 12 | 33 | 9 |
| | | | 90.9 | 32 | 12 | 67 | 8 |
| | | | 294.2 | 32 | 12 | 27 | 15 |
| | | | 311.2 | 32 | 12 | 21 | 7 |
| Lansoprazole | 9.29 | 370 | 252.2 | 45 | 5 | 15 | 2 |
| | | | 119.2 | 45 | 5 | 27 | 2 |
| Levofloxacin | 6.25 | 362.1 | 261.2 | 80 | 8 | 40 | 10 |
| | | | 318.2 | 80 | 8 | 26 | 15 |
| Lidocaine | 6.52 | 235 | 86 | 70 | 7 | 20 | 5 |
| | | | 58 | 70 | 8 | 50 | 4 |
| Lincomycin | 5.86 | 407.1 | 126.3 | 50 | 5 | 45 | 2 |
| | | | 359.3 | 50 | 5 | 23 | 2 |
| Loratadine | 10.7 | 383.1 | 337.3 | 50 | 5 | 29 | 2 |
| | | | 267.2 | 50 | 5 | 40 | 2 |
| Mefanamic acid | 11.68 | 242.2 | 224.2 | 36 | 5 | 34 | 2 |
| | | | 180.2 | 36 | 5 | 53 | 2 |
| Memantine | 8.1 | 180.3 | 163.1 | 28 | 12 | 22 | 10 |
| | | | 107.1 | 28 | 12 | 36 | 9 |
| Mepivacaine | 6.67 | 247.4 | 98.1 | 28 | 5 | 23 | 2 |
| | | | 70.1 | 28 | 5 | 53 | 2 |
| Metalaxyl | 9.76 | 280 | 220 | 85 | 12 | 20 | 12 |
| | | | 220 | 100 | 12 | 19 | 9 |
| | | | 192 | 70 | 12 | 25 | 9 |
| Methadone | 8.55 | 310.2 | 265.1 | 70 | 13 | 22 | 7 |
| | | | 105 | 70 | 11 | 40 | 20 |
| | | | 223 | 70 | 13 | 30 | 11 |
| Methiocarb | 10.33 | 226 | 169 | 44 | 14 | 13 | 9 |
| | | | 121 | 44 | 9 | 25 | 6 |
| | | | 107 | 44 | 9 | 51 | 5 |
| Methotrexate | 6.1 | 455.2 | 308 | 80 | 12 | 28 | 15 |
| | | | 175 | 90 | 12 | 55 | 15 |
| | | | 134 | 90 | 12 | 48 | 15 |
| Metoclopramide | 6.57 | 300 | 184 | 80 | 6 | 42 | 11 |
| | | | 141 | 80 | 11 | 66 | 10 |

| Compound | Rt (min) | Precursor ion | Quantifier/ qualifyer | DP[a] (V) | EP[b] (V) | CE[c] (eV) | CXP[d] (V) |
|---|---|---|---|---|---|---|---|
| Metoprolol | 6.9 | 268.2 | 116.2 | 30 | 5 | 25 | 2 |
| | | | 159.2 | 30 | 5 | 28 | 2 |
| Metronidazol | 5.63 | 172.1 | 128.1 | 35 | 5 | 20 | 2 |
| | | | 82.1 | 35 | 5 | 30 | 2 |
| Mevastatin | 11.4 | 391.3 | 185.2 | 55 | 5 | 25 | 2 |
| | | | 159.3 | 55 | 5 | 30 | 2 |
| Myclobutanil | 10.38 | 289.2 | 70.2 | 100 | 10 | 36 | 4 |
| | | | 125.1 | 100 | 10 | 44 | 4 |
| Nadolol | 6.15 | 310.2 | 254.4 | 45 | 5 | 30 | 2 |
| | | | 201.2 | 45 | 5 | 30 | 2 |
| Nalidixic acid | 9.25 | 233.2 | 187 | 45 | 10 | 35 | 12 |
| | | | 104 | 45 | 10 | 55 | 11 |
| Naproxen | 10.23 | 231.2 | 185.1 | 86 | 5 | 17 | 10 |
| | | | 170.1 | 86 | 5 | 35 | 10 |
| N-desmethylcitalopram | 7.85 | 311.3 | 109.1 | 66 | 12 | 31 | 7 |
| | | | 262.1 | 66 | 11 | 23 | 13 |
| Nicotinamide | 3.16 | 123.1 | 53.1 | 35 | 8 | 42 | 10 |
| | | | 80 | 35 | 12 | 28 | 8 |
| | | | 78 | 35 | 12 | 33 | 12 |
| Nicotine | 2.77 | 163.3 | 130 | 60 | 4 | 26 | 7 |
| | | | 132 | 60 | 10 | 20 | 7 |
| | | | 106 | 60 | 15 | 23 | 6 |
| Nicotinic acid | 3.34 | 124 | 80.1 | 76 | 6 | 29 | 13 |
| | | | 78.1 | 76 | 8 | 30 | 12 |
| Nitrendipine | 10.46 | 361 | 315 | 80 | 10 | 18 | 17 |
| | | | 329.1 | 80 | 10 | 15 | 15 |
| | | | 254.2 | 80 | 10 | 45 | 15 |
| Norfloxacin | 6.41 | 320 | 302.2 | 220 | 12 | 33 | 17 |
| | | | 233.1 | 220 | 12 | 33 | 5 |
| O-desmethyltramadol | 5.91 | 250.3 | 58.1 | 70 | 12 | 45 | 7 |
| | | | 232.2 | 70 | 13 | 17 | 11 |
| O-desmethylvenlafaxine | 6.76 | 264.1 | 57.9 | 190 | 9 | 50 | 6 |
| | | | 107 | 190 | 13 | 25 | 6 |
| Oxcarbamazepine | 8.68 | 253 | 180 | 73 | 10 | 44 | 11 |
| | | | 208.1 | 73 | 10 | 28 | 13 |
| | | | 235.9 | 150 | 10 | 47 | 11 |
| Oxytetracycline | 6.62 | 461.3 | 426.1 | 90 | 10 | 27 | 11 |
| | | | 443.1 | 90 | 10 | 19 | 11 |
| Paraxanthine | 6.19 | 181.2 | 124.2 | 50 | 5 | 25 | 2 |
| | | | 69.2 | 50 | 5 | 43 | 2 |
| Paroxetin | 8.46 | 330.3 | 192.2 | 70 | 5 | 25 | 2 |
| | | | 151.2 | 70 | 5 | 30 | 2 |
| Pentoxifylline | 8.02 | 279 | 181 | 60 | 10 | 23 | 10 |
| | | | 138 | 60 | 10 | 35 | 10 |

| Compound | Rt (min) | Precursor ion | Quantifier/ qualifyer | DP[a] (V) | EP[b] (V) | CE[c] (eV) | CXP[d] (V) |
|---|---|---|---|---|---|---|---|
| Phenacetin | 8.68 | 180.3 | 110.1 | 70 | 10 | 29 | 6 |
| | | | 138 | 70 | 10 | 22 | 9 |
| | | | 152 | 70 | 10 | 21 | 7 |
| Pirimicarb | 8.02 | 239 | 72.1 | 100 | 10 | 38 | 4 |
| | | | 182.1 | 100 | 10 | 23 | 4 |
| Primidone | 8.02 | 219.2 | 91.1 | 35 | 5 | 35 | 2 |
| | | | 162.3 | 35 | 5 | 16 | 2 |
| Prochloraz | 10.94 | 376.1 | 308 | 80 | 10 | 18 | 4 |
| | | | 266 | 80 | 10 | 23 | 4 |
| Propafenone | 8.47 | 342.4 | 116 | 69 | 8 | 32 | 7 |
| | | | 98.1 | 69 | 12 | 29 | 6 |
| Propamocarb | 4.97 | 189.1 | 101.9 | 29 | 10 | 25 | 4 |
| | | | 144.1 | 29 | 10 | 16 | 4 |
| Propanolol | 7.93 | 260 | 116.2 | 35 | 5 | 23 | 2 |
| | | | 183.2 | 35 | 5 | 23 | 2 |
| Propyphenazone | 9.43 | 231.3 | 189.2 | 55 | 5 | 22 | 2 |
| | | | 201.2 | 55 | 5 | 30 | 2 |
| Pyrimethanil | 10.13 | 200.1 | 107 | 246 | 12 | 33 | 6 |
| | | | 82.1 | 246 | 8 | 35 | 7 |
| Quinmerac | 8.37 | 222 | 204 | 47 | 10 | 25 | 12 |
| | | | 141 | 47 | 13 | 45 | 10 |
| | | | 206 | 46 | 10 | 24 | 6 |
| Quinoxyfen | 12.25 | 308 | 197 | 300 | 12 | 49 | 5 |
| | | | 162 | 300 | 12 | 61 | 8 |
| Ranitidine | 3.94 | 315.3 | 176.2 | 38 | 5 | 21 | 2 |
| | | | 130.1 | 38 | 5 | 30 | 2 |
| Roxithromycin | 8.91 | 837.5 | 158 | 140 | 8 | 43 | 15 |
| | | | 679.4 | 140 | 8 | 31 | 10 |
| Salbutamol | 3.42 | 240.3 | 148.2 | 44 | 5 | 26 | 2 |
| | | | 222.2 | 44 | 5 | 14 | 2 |
| Sertraline | 7.87 | 360.3 | 158.9 | 21 | 12 | 40 | 8 |
| | | | 275.1 | 21 | 12 | 18 | 6 |
| Simazine | 9.37 | 202.1 | 132 | 45 | 5 | 26 | 2 |
| | | | 124.2 | 45 | 5 | 23 | 2 |
| Simvastatin | 11.96 | 419.1 | 285.3 | 45 | 5 | 15 | 2 |
| | | | 199.1 | 45 | 5 | 15 | 2 |
| Sotalol | 3.4 | 273.3 | 255.2 | 45 | 6 | 14 | 2 |
| | | | 133.2 | 45 | 6 | 37 | 2 |
| Sulfadiazine | 5.68 | 251.2 | 92.1 | 40 | 5 | 35 | 2 |
| | | | 108.1 | 40 | 5 | 30 | 2 |
| Sulfamethazine | 6.8 | 279 | 186.2 | 42 | 5 | 20 | 2 |
| | | | 156.1 | 42 | 5 | 26 | 2 |
| Sulfamethizole | 6.76 | 271.1 | 156.1 | 80 | 6 | 20 | 8 |
| | | | 92 | 80 | 6 | 37 | 10 |

| Compound | Rt (min) | Precursor ion | Quantifier/ qualifyer | DP[a] (V) | EP[b] (V) | CE[c] (eV) | CXP[d] (V) |
|---|---|---|---|---|---|---|---|
| | | | 108.1 | 80 | 6 | 34 | 10 |
| Sulfamethoxazole | 7.21 | 254.2 | 156.1 | 47 | 5 | 21 | 2 |
| | | | 108.1 | 47 | 5 | 30 | 2 |
| Sulfapyridine | 6.06 | 250.1 | 156.1 | 47 | 5 | 21 | 2 |
| | | | 108.3 | 47 | 5 | 34 | 2 |
| Sulfathiazole | 5.87 | 256.2 | 156 | 45 | 5 | 18 | 2 |
| | | | 92.2 | 45 | 5 | 34 | 2 |
| Sulpiride | 3.66 | 342.3 | 112 | 47 | 11 | 34 | 15 |
| | | | 214.1 | 47 | 12 | 48 | 11 |
| Tamoxifen | 9.69 | 372 | 72 | 50 | 10 | 32 | 8 |
| | | | 70 | 50 | 8 | 75 | 10 |
| | | | 129 | 50 | 6 | 38 | 7 |
| Tebuconazole | 10.95 | 308 | 70 | 80 | 7 | 50 | 11 |
| | | | 125 | 80 | 10 | 50 | 6 |
| | | | 70 | 80 | 10 | 63 | 10 |
| Telmisartan | 9.14 | 515.5 | 497.3 | 40 | 12 | 47 | 11 |
| | | | 305.2 | 40 | 12 | 58 | 15 |
| | | | 276.2 | 40 | 12 | 60 | 7 |
| Terbutaline | 3.42 | 226.3 | 152.2 | 47 | 5 | 20 | 2 |
| | | | 107.1 | 47 | 5 | 40 | 2 |
| Terbutryn | 10.05 | 242 | 186 | 100 | 13 | 27 | 10 |
| | | | 68 | 100 | 12 | 60 | 4 |
| Tetracycline | 6.47 | 445.2 | 154.2 | 75 | 10 | 40 | 11 |
| | | | 410.2 | 75 | 10 | 27 | 9 |
| Theophylline | 6.45 | 181.1 | 124.2 | 50 | 8 | 24 | 19 |
| | | | 69.1 | 50 | 8 | 35 | 12 |
| Thiabendazole | 6.72 | 202 | 131.1 | 150 | 10 | 47 | 11 |
| | | | 175.1 | 150 | 10 | 47 | 11 |
| Tramadol | 6.85 | 264 | 246.1 | 15 | 8 | 15 | 3 |
| | | | 58 | 15 | 8 | 7 | 3 |
| Tramadol N-oxide | 7.04 | 280.4 | 135.1 | 70 | 13 | 32 | 11 |
| | | | 201.1 | 70 | 13 | 27 | 10 |
| | | | 58 | 70 | 14 | 47 | 15 |
| | | | 159 | 70 | 13 | 37 | 10 |
| Trazodone | 7.4 | 372.4 | 148.1 | 73 | 12 | 48 | 8 |
| | | | 176 | 73 | 12 | 35 | 10 |
| Triamterene | 6.66 | 254.6 | 238.1 | 29 | 12 | 39 | 12 |
| | | | 168.1 | 29 | 12 | 47 | 10 |
| Trigonelline | 2.65 | 138.2 | 78.2 | 45 | 8 | 33 | 12 |
| | | | 92.2 | 150 | 10 | 47 | 11 |
| Trimethopim | 5.95 | 291.3 | 230.2 | 45 | 5 | 28 | 2 |
| | | | 123.2 | 45 | 5 | 30 | 2 |
| Vancomycin | 4.75 | 725.3 | 100.3 | 150 | 10 | 47 | 11 |
| | | | 144.3 | 150 | 10 | 47 | 11 |

| Compound | Rt (min) | Precursor ion | Quantifier/ qualifyer | DP[a] (V) | EP[b] (V) | CE[c] (eV) | CXP[d] (V) |
|---|---|---|---|---|---|---|---|
| Venlafaxine | 7.71 | 278.4 | 58.1 | 50 | 5 | 45 | 2 |
| | | | 260.4 | 50 | 5 | 15 | 2 |
| Verapamil | 8.07 | 455.5 | 303.3 | 52 | 10 | 36 | 8 |
| | | | 260 | 52 | 12 | 41 | 14 |

713 [a]DP: Declustering Potential; [b]EP: Entrance Potential; [c]CE; Collision Energy; [d]CXP: Collision
714 Cell Exit Potential

715

716 **Table SI-5.** Evolution of OMC removal detected in the retentate during solar-assisted AO treatment

| | Concentration (ng $L^{-1}$) | | | | | | | | | | |
|---|---|---|---|---|---|---|---|---|---|---|---|
| **OMCs** | **0 min** | **15 min** | **30 min** | **45 min** | **60 min** | **75 min** | **90 min** | **120 min** | **150 min** | **180 min** | **Removal (%)** |
| 4AA | 4579 | 173 | 101 | | | | | | | | >99 |
| 4AAA | 14347 | | 11136 | 8589 | 8346 | 7792 | 5041 | 4015 | 1287 | 362 | 98 |
| 4FAA | 28357 | | 21905 | 20859 | 18779 | 14167 | 11298 | 6491 | 2585 | 780 | 97 |
| Carbamazepine | 7068 | 6732 | | 6532 | 6091 | | 5159 | 4703 | 4651 | 3942 | 44 |
| Citalopram | 878 | | 560 | 557 | 295 | 175 | 85 | | | | >99 |
| Diatrizoic acid | 1461 | 1382 | | | | | 1043 | 969 | 766 | 693 | 53 |
| Pentoxifylline | 842 | 726 | 541 | 564 | 464 | | | | | 442 | 48 |
| Venlafaxine | 2928 | 2127 | 1934 | 1747 | 1152 | 1042 | 806 | 195 | 50 | | >99 |
| Gabapentin | 12385 | | 9450 | | 7035 | 6741 | 6258 | 4918 | 3726 | 2727 | 78 |
| Acetamiprid | 471 | | | | | | | | | 438 | 7 |
| Azoxistrobin | 57 | 54 | | 49 | | | 48 | 43 | 39 | 36 | 37 |
| Imidacloprid | 4525 | 4479 | 4116 | | | | 3695 | 3227 | 2316 | 2087 | 54 |
| Terbutryn | 172 | | | | | | | | | 155 | 10 |
| Azithromycin | 537 | 414 | | 234 | 182 | 108 | 56 | | | | >99 |
| Lincomycin | 705 | 421 | 0 | | | | | | | | >99 |
| Cetirizine | 1693 | 1624 | 1584 | | 1510 | 1425 | 1312 | 1276 | 1147 | 1026 | 39 |
| Sulpiride | 4056 | 3805 | 3058 | 2182 | 1720 | 1173 | 846 | 396 | 256 | 13 | >99 |
| Telmisartan | 1586 | | 1562 | | | 1540 | | 1533 | 1295 | 1274 | 20 |
| N-desmethylcitalopram | 479 | | | 391 | | | | | | 350 | 27 |
| Flecainide | 403 | 341 | 257 | | 209 | 189 | 162 | | 107 | 96 | 76 |
| Irbesartan | 1554 | 1482 | | 1334 | 1332 | 1313 | | 1186 | 993 | 905 | 42 |
| Iminostilbene | 5775 | | | | 5557 | 4953 | | 4565 | | 3406 | 41 |
| Diazepam | 25 | | | 25 | | 24 | | | | 22 | 15 |
| Fenofibric acid | 370 | 264 | 181 | 111 | 62 | 35 | | | | | >99 |

| | | | | | | | | | | | |
|---|---|---|---|---|---|---|---|---|---|---|---|
| Indomethacin | 68 | 37 | | | | | | | | | >99 |
| Naproxen | 928 | 811 | 775 | 705 | | | | | | | >99 |
| Propanolol | 215 | 137 | | | | | | | | | >99 |
| Carbendazim | 138 | | 127 | 112 | 116 | 104 | 105 | 99 | 80 | 65 | 53 |
| Dimethoate | 127 | 118 | | 100 | 77 | | | | | | >99 |
| Diuron | 70 | | 67 | | | 65 | | 59 | 57 | 47 | 33 |
| Isoproturon | 85 | 74 | 73 | 62 | 61 | 50 | 39 | 21 | | | >99 |
| Metalaxyl | 18 | | | 17 | | 17 | | | 15 | 15 | 16 |
| Myclobutanil | 41 | | 41 | | | | 39 | | 39 | 37 | 11 |
| Tebuconazole | 34 | | 33 | 33 | 33 | | 30 | | 28 | 27 | 20 |
| Erithromycin | 19 | 14 | 5 | 3 | | | | | | | >99 |
| Metronidazole | 161 | 141 | | 135 | 116 | 109 | 106 | 87 | | | >99 |
| Sulfathiazole | 43 | | | | | | | | | | >99 |
| Trimethoprim | 272 | 185 | 94 | | | | | | | | >99 |
| Levofloxacin | 1929 | 1758 | | 1557 | 918 | 879 | 451 | 168 | | | >99 |
| Alfuzosin | 9 | 8 | 6 | 6 | | | | | | | >99 |
| Domperidone | 34 | 33 | | | | | | | | | >99 |
| Propafenone | 18 | 11 | | | | | | | | | >99 |
| Memantine | 194 | 178 | 140 | 139 | 109 | 96 | 74 | 41 | | | >99 |
| Trazodone | 85 | 51 | | | | | | | | | >99 |

717

**Author statement:**

**Irene Salmerón:** Methodology, Investigation, Preparation, creation and/or presentation of the published work, writing the initial draft; **Gracia Rivas:** Data Curation, Visualization; **Isabel Oller:** Term, Conceptualization, Writing Review and Editing; **Ana Martínez-Piernas:** Specific Methodology on liquid chromatography coupled to mass spectrometry, Investigation; **Ana Agüera:** Supervision, Data curation and visualization liquid chromatography coupled to mass spectrometry, Resources; **Sixto Malato**: Project administration, Funding acquisition.

Process Safety and Environmental Protection

# Electrochemically Assisted Photocatalysis for the Simultaneous Degradation of Organic Micro-Contaminants and Inactivation of Microorganisms in Water

--Manuscript Draft--

| | |
|---|---|
| **Manuscript Number:** | PSEP-D-20-00435 |
| **Article Type:** | SI: Advanced Oxidation - Full Length Article |
| **Keywords:** | Carbon-felt cathode; Escherichia coli; organic microcontaminants; photoelectrocatalysis; TiO2 nanotubes photoanode; water purification |
| **Corresponding Author:** | Pilar Fernandez-Ibanez<br>Ulster University<br>United Kingdom |
| **First Author:** | I. Salmerón |
| **Order of Authors:** | I. Salmerón |
| | P. K. Sharma |
| | M.I. Polo-López |
| | A. Tolosana |
| | I. Oller |
| | J.A. Byrne |
| | Pilar Fernandez-Ibanez |
| **Manuscript Region of Origin:** | Europe |
| **Abstract:** | This study presents the assessment of the performance of a photoelectrochemical reactor for the simultaneous degradation of organic microcontaminants (OMCs) and inactivation of bacteria in real surface water. Target OMCs were terbutryn, clorfenvinphos and diclofenac (500 µg L-1 each), and E. coli K12 (10 6 CFU mL -1 ) was used as the model microorganism. The reactor utilised a photoanode consisting of two Ti mesh electrodes anodised to give aligned self-assembled TiO 2 nanotubes on the surface. Two cathode materials were investigated i.e. Pt and carbon felt. Higher E. coli inactivation rates were observed with electrochemically assisted photocatalysis (EAP) with a 2-Log Reduction Value (LRV) for Pt CE and 2.7-LRV in 2h for carbon felt cathode, as compared to only a 0.8 LRV for photocatalysis (open circuit). For the simultaneous degradation of OMCs and inactivation of bacteria a 4.5-LRV was achieved in 90 min with applied potential and a carbon felt cathode. Similar degradation kinetics were observed for the OMC for both electrochemically assisted photocatalysis and photocatalysis (open circuit) with ca 70% of the removal of the total OMCs in 60 min. Hydroxyl radical, H 2 O 2 and chlorine generation were also evaluated to elucidate the mechanisms of degradation and disinfection. This work suggests that electrochemically assisted photocatalysis is more efficient than photocatalysis alone for the combined removal of OMCs and disinfection of water. |
| **Suggested Reviewers:** | Cristina Adan<br>cristina.adan@urjc.es<br>She has already several publications in this area. |
| | Dionissios Mantzavinos<br>mantzavinos@chemeng.upatras.gr<br>He is an expert on AOPs and has some contributions in the area of PEC cells. |
| | Adrian Silva<br>adrian@fe.up.pt<br>expert on AOPs fro water and wastewater purification |
| | Ignasi Sires<br>i.sires@ub.edu<br>Expert on photo-electro-chemistry for water applications |

Ulster University
NIBEC
Shore Road
Newtownabbey
BT37 0QB

T: +44 (0)28 9036 8664
W: nibec.ulster.ac.uk

Professor Adisa Azapagic
Editor-in-Chief
Process Safety and Environmental Protection

July 8, 2020

Dear Dr. Azapagic,

We wish to submit our manuscript entitled “Electrochemically Assisted Photocatalysis for the Simultaneous Degradation of Organic Micro-Contaminants and Inactivation of Microorganisms in Water” for consideration as a Process Safety and Environmental Protection full research article. This paper is co-authored by researchers at CIEMAT – Plataforma Solar de Almeria, Spain, and Ulster University, UK.

We believe that this full research paper is timely for publication in Process Safety and Environmental Protection because it addresses a novel photoelectrochemical cell where the traditionally investigated platinum is substituted by carbon felt with the aim of reducing costs of further applications. The goal of this study is to compare electrochemically assisted photocatalysis using a photo-electrochemical cell with titania-nanotubes photoanode with either a carbon felt or Pt cathode for the simultaneous degradation of organic micropollutants and inactivationof bacteria in surface water. In this work three selected emerging pollutants, terbutryn, chlorfenvinphos and diclofenac and *E. coli* K12 were used at the same concentrations that they are usually found in the environment in natural surface water. This paper contributes with a clear research impact in the area of electrochemical cells and water remediation.

We confirm that this work is original and has not been published elsewhere, nor is it currently under consideration for publication elsewhere. We have no conflicts of interest to disclose.

Thank you for your consideration of this manuscript.

Yours truly,

Dr Pilar Fernandez-Ibanez
p.fernandez@ulster.ac.uk

Graphical Abstract

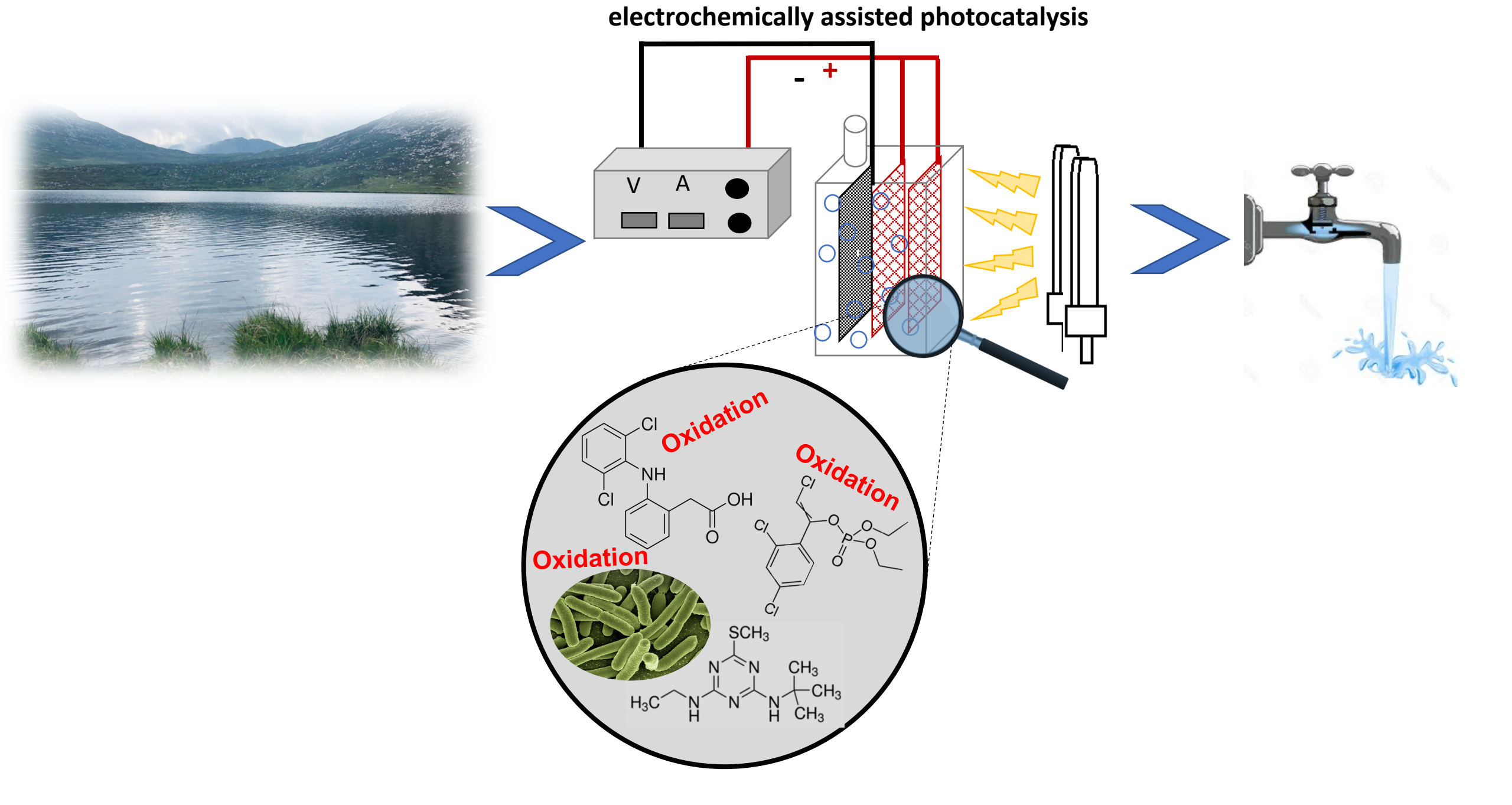

**Title:** Electrochemically Assisted Photocatalysis for the Simultaneous Degradation of Organic Micro-Contaminants and Inactivation of Microorganisms in Water

**Authors**: I. Salmerón[a], P. K. Sharma[b], M.I. Polo-López[a], A. Tolosana[b], I. Oller[a], J.A. Byrne[b], P. Fernández-Ibañez[b*]

[a]Plataforma Solar de Almería-CIEMAT. Ctra Senés km 4, 04200 Tabernas (Almería), Spain.

[b]Nanotechnology and Integrated BioEngineering Centre, School of Engineering, Ulster University, Northern Ireland, BT37 0QB, United Kingdom

* Corresponding author:

Pilar Fernandez: p.fernandez@ulster.ac.uk

**Title:** Electrochemically Assisted Photocatalysis for the Simultaneous Degradation of Organic Micro-Contaminants and Inactivation of Microorganisms in Water

**Authors**: I. Salmerón[a], P. K. Sharma[b], M.I. Polo-López[a], A. Tolosana[b], I. Oller[a], J.A. Byrne[b], P. Fernández-Ibañez[b*]

[a]Plataforma Solar de Almería-CIEMAT. Ctra Senés km 4, 04200 Tabernas (Almería), Spain.

[b]Nanotechnology and Integrated BioEngineering Centre, School of Engineering, Ulster University, Northern Ireland, BT37 0QB, United Kingdom

* Corresponding authors:

Pilar Fernandez: p.fernandez@ulster.ac.uk

**ABSTRACT**

This study presents the assessment of the performance of a photoelectrochemical reactor for the simultaneous degradation of organic microcontaminants (OMCs) and inactivation of bacteria in real surface water. Target OMCs were terbutryn, clorfenvinphos and diclofenac (500 µg L-1 each), and *E. coli* K12 ($10^6$ CFU $mL^{-1}$) was used as the model microorganism. The reactor utilised a photoanode consisting of two Ti mesh electrodes anodised to give aligned self-assembled $TiO_2$ nanotubes on the surface. Two cathode materials were investigated i.e. Pt and carbon felt. Higher *E. coli* inactivation rates were observed with electrochemically assisted photocatalysis (EAP) with a 2-Log Reduction Value (LRV) for Pt CE and 2.7-LRV in 2h for carbon felt cathode, as compared to only a 0.8 LRV for photocatalysis (open circuit). For the simultaneous degradation of OMCs and inactivation of bacteria a 4.5-LRV was achieved in 90 min with applied potential and a carbon felt cathode. Similar degradation kinetics were observed for the OMC for both electrochemically assisted photocatalysis and photocatalysis (open circuit) with ca 70% of the removal of the total OMCs in 60 min. Hydroxyl radical, $H_2O_2$ and chlorine generation were also evaluated to elucidate the mechanisms of degradation and disinfection. This work suggests that electrochemically assisted photocatalysis is more efficient than photocatalysis alone for the combined removal of OMCs and disinfection of water.

**Keywords:** Carbon-felt cathode, *Escherichia coli*, organic microcontaminants, photoelectrocatalysis, $TiO_2$ nanotubes photoanode, water purification.

## 1. Introduction

The increase of the pharmaceutical and agricultural industry during the last decades has led to the appearance of new organic substances into the environment. These compounds are commonly present at very low concentrations, from ng $L^{-1}$ to µg $L^{-1}$, however they are highly toxic or non-biodegradable and their effects into the ecosystems and humans are still unknown. Their recalcitrant character makes them unable to be removed by biological treatments thus in wastewater treatment plants (WWTP) without a proper tertiary treatment they are directly discharged into water bodies. Furthermore, wastewater will contain pathogenic microorganisms which should be inactivated before discharge to certain catchments or before reuse for irrigation. In this context Advanced Oxidation Processes, able to generate a highly oxidative species, appear as a useful tool for the simultaneous removal of organic microcontaminants (OMCs) and bacteria.

Titanium dioxide ($TiO_2$) is a semiconductor photocatalyst widely investigated for the degradation of pollutants and inactivation of microorganisms.; however, $TiO_2$ photocatalysis requires UV excitation, and typically displays low quantum efficiencies due to fast charge carrier recombination. Where the $TiO_2$ is immobilised on an electrically conducting support, the application of an external electrical bias improves the separation of the photogenerated charge carriers, and thus improves the overall efficiency (Byrne et al., 2002). This process is normally referred to as electrochemically assisted photocatalysis (EAP), photoelectrocatalysis or sometimes, photoelectrolysis. The immobilization or formation of the catalyst on a support can decrease the effective surface area available for reaction, and may result in mass transfer limitations in the reactor (Leng et al., 2006; Pablos et al., 2017a). However, in EAP, mass transport might be improved due to the electromigration of negatively charged bacteria to a positively biased photoanode (Pablos et al., 2017a).

With EAP, oxidation of water at the semiconductor electrode (photoanode) gives hydroxyl radicals and reduction of molecular oxygen at the cathode can generate superoxide radical anion, hydrogen peroxide, and hydroxyl radicals. In natural water matrices containing dissolved ions, the EAP leads to the generation of other species including active chlorine species (ACS), HClO ($E^0$= 1.49 V/SHE) and $ClO^-$ ($E^0$=0.89 V/SHE) (Moreira et al., 2017), which are widely recognized as key oxidants in electrolytic water treatment. In a photoelectrochemical cell (PEC), the sites for oxidation and reduction are spatially separated avoiding surface recombination reactions, and photogenerated charge carriers are separated under the influence of the electric field, decreasing the rate of bulk recombination.

Generally, Pt has been used as counter electrode because its good chemical resistance to corrosion even in strongly aggressive media (Panizza, 2010) and low overpotential for reduction reactions

such as $H_2$ evolution. However, carbon-based electrodes have been extensively studied as cathodes (Cotillas et al., 2015; Le et al., 2017) due to their selective reduction of molecular oxygen to hydrogen peroxide (Panizza, 2010). The use of carbon cathodes is widespread in other electro-oxidative processes for the in situ generation of Fenton reagent, such as electro-Fenton (Le et al., 2017) or solar photoelectro-Fenton. Most published research does not specifically consider the nature of the counter electrode in EAP, however, Xie and Li (2006) reported a significant increase in the degradation of orange-G dye from 3.4% with a Pt cathode to 25.1% using reticulated vitreous carbon (RVC).

Previous research has reported that EAP using titanium dioxide nanotube ($TiO_2$-NTs) electrodes can achieve high inactivation rates for bacteria (Baram et al., 2009; Pablos et al., 2017b), even in seconds (Liu et al., 2013) depending on the reactor configuration, electrical potential applied, and the electrolyte solution. For degradation of organic micropollutants, $TiO_2$-NTs PEC have been applied for contaminants removal such as diclofenac (Cheng et al., 2016), pentachlorophenol (Quan et al., 2007), or even aromatic amines (Cardoso et al., 2010). However, the use of these systems for real waters with the aim of simultaneous disinfection and elimination of OMCs, in a realistic range of μg $L^{-1}$, has not been reported.

The goal of this study is to compare electrochemically assisted photocatalysis using a PEC reactor with a $TiO_2$-NT photoanode with either a carbon felt or Pt cathode for the simultaneous degradation of OMCs and inactivation of bacteria. In this work terbutryn (TBT), chlorfenvinphos (CVP), and diclofenac (DFC), were selected as OMCs and *E. coli* K12 (at $10^6$ CFU $mL^{-1}$) was used as model microorganism. Natural (non-autoclaved or filtered) surface water was used for all experiments.

## 2. Materials and methods

### *2.1 Water matrix characterization*

The water matrix used in this study was surface water. It was collected from a natural stream in Whiteabbey (Newtownabbey, UK). The characterization of this water matrix was done using a pH meter (multi720, WTW, Germany), conductivity meter (GLP31, CRISON, Spain), and turbidimeter (Model 2100N, Hach, USA). Ionic composition was measured using an ion chromatograph (IC) (Model 850, Metrohm, Switzerland). Dissolved organic carbon (DOC) was measured with a TOC analyser (Shimadzu TOC 5000A, Japan). Main characteristics of the water are pH 7.35, electric conductivity of 697 μS $cm^{-1}$, 0.1 NTU of turbidity, 6.9 mg $L^{-1}$ of DOC and 18.4 mg $L^{-1}$ of chloride. The detailed characterization is shown in Table SI-1.

### *2.2 Bacterial enumeration and quantification*

*E. coli* K12 was obtained from the Spanish Culture Collection (CECT 4624). Fresh liquid cultures were prepared in Tryptone Soya Broth CM0129 (OXOID) and incubated during 20 h at 37 °C with rotary shaking, in order to achieve the stationary phase of $10^9$ CFU $mL^{-1}$. Bacterial suspensions were diluted in the reactor to reach an initial concentration of $10^6$ CFU $mL^{-1}$. The bacteria stock solution added to the water sample a DOC concentration of 6.7 mg $L^{-1}$. All samples were enumerated using the standard plate counting method with Tryptone Soya Agar CM0131 (OXOID). Six 20 µL drops of each dilution were plated. Colonies were counted after incubation at 37 °C for 24 h. The limit of detection (DL) was 9 CFU $mL^{-1}$.

For hole-acceptor experiments bacterial suspensions were harvested by centrifugation at 3000 rpm for 10 min. Then, the pellet was re-suspended in Phosphate Buffer Saline (PBS) solution and diluted directly into the sample to reach the initial concentration of $10^6$ CFU $mL^{-1}$. Water samples taken during the experiments were enumerated using the standard plate counting method with ChromoCult®Coliform Agar (Merck KGaA, Darmstadt, Germany). 10-fold dilutions of water samples were done in PBS, and volumes ranged between 50-500 µL were spread onto Petri-dishes surface. Colonies were counted after an incubation period of 24 h at 37 ºC. Detection limit of this procedure was 2 CFU $mL^{-1}$.

### *2.3 Organic Microcontaminant Analysis*

TBT, CVP, and DFC were used as a representative mixture of OMCs since they cover a wide spectrum of commonly found chemical anthropogenic contamination in surface waters (herbicide, pesticide and drugs respectively). The OMCs used were analytical grade, purchased from Sigma-Aldrich. Stock solutions containing the three OMCs at 2.5 g $L^{-1}$/OMCs were prepared in methanol (organic matrix to dissolve the OMCs) and stored at 4ºC. stock solution (38 µL) was diluted in the sample to reach an initial concentration of 500 µg $L^{-1}$/OMCs. The dilution of OMCs added 60 mg $L^{-1}$ of extra DOC concentration to the water matrix. The OMC concentration was monitored by high performance liquid chromatography using a HPLC/UV Agilent Technologies Series 1100, equipped with an analytical column Luna C18 (4.6 mm x 150 mm, 3µm) from Phenomenex. Injection volume was 100µL. The three OMCs were simultaneously detected using a gradient method, from 90/10 (v/v) of formic acid (25 mM)/acetonitrile (ACN) to 100% ACN after 14 min with a flow rate 1 mL $min^{-1}$.

For HPLC measurements, samples were prepared mixing 900 µL of sample and 100 µL of ACN that were filtered through a Millipore Millex-GN 0.20 µm nylon membrane filter. Then, the solution was transferred into HPLC vials, put in the HPLC and results analysed. Quantification of each OMC was done according to a standard curve previously prepared in the range of 10 to

1000 µg $L^{-1}$. Retention time, limit of quantification (LOQ), limit of detection (LOD), and maximum absorption for each OMCs are shown in Table SI-2.

### *2.4 Electrode preparation and characterization*

The $TiO_2$-NT photoanodes were fabricated by electrochemical anodization of titanium mesh (Sigma-Aldrich) using the method described elsewhere (Shin and Lee, 2008). Briefly, titanium mesh (75 x 95 $mm^2$) were sonicated and washed in 5% Decon90 detergent, distilled water and ethanol, sequentially. Electrochemical cell for anodization consisted of Pt coated Ti mesh cathode and titanium mesh as anode on each side of cathode, in a polypropylene beaker. The anodization process was repeated on the opposite side of the Ti mesh to have uniform nanotubes growth on both sides of the Ti mesh. The electrolyte solution was prepared by mixing $NH_4F$ (0.3 wt%) in distilled water (3.0 vol%) and ethylene glycol (97 vol%). The anodization was performed at 30 V for 3 h using a PLH120 Power Supply. After anodization, the foils were rinsed multiple times in distilled water and then annealed at 500°C in air for 20 h (ramp 2°C $min^{-1}$ up and 1°C $min^{-1}$ down) in a Lenton AWF 12/5 Chamber Furnace.

The growth, coverage and dimensions of the $TiO_2$-NTs were examined using scanning electron microscopy (SEM) at 10 kV (Hitachi SU5000 FESEM). Energy dispersive X-ray analysis (EDX) was performed using Oxford Instruments EDX coupled with FESEM system.

### *2.5 Photoelectrochemical cell configuration*

The total volume of the PEC reactor was 190 mL, which was irradiated through a quartz window (Figure 1a). $TiO_2$-NTs and platinized Ti mesh (Ti-Pt) mesh (Sigma-Aldrich) or carbon felt (Sigracet GDL 28 BC from Ion Power) were used as photoanode and cathodes for the different experiments, respectively. Electrode dimensions were 7.5 cm x 9.5 cm, with a total surface area of 71.25 $cm^2$ each. The electrodes were assembled following an anode-anode-cathode configuration in order to maximise the absorption of irradiated photons. The nanotubes were grown on Ti mesh that allowed 50% of the light to pass through its faces (experimentally determined). The misaligned mesh electrodes combination allowed only 25% of the light to pass through, so at least 75% of the direct photons interacted with the photoanodes. The reactor was operated in batch mode and electrodes were biased with a PLH120 Power Supply.

An air-blower was connected to the reactor with a flow rate of 0.36 mL $min^{-1}$ to avoid the depletion of dissolved oxygen during the photocatalytic process and simultaneously kept the solution stirred. Two 9W UVA black light lamps were placed in front of the Ti-mesh side of the PEC (Phillips, Actinic BL PL-S 9W/10/2P; 370 nm-peak wavelength). The irradiation profile of the lamps (Fig SI-1) was determined by the use of a GEMINI 180 scanning monocromator from

HORIBA, measuring at different distances of the source aiming to achieve an incident irradiance of 50 W $m^{-2}$ in the UVA, equivalent to high intensity solar UV with Air Mass of 1.5 (ASTM E-490-00). A scheme of the complete system is shown in Figure 1b

**FIGURE 1**

### *2.6 Photoelectrochemical experiments*

The reactor operational potential was determined according to the minimum potential at which maximum photocurrent (plateau) is reached (see section 3.3). For this purpose, several potentials were applied to the cell, increasing the interval by 0.1 V each time, measuring the current response in dark conditions and under irradiation for each applied potential. The photocurrent is calculated thought the difference between the current response under radiation and in dark. Current densities and applied potentials were measured using LAP MAS830B multimeter.

For OMCs and bacterial removal experiments the reactor was filled with surface water in natural conditions (without any pre-treatment or addition of reagents), at pH 7.4 and air sparged. After a few minutes the target contaminant was added, whether it was the microorganism, the OMCs, or both, leaving to equilibrate for 10 min. An initial sample t=0 was taken and the reactor was biased and exposed to irradiation. The samples were taken at 5 min interval till 20 min, every 15 min till 60 min and then every 30 min until the end of the. Before and after carrying out each experiment, the reactor was washed with a solution of 10 mg $L^{-1}$ hydrogen peroxide and was rinsed three times with distilled water.

### *2.7 ROS determination*

Several oxidative agents generated during PEC operation were detected by spectrophotometric methods. A JENWAY 6300 UV-VIS spectrophotometer was used with glass cuvettes of 1 cm path length.

*i) Hydroxyl radicals* generated were measured by spectrophotometry following procedure described elsewhere (Cruz-Ortiz et al., 2017; Muff et al., 2011). Briefly, it consists of detecting the bleaching of a solution with 17 µM P-nitrosodimethylaniline (RNO) (Sigma-Aldrich) by measuring light absorbance at 440 nm. Quantification was made in the range from 1 to 20 µM. It has to be considered that the presence of other oxidant could generate interferences in this method.

*ii) Free chlorine* (FC) was determined following N,N-diethyl-p-phenylenediamine (DPD) method 10069 from HACH. It consists on the addition of DPD powder pillows from HACH to the sample, mixing for 30 seconds and measuring at 530 nm.

*iii) Hydrogen peroxide* concentration was determined by direct reaction with titanium (IV) oxysulfate. For that, 2 mL of 280 mM solution of $TiOSO_4$ (Sigma-Aldrich) were mixed with 2 mL of sample (Cruz-Ortiz et al., 2017). The yellow complex formed from the reaction of titanium IV oxysulfate with $H_2O_2$ is measured at 410 nm. Absorbance was read after 5 min equilibration time against a standard curve in the $H_2O_2$ concentration range 1-60 mg $L^{-1}$.

## 3. Results and discussion

### *3.1 Anodised $TiO_2$-NTs characterisation*

Figure 2a shows SEM images of the nanotubes fabricated by the electrochemical anodisation of Ti mesh. There was a reasonable uniform coverage of the mesh with $TiO_2$-NT with an average outer diameter of 95.2 nm, inner diameter of 73.6 nm diameter, tube wall thickness of 21.6 nm and average length of 1.05 μm.

The SEM-EDX measurements of the annealed nanotubes show the peaks corresponding to Ti and O elements, indicating the formation of the $TiO_2$ nanotubes (data not shown). The XRD analysis of the samples was performed on annealed nanotubes, (Figure 2b). As shown in the figure, the major peaks correspond to anatase planes A(101) and A(004). Other peaks corresponding to A(200), rutile R(110) and titanium metal were obtained. The titanium metal peaks are coming from the Ti substrate used for the nanotubes growth. Presence of significantly less intense rutile peaks indicates that the nanotubes are mostly anatase with very little contribution from rutile phase.

**FIGURE 2**

### *3.2 Assessment of boundary effects on PEC cell: dark and photocatalytic (PC) tests*

To discriminate the influence of any possible parameter on the water disinfection and decontamination performance of PEC a series of different tests were carried out. Firstly, the viability of *E. coli* in the presence of OMCs were assessed in the dark. Results obtained demonstrated that the initial concentration of bacteria ($10^6$ CFU $mL^{-1}$) remained constant for 3 h (Fig. SI-2). This result discarded therefore any toxic effect over bacterial viability due to the presence of 500 μg $L^{-1}$ of each contaminant (including the 158 mg $L^{-1}$ -approximately 5 mM- of methanol added from the OMCs stock solution).

The photocatalytic activity of $TiO_2$-NT to inactivate *E. coli* and remove OMCs from water was also investigated using the same PEC without applying the electrical bias (open circuit = photocatalysis). Figure 4a shows a very small decay of *E. coli* concentration in 2 h of photocatalytic (PC) treatment, attaining only 0.8-Log Reduction Value (LRV) after 2 h of PC. This low efficiency is not surprising in an immobilized catalyst configuration. It is very well known that its photocatalytic disinfection efficiency is lower compared with similar load of catalyst in slurry, especially if the catalyst is disposed as a flat plate as mode of immobilisation. This is due to the reduced catalytic surface area available ROS generation, and mass transport limitations from bulk solution to the electrode surface.

Prior to any OMCs degradation test, controls were performed to determine dark adsorption of the OMCs on the electrodes. For that, OMCs were added to the reactor leaving in dark during 1h, being the decay negligible. The removal of the ∑OMCs by PC during 60 min of treatment was studied (Figure 4b). The mixture of OMCs illustrated a representative mixture of different anthropogenic contaminants that could be found in surface waters, therefore the ∑OMCs was monitored during the experiment which permitted the comparison with different operating conditions. A linear decrease was observed in this case, reaching ca. 70% of degradation of the mixture, with a zero order rate constant $k$ =1.07 ± 0.08 ($10^{-2}$ $min^{-1}$). Nevertheless, the removal was not similar for each OMC, a degradation of 57%, 60% and 87% of TBT, CVP and DCF, respectively were attained (Fig SI-3). After 60 min of PC treatment, OMCs concentrations were below their limit of quantification (see Table SI-2). TBT and CVP presented similar behaviour, with a slower degradation rates that shows its greater recalcitrant character when compared to DCF, which almost eliminated. The removal of ∑OMCs achieved (ca. 70%) without system optimisation was near to that established as target by Switzerland regulations for WWTP effluents (80% of ∑OMCs removal), being a reference for the rest of countries since it is the first water regulation addressing OMCs concern (Bourgin et al., 2018) in Europe. DOC effect was also followed in other study (Gao et al., 2020) determining that in a concentration higher than 10 mg $L^{-1}$ produces a decrease in the degradation rates of DFC due to competition for active sites and ROS. In the present study, with at least 60 mg $L^{-1}$ of DOC, a marked reduction in the degradation efficiency of the PEC for both, organics and bacteria, was expected. In fact, this study is focused on a real water matrix scenario, where naturally present ions interfere and the total organic matter acts as background organic matter.

### *3.3 Photoelectrocatalysis with cathode of Pt*

The optimal current density (calculate photocurrent) for the Pt cathode PEC (PEC-Pt) was established by measuring current response in the dark and under UVA irradiation with applied cell potential between 0.0 V to 1.5 V, using surface water as electrolyte. Figure 3 shows that the

photocurrent rises significantly till 0.5 V, from which the increase was moderated reaching a plateau after the application of 1.0 V. Therefore, 1.0 V was selected as the operating potential for EAP tests, corresponding to a photocurrent response of 3 mA (estimated current density of 21 µA $cm^{-2}$).

**FIGURE 3**

As this is an electrochemical process, the PEC efficiency is clearly influenced by the concentration of salts in the water to be treated, not only due to the impedance presented for the electrical current, but also from the specific ionic content. It has been demonstrated that the ionic species dissolved in the water determine the oxidant species generated during the electrochemical treatment (Farhat et al., 2017, 2018) since ACS are produced from chlorides oxidation and sulphate radicals ($E^0$ = 2.5 – 3.1 V) from sulphates, adding their oxidative effect to that of the hydroxyl radicals.

The content of salts from the actual stream under study (see Table SI-1) was far from the majority of studies previously published, in which highly concentrated solutions of $Na_2SO_4$, NaCl or $NaNO_3$, etc., are used as electrolytes, thus the behaviour of our system was very different. The matrix effect is also remarked by Moles et al. (2020) where it was clear the difference between a NaCl solution and a real effluent as water matrix, since disinfection with saline solution achieved 7-LRV while in the wastewater effluent was reached ca. 1-LRV, evidencing the influence of the water composition in the disinfection process by PEC.

Despite the low salinity of the surface water (697 µS $cm^{-1}$ vs 8.8 mS $cm^{-1}$ of a 50 mM $Na_2SO_4$ supporting electrolyte solution), the PEC-Pt system gave a 2-LRV in 120 min of treatment as is shown in Figure 4a. In comparison with PC alone, a similar pattern of bacteria inactivation was obtained with PEC-Pt, but with a slight increase on the bacterial reduction at the end of the treatment. This enhancement can be attributed to the enhanced charge carrier separation.

The application of an electrical bias has been reported to give also an enhancement in the degradation of OMCs as compared to PC (Cheng et al., 2016; Nie et al., 2013). In this work no real difference was observed in the rate of OMC degradation with EAP ($k$ =1.15 ± 0.12 ($10^{-2}$ $min^{-1}$)) as compared to PC ($k$ =1.07 ± 0.08 ($10^{-2}$ $min^{-1}$)) (Fig. 4b). This behaviour remarked the influence of the high amount of organic matter provided by the stock solution, that competed with OMCs for oxidizing radicals.

The direct comparison with previous work on the EAP degradation of OMCs is not realistic due differences in experimental parameters (mainly a high OMCs concentration in the range of several mg $L^{-1}$). However Mazierski et al. (2019) studied the removal of 0.385 mM (50 mg $L^{-1}$) of 5-fluorouracil in a 42 mM $Na_2SO_4$ solution with a $TiO_2$-NT photoanode, using in a solar simulator with a Xenon lamp applying an UV-A irradiation of 4.5 mW $cm^{-2}$ (45 W $m^{-2}$). When applied a potential of 1 V, more than 60 min were needed to remove the 80% of the initial concentration of 5-fluorouracil, approximately the same time as was needed to our system to remove the same percentage starting from a lower concentration of pollutant. In other cases, as Cheng et al. (2016), the treatment time is much longer, since using a $TiO_2$-NT anode (4 $cm^2$) and a 35W Xenon lamp, needed more than 5 h to remove the 80% of 5 mg $L^{-1}$ of DCF in a 0.1M solution of $Na_2SO_4$ applying 0.4 V.

**FIGURE 4**

### *3.4 Photoelectrocatalysis with cathode of C-felt*

The working potential for PEC with C-felt cathode (PEC-C felt) was determined by monitoring the photocurrent response with the cell potential increasing from 0.0 V to 1.5 V and observing the maximum photocurrent value (Fig. 3). The photocurrent behaviour was similar to PEC-Pt, reaching the maximum at 1V, but with a lower current density value, 1.8 mA (12.5 µA$cm^{-2}$) due to the higher resistance of the carbon felt as compared to Ti-Pt mesh.

Figure 5a shows the *E. coli* inactivation profile obtained by PEC-C felt. Although a lower photocurrent was observed, there was a greater LRV of 2.7 achieved. It has been reported previously that the rate of disinfection is not directly proportional to the photocurrent in EAP (Pablos et al., 2017b). The improvement in the rate of disinfection may be attributed to the selective production of hydrogen peroxide ($H_2O_2$) at the carbon cathode.

It is well known that $H_2O_2$ is a disinfectant that even at low concentrations it can enhance the rate of photo-inactivation of microorganisms (Polo-López et al., 2011). This phenomenon is explained by the diffusion of $H_2O_2$ across the cell membrane as it is a non-charged molecule. Once inside the cell, the equilibrium of ROS changes, releasing the iron naturally occurring in cells that reacts with $H_2O_2$ to produce internal $^{\bullet}OH$ which accumulation and reaction with internal structures (DNA, proteins, enzymes, etc) finally determines the cell death (Giannakis et al., 2016). In fact, the use of a carbon cathode for in situ generation of $H_2O_2$ as an enhancement for solar disinfection (SODIS) process was investigated by Jin et al. (2020) that reach approximately 6-LRV on *E. coli K12* concentration in 180 min while 3-LRV was attained by only SODIS and electrolysis 1-LRV.

For the PEC-C felt system it is possible to calculate the theoretical maximum amount of $H_2O_2$ electrogenerated that could be obtained in the system. Knowing the electrical charge ($Q$), with the Faraday constant ($F$, 96485 Q $mol^{-1}$), the $e^-$ moles ($n_e$) can be calculated based on equation 1. The maximum accumulated $H_2O_2$ that could be generated in our experimental system, assuming that all $e^-$ are employed in its production, was 15 mg $L^{-1}$ after 120 min. However, as it was consumed as being generated, we were not able to detect the level of $H_2O_2$ using the titanium oxysulphate method as the limit of quanitifation was only 1 ppm.

$$Q = n_e \cdot F \qquad \text{Eq. 1}$$

In addition, FC is generated simultaneously due to chlorine oxidation, being able to react with the electrogenerated $H_2O_2$ (reaction 1). In fact the use of $H_2O_2$ as quencher for FC in drinking water is commonly used (Wang et al., 2006). Thus apart from $H_2O_2$ internal diffusion across cell membranes, $H_2O_2$ could generate $O_2$ through reaction 1, so producing ROS according to reactions 2-5, explaining the subsequently enhance of bacteria inactivation.

$$HOCl + H_2O_2 \rightarrow O_2 + H_2O + HCl \qquad (R.1)$$

$$e_{CB}^- + O_2 \rightarrow O_2^{\bullet -} \qquad (R.2)$$

$$O_2^{\bullet -} + H^+ \rightarrow HO_2^{\bullet} \qquad (R.3)$$

$$2HO_2^{\bullet} \rightarrow H_2O_2 + O_2 \qquad (R.4)$$

$$H_2O_2 + O_2^{\bullet -} \rightarrow {}^{\bullet}OH + OH^- + O_2 \qquad (R.5)$$

**FIGURE 5**

There was no improvement in the degradation rate of the OMCs using the carbon cathode (Figure 5b). The degradation of the sum of OMCs was similar to that observed with the Pt cathode, with $k$ =1.17 ± 0.05 ($10^{-2}$ $min^{-1}$). The % degradation achieved for the individual OMCs was 63% of TBT, 57% of CVP and >90% of DCF in 60 min (Figure SI-3).

In other studies it was demonstrated that $H_2O_2$ itself is not able to remove OMCs, as in Michael et al. (2020) where the combination of sunlight and $H_2O_2$, in a concentration of 30 mg $L^{-1}$, after 5 h of treatment only achieved the removal of the 46% of sulfamethoxazole in an urban wastewater with 15 mg $L^{-1}$ of DOC. Moreover, in Jiménez-Tototzintle et al. (2015), it was studied the effects of $H_2O_2$ addition to a $TiO_2$ supported catalyst for the removal of imazalil, thiabendazole and acetamiprid (200 µg $L^{-1}$ each) in a wastewater treatment plant effluent with 25.2 mg $L^{-1}$ of DOC, being required 500 mg $L^{-1}$ of $H_2O_2$ to achieve a remarkable improvement, evidencing its low efficiency to remove OMCs even acting as electron acceptor. Therefore in our system, where

peroxide production is very low, no improvement is expected. Moreover if it reacts with FC generating producing finally ROS, consequently the amount generated will be also very low and, even if they improves the inactivation of bacteria, they will probably not be enough to mineralize the OMCs.

The simultaneous removal of OMCs and *E. coli* was also investigated aiming to evaluate any possible competition effect between both targets during the PEC-C felt treatment. Results are shown in Figure 5a and b for *E. coli* and OMCs, respectively.

The PEC-C felt system for the simultaneous treatment improved the rate of *E. coli* inactivation as compared to the disinfection results in the absence of OMCs. The detection limit was reached in 90 min of treatment (approximately 4.5-LRV). The enhancement in bacterial inactivation could be cause due to the methanol added from the OMCs stock solution. On the one hand the oxidation of methanol generates formaldehyde (HCHO) (Pablos et al., 2014) which is bactericidal even at low concentrations ($LC_{50}$ for *E. coli* = 1 mg $L^{-1}$ or 33 µM) (Bae et al., 2008; Verschueren, 2001). On the other hand, methanol is a hole scavenger that increases the photocurrent and may led to the generation of more $H_2O_2$ at the cathode. The action of hole scavengers is described in detail in section 3.6. Regarding ∑OMCs a slight enhancement is observed with a rate constant of $k$ =1.38 ± 0.07 ($10^{-2}$ $min^{-1}$).

### *3.5 Oxidant species generated during PEC*

The generation oxidant species was monitored during PC (as reference) and for EAP with the carbon electrode. Figure 6a shows the results of of RNO bleaching measured •OH when using PEC-C felt system in comparison with PC. It should be considered that in waters containing chlorides, ACS are produced which are able to bleach RNO by themselves, being an interference for •OH determination (Muff et al., 2011). For that reason the RNO bleaching was considered as a parameter to evaluate the oxidative power of the electrochemical system.Specifically, after 30 min of EAP with the carbon cathode, 66% of the RNO was removed while 27% with PC. These results support the benefits of EAP for the inactivation and degradation of *E. coli* and OMCs (Fig. 5a and 5b, respectively) in comparison with PC in water. The application of an external electrical bias serves to separate the charge carriers and therefore should increase oxidant species production at the photoanode.

$H_2O_2$ quantification was not feasible as the detected amount was but below the quantification limit (1 mg $L^{-1}$). As described in section 3.4, electrogenerated $H_2O_2$ rapidly reacts with FC thus avoid its proper quantification.

The generation of FC measured with the PEC-C felt and PC is shown in Figure 6b. It is observed that values of FC detected was higher in the case of EAP than in PC. FC is formed by the oxidation of chloride present in the surface water (18.4 mg $L^{-1}$). With EAP, the separation of charge carriers means the holes are longer lived and more likely to react with chloride. Moreover, according to reaction 1, part of the FC produced is quenched by the electrogenerated $H_2O_2$, so the measurement represents residual FC in the solution. The concentration of FC detected during PEC-C felt treatment was very low (< 0.5 mg $L^{-1}$) in 30 min of treatment. This is below the recommended free chlorine level for residual disinfection of water (WHO, 2017) .

**FIGURE 6**

***3.6 Influence of hole acceptors in PEC disinfection***

In this study, the bacteria inactivation by PEC-C felt cathode was tested in the presence of 5 mM of methanol and acetate as hole-acceptors (Fig. 7), as this was the concentration of methanol added with the stock solution of OMCs. In EAP processes with $TiO_2$ photoanodes, hole-acceptors such as methanol and acetate, generate an increase in the photocurrent studied in detail by Byrne et al. (1998). The one electron oxidation of methanol generates a radical which injects a second electron to the conduction band, giving rise to photocurrent doubling. However, acetate is not a current doubling agent. For that reason, in our study the average of photocurrent with methanol was a 38% higher than without hole scavengers while for acetate was a 20% higher.

Regarding disinfection, the inactivation rates obtained in the presence of hole acceptors are much higher (Fig. 7). For methanol, this enhancement was previously explained due to the formation of formaldehyde which is highly toxic for microorganism and the generation of ROS derived from oxygen reduction reactions (reactions 2-5) while for acetate, the improvement have to be caused mainly for the ROS.

That way, extracellular ROS and intracellular •OH can inactivate bacteria through DNA/RNA damage, membrane rupture, interruption of respiratory pathways or increased ion permeability (Sun et al., 2016). Previous studies pointed out the sensitivity of *E. coli* to $H_2O_2$ (Morais et al., 2016) and the effective inactivation in the presence of superoxide radicals ($O_2^{\cdot-}$) (Gupta et al., 2019). Therefore, using a hole scavenger and carbon felt as a cathode simultaneously could lead to a lower electron-hole recombination rate, allowing increasing the number of photoinduced electrons that are able to reduce oxygen and produce higher concentrations of ROS, such as $H_2O_2$ and $O_2^{\cdot-}$.

**FIGURE 7**

## 4. Conclusions

PEC systems based on $TiO_2$-NTs has been evaluated as an alternative for the treatment of real surface water, in which salt concentration is substantially lower than in the solutions used as supporting electrolytes, eg., $Na_2SO_4$ that is commonly used in concentrations of 50 mM or higher. This research has confirmed the suitability of using C-felt cathode for a PEC cell as promising alternative to Pt. Carbon-based electrodes at the same current, without additional energy cost, are able to simultaneously produce $H_2O_2$, improving current efficiency of the system. The simultaneous removal of OMCs and *E. Coli* has been successfully proven in the PEC - C felt system for surface water depuration being the first step for the application of this system in conditions closer to reality. The presence of a significant amount of background organic matter (60 mg $L^{-1}$) had a critical effect on the efficiency since it caused a scavenger effect for the oxidant radicals. Despite this, 70% degradation of the OMCs was reached. The study of oxidizing species confirmed that the generation of $H_2O_2$ and FC represents a great improvement for disinfection purposes, despite they do not significantly affect the removal of OMCs. Nevertheless, it is important to highlight that further research must be tackled to better distinguish and define the inactivation mechanism when PEC-C felt system is applied.


## Acknowledgements

This research has received funding from the European Union's Horizon 2020 via the Marie Curie Action under the grant agreement number 734560 (ALICE), and the research and innovation program under the grant agreement number 820718 , which is jointly funded by the European Commission and the Department of Science and Technology of India (PANIWATER).

**Declarations of interest:** none


## References


Bae, E., Lee, J.W., Hwang, B.H., Yeo, J., Yoon, J., Cha, H.J., Choi, W., 2008. Photocatalytic bacterial inactivation by polyoxometalates. Chemosphere 72, 174-181.

Baram, N., Starosvetsky, D., Starosvetsky, J., Epshtein, M., Armon, R., Ein-Eli, Y., 2009. Enhanced inactivation of E. coli bacteria using immobilized porous $TiO_2$ photoelectrocatalysis. Electrochim. Acta 54, 3381-3386.

Bourgin, M., Beck, B., Boehler, M., Borowska, E., Fleiner, J., Salhi, E., Teichler, R., von Gunten, U., Siegrist, H., McArdell, C.S., 2018. Evaluation of a full-scale wastewater treatment plant upgraded with ozonation and biological post-treatments: Abatement of micropollutants, formation of transformation products and oxidation by-products. Water Res. 129, 486-498.

Byrne, J.A., Davidson, A., Dunlop, P.S.M., Eggins, B.R., 2002. Water treatment using nano-crystalline $TiO_2$ electrodes. J Photoch Photobio A 148, 365-374.

Byrne, J.A., Eggins, B.R., Linquette-Mailley, S., Dunlop, P.S.M., 1998. The effect of hole acceptors on the photocurrent response of particulate $TiO_2$ anodes. Analyst 123, 2007-2012.

Cardoso, J.C., Lizier, T.M., Zanoni, M.V.B., 2010. Highly ordered $TiO_2$ nanotube arrays and photoelectrocatalytic oxidation of aromatic amine. Appl Catal B-Environ 99, 96-102.

Cheng, X., Cheng, Q., Deng, X., Wang, P., Liu, H., 2016. A facile and novel strategy to synthesize reduced TiO2 nanotubes photoelectrode for photoelectrocatalytic degradation of diclofenac. Chemosphere 144, 888-894.

Cotillas, S., Llanos, J., Rodrigo, M.A., Canizares, P., 2015. Use of carbon felt cathodes for the electrochemical reclamation of urban treated wastewaters. Appl Catal B-Environ 162, 252-259.

Cruz-Ortiz, B.R., Hamilton, J.W.J., Pablos, C., Díaz-Jiménez, L., Cortés-Hernández, D.A., Sharma, P.K., Castro-Alférez, M., Fernández-Ibañez, P., Dunlop, P.S.M., Byrne, J.A., 2017. Mechanism of photocatalytic disinfection using titania-graphene composites under UV and visible irradiation. Chem. Eng. J. 316, 179-186.

Farhat, A., Keller, J., Tait, S., Radjenovic, J., 2017. Assessment of the impact of chloride on the formation of chlorinated by-products in the presence and absence of electrochemically activated sulfate. Chem. Eng. J. 330, 1265-1271.

Farhat, A., Keller, J., Tait, S., Radjenovic, J., 2018. Oxidative capacitance of sulfate-based boron-doped diamond electrochemical system. Electrochem. Commun. 89, 14-18.

Gao, L., Zhou, B., Wang, F., Yuan, R., Chen, H., Han, X., 2020. Effect of dissolved organic matters and inorganic ions on $TiO_2$ photocatalysis of diclofenac: mechanistic study and degradation pathways. Environ Sci Pollut Res Int 27, 2044-2053.

Giannakis, S., Polo López, M.I., Spuhler, D., Sánchez Pérez, J.A., Fernández Ibáñez, P., Pulgarin, C., 2016. Solar disinfection is an augmentable, in situ -generated photo-Fenton reaction—Part 1: A review of the mechanisms and the fundamental aspects of the process. Appl Catal B-Environ 199, 199-223.

Gupta, R., Modak, J.M., Madras, G., 2019. Behavioral analysis of simultaneous photo-electro-catalytic degradation of antibiotic resistant E. coli and antibiotic via ZnO/CuI: a kinetic and mechanistic study. Nanoscale Advances 1, 3992-4008.

Jiménez-Tototzintle, M., Oller, I., Hernández-Ramírez, A., Malato, S., Maldonado, M.I., 2015. Remediation of agro-food industry effluents by biotreatment combined with supported $TiO_2/H_2O_2$ solar photocatalysis. Chem. Eng. J. 273, 205-213.

Jin, Y., Shi, Y., Chen, Z., Chen, R., Chen, X., Zheng, X., Liu, Y., Ding, R., 2020. Enhancement of solar water disinfection using $H_2O_2$ generated in situ by electrochemical reduction. Appl Catal B-Environ 267.

Le, T.X.H., Bechelany, M., Cretin, M., 2017. Carbon felt based-electrodes for energy and environmental applications: a review. Carbon 122, 564-591.

Leng, W.H., Zhu, W.C., Ni, J., Zhang, Z., Zhang, J.Q., Cao, C.N., 2006. Photoelectrocatalytic destruction of organics using $TiO_2$ as photoanode with simultaneous production of $H_2O_2$ at the cathode. Appl Catal A-Gen 300, 24-35.

Liu, X., Han, Y., Li, G., Zhang, H., Zhao, H., 2013. Instant inactivation and rapid decomposition of Escherichia coli using a high efficiency $TiO_2$ nanotube array photoelectrode. RSC Advances 3, 20824-20828.

Mazierski, P., Borzyszkowska, A.F., Wilczewska, P., Bialk-Bielinska, A., Zaleska-Medynska, A., Siedlecka, E.M., Pieczynska, A., 2019. Removal of 5-fluorouracil by solar-driven photoelectrocatalytic oxidation using Ti/$TiO_2$(NT) photoelectrodes. Water Res. 157, 610-620.

Michael, S.G., Michael-Kordatou, I., Nahim-Granados, S., Polo-López, M.I., Rocha, J., Martínez-Piernas, A.B., Fernández-Ibáñez, P., Agüera, A., Manaia, C.M., Fatta-Kassinos, D., 2020. Investigating the impact of UV-C/$H_2O_2$ and sunlight/$H_2O_2$ on the removal of antibiotics, antibiotic resistance determinants and toxicity present in urban wastewater. Chem. Eng. J. 388, 124383

Moles, S., Valero, P., Escuadra, S., Mosteo, R., Gomez, J., Ormad, M.P., 2020. Performance comparison of commercial $TiO_2$: separation and reuse for bacterial photo-inactivation and emerging pollutants photo-degradation. Environ Sci Pollut Res 27, 9099–9113

Morais, L.A., Adán, C., Araujo, A.S., Guedes, A.P.M.A., Marugán, J., 2016. Photocatalytic Activity of Suspended and Immobilized Niobium Oxide for Methanol Oxidation and Escherichia coli Inactivation. J Adv Oxid Technol 19, 256-265.

Moreira, F.C., Boaventura, R.A.R., Brillas, E., Vilar, V.J.P., 2017. Electrochemical advanced oxidation processes: a review on their application to synthetic and real wastewaters. Appl Catal B-Environ 202, 217-261.

Muff, J., Bennedsen, L.R., Søgaard, E.G., 2011. Study of electrochemical bleaching of p-nitrosodimethylaniline and its role as hydroxyl radical probe compound. J. Appl. Electrochem. 41, 599-607.

Nie, X., Chen, J., Li, G., Shi, H., Zhao, H., Wong, P.-K., An, T., 2013. Synthesis and characterization of TiO2nanotube photoanode and its application in photoelectrocatalytic degradation of model environmental pharmaceuticals. J Chem Technol Biot 88, 1488-1497.

Pablos, C., Marugán, J., Adán, C., Osuna, M., van Grieken, R., 2017a. Performance of $TiO_2$ photoanodes toward oxidation of methanol and E. coli inactivation in water in a scaled-up photoelectrocatalytic reactor. Electrochim. Acta 258, 599-606.

Pablos, C., Marugán, J., van Grieken, R., Adán, C., Riquelme, A., Palma, J., 2014. Correlation between photoelectrochemical behaviour and photoelectrocatalytic activity and scaling-up of P25-$TiO_2$ electrodes. Electrochim. Acta 130, 261-270.

Pablos, C., Marugán, J., van Grieken, R., Dunlop, P., Hamilton, J., Dionysiou, D., Byrne, J., 2017b. Electrochemical enhancement of photocatalytic disinfection on aligned $TiO_2$ and nitrogen doped $TiO_2$ nanotubes. Molecules 22, 704.

Panizza, M., 2010. Importance of electrode material in the electrochemical treatment of wastewater containing organic pollutants, in: Comninellis, C., Chen, G. (Eds.), Electrochemistry for the Environment. Springer, pp. 25-54.

Polo-López, M.I., García-Fernández, I., Oller, I., Fernández-Ibáñez, P., 2011. Solar disinfection of fungal spores in water aided by low concentrations of hydrogen peroxide. Photoch Photobio Sci 10, 381-388.

Quan, X., Ruan, X., Zhao, H., Chen, S., Zhao, Y., 2007. Photoelectrocatalytic degradation of pentachlorophenol in aqueous solution using a TiO2 nanotube film electrode. Environ. Pollut. 147, 409-414.

Shin, Y., Lee, S., 2008. Self-Organized Regular Arrays of Anodic TiO2 Nanotubes. Nano Lett. 8, 3171-3173.

Sun, H., Li, G., An, T., Zhao, H., Wong, P.K., 2016. Unveiling the photoelectrocatalytic inactivation mechanism of Escherichia coli: Convincing evidence from responses of parent and anti-oxidation single gene knockout mutants. Water Res. 88, 135-143.

Verschueren, K., 2001. Handbook of environmental data on organic chemicals: Vol. 1. John Wiley and Sons, Inc.

Wang, L., Hung, Y.-T., Shammas, N., 2006. Advanced Physicochemical Treatment Processes.

WHO, W.H.O., 2017. Guidelines for drinking-water quality. Fourth edition incorporating the first adenddum.

Xie, Y.B., Li, X.Z., 2006. Interactive oxidation of photoelectrocatalysis and electro-Fenton for azo dye degradation using $TiO_2$–Ti mesh and reticulated vitreous carbon electrodes. Mater. Chem. Phys. 95, 39-50.

Figure 1

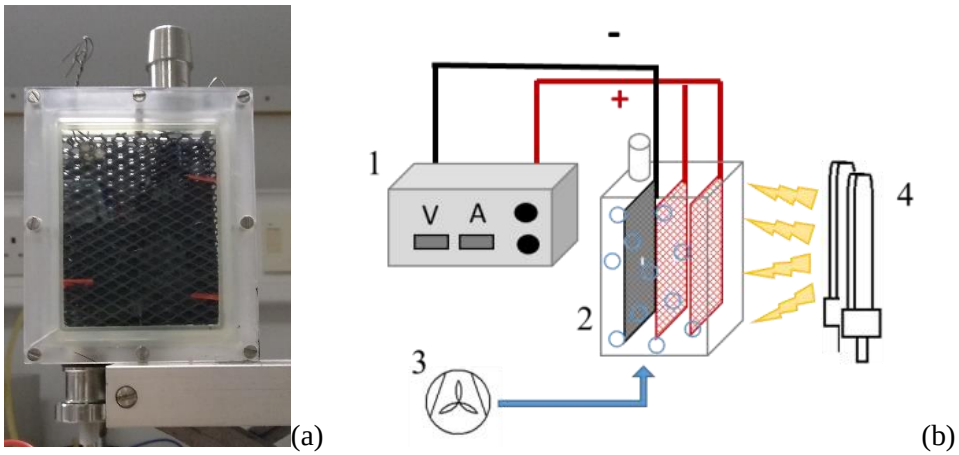


(a) (b)

**Figure 1**. a) photograph of PEC reactor b) Experimental setup: (1) power supply (2) PEC cell (cathode in black, anodes in red), (3) air-blower, (4) UVA lamps.

Figure 2

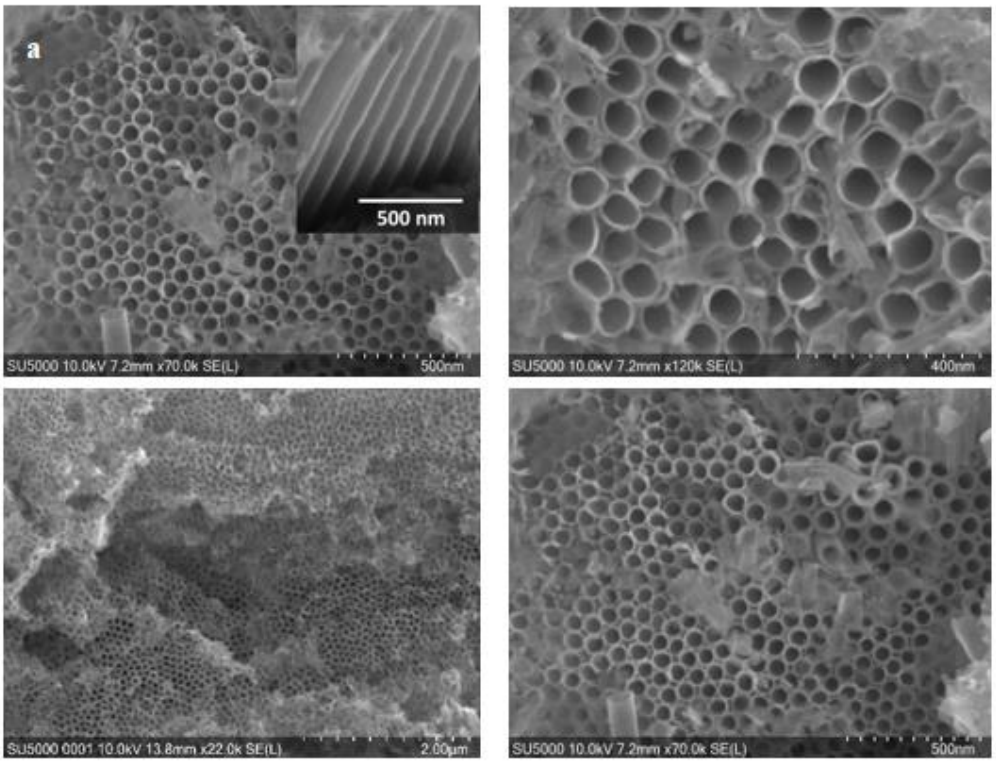


a)

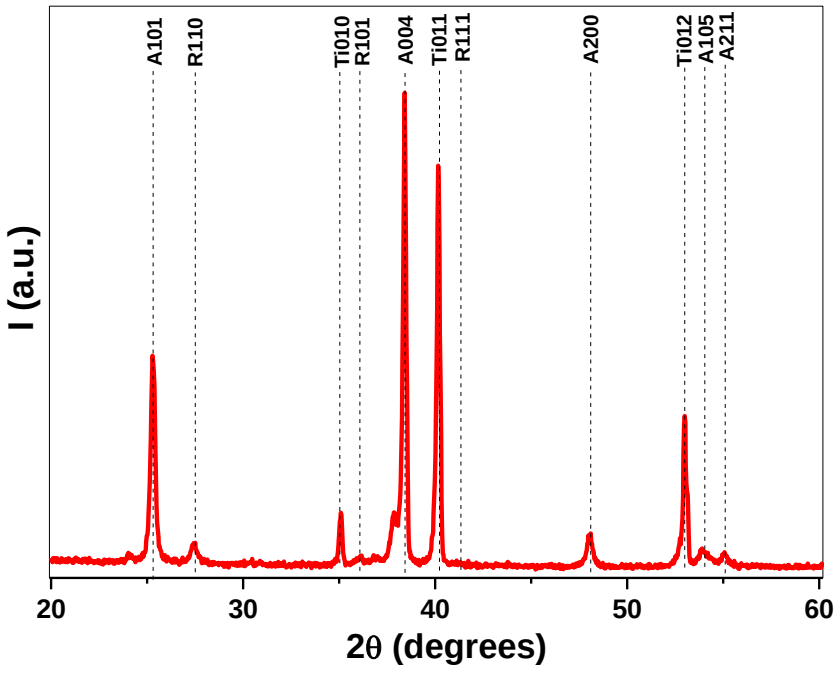


b)

**Figure 2.** Characterization of $TiO_2$-NTs prepared by electrochemical anodization of Ti mesh: a) SEM images with inset(a) view of cross-section of the nanotubes and b) XRD analysis.

Figure 3

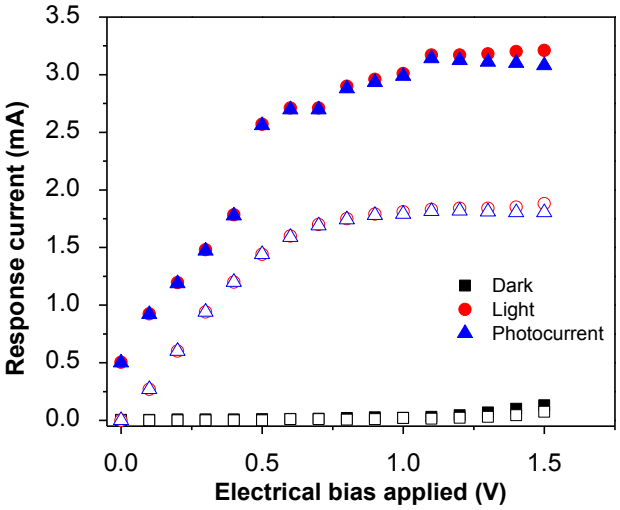


**Figure 3.** Response current densities in dark and under radiation, and the calculated photocurrent, obtained by the application of a serial of potentials from 0 to 1.5 V using a Pt cathode (full symbol) and C-felt cathode (open symbol).

Figure 4

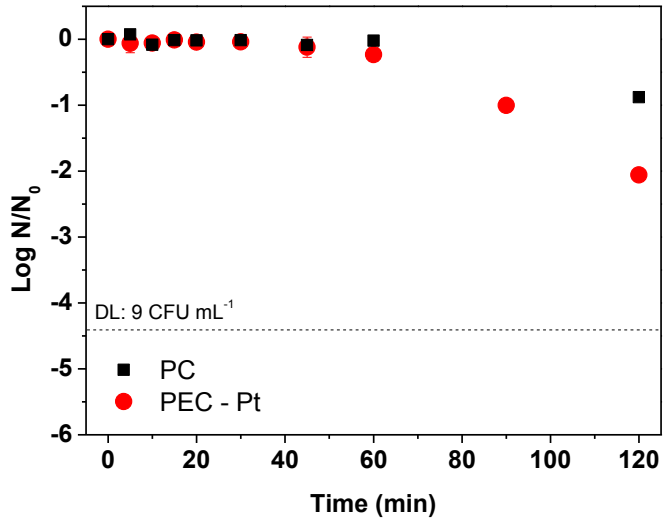


a)

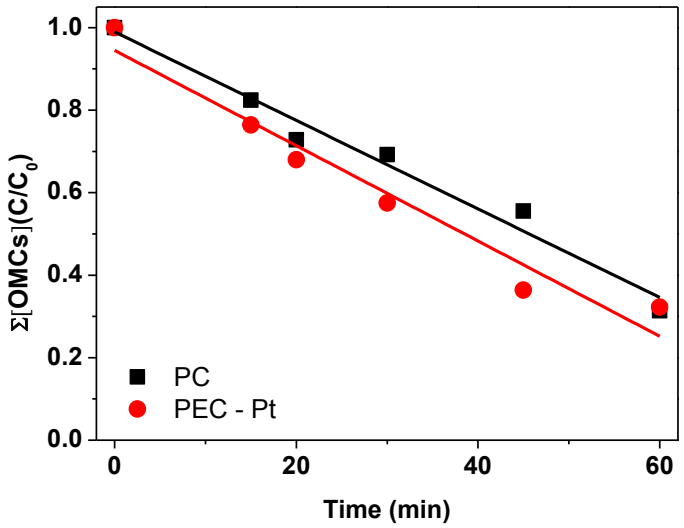


b)

**Figure 4.** a) *E. coli* inactivation and b) ΣOMCs concentration during photocatalysis (PC), EAP with Pt cathode (PEC-Pt) in surface water.

Figure 5

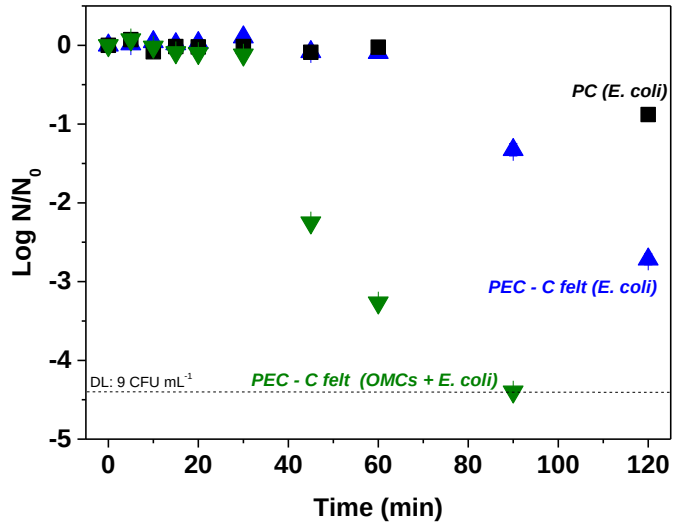


a)

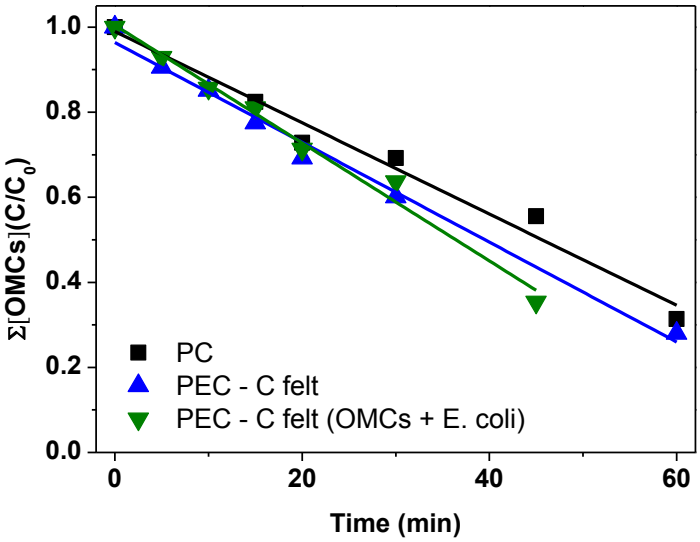


b)

**Figure 5.** a) *E. coli* inactivation and b) OMCs degradation profiles obtained by photocatalysis (PC), photoelectrocatalysis with carbon-felt cathode (PEC-C felt) in surface water.

Figure 6

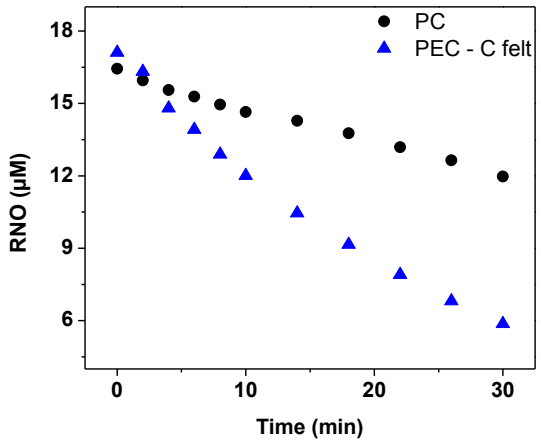


a)

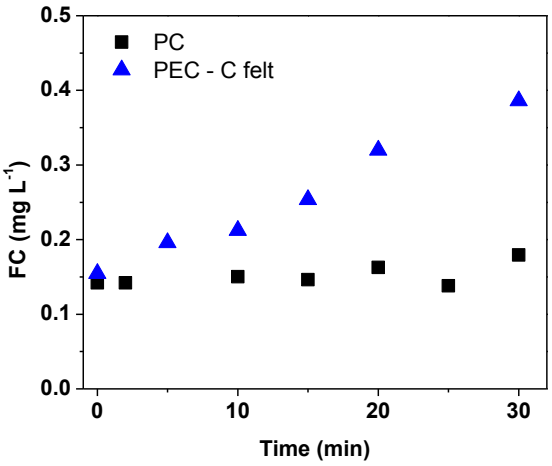


b)

**Figure 6.** Generation of a) RNO bleaching and b) FC during PC and EAP in a PEC-C felt cathode.

Figure 7

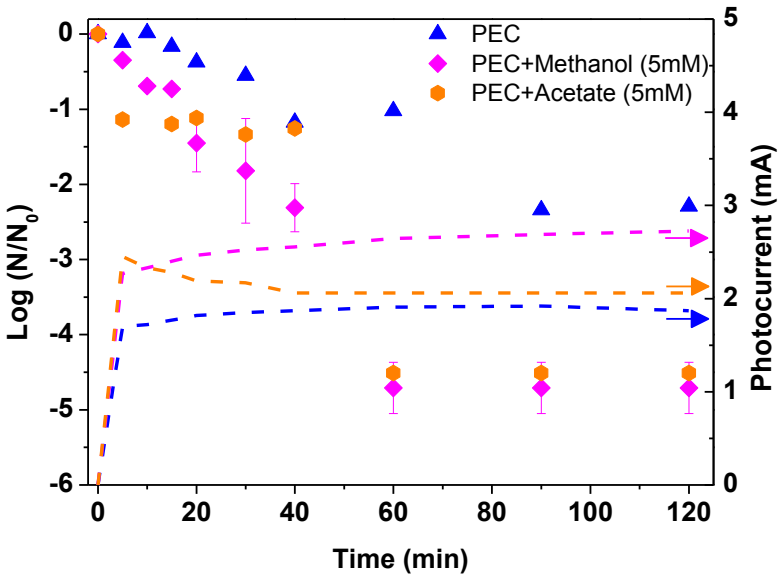


**Figure 7.** *E. coli* inactivation profile for PEC with C-felt cathode with methanol and acetate as hole acceptors.